

**NUMERICAL SOLUTION OF FORCED CONVECTIVE  
FLOW OF BIO-NANOFLUID ALONG A WEDGE WITH  
STEFAN BLOWING AND MULTIPLE SLIPS EFFECTS**

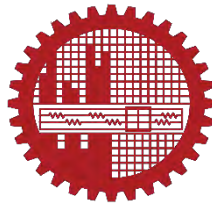
by

**Debasis Kumar**

Student No. 0412093004p

Session: April-2012

MASTER OF PHILOSOPHY  
IN  
MATHEMATICS



Department of Mathematics  
BANGLADESH UNIVERSITY OF ENGINEERING AND  
TECHNOLOGY, DHAKA-1000

March – 2019

The thesis entitled “NUMERICAL SOLUTION OF FORCED CONVECTIVE FLOW OF BIO-NANOFLUID ALONG A WEDGE WITH STEFAN BLOWING AND MULTIPLE SLIPS EFFECTS”, submitted by **Debasis Kumar**, Student No. 0412093004p, Session: April-2012, has been accepted as satisfactory in partial fulfillment for the degree of Master of Philosophy in Mathematics on 9th March 2019.

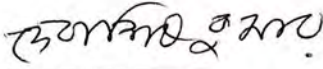
### Board of Examiners

*A. Alim*

- (i) \_\_\_\_\_  
**Dr. Md. Abdul Alim**  
Professor  
Department of Mathematics, BUET, Dhaka-1000  
**Chairman (Supervisor)**
- (ii) *Palan*  
\_\_\_\_\_  
**Head**  
Department of Mathematics, BUET, Dhaka-1000  
**Member (Ex-Officio)**
- (iii) *Mab Khan*  
\_\_\_\_\_  
**Dr. Md. Abdul Hakim Khan**  
Professor  
Department of Mathematics, BUET, Dhaka-1000  
**Member**
- (iv) *Lamir*  
\_\_\_\_\_  
**Dr. Md. Manirul Alam Sarker**  
Professor  
Department of Mathematics, BUET, Dhaka-1000  
**Member**
- (v) *Jashim*  
\_\_\_\_\_  
**Dr. Md. Jashim Uddin**  
Professor and Head  
Department of Mathematics  
Faculty of Science & Information Technology  
American International University-Bangladesh (AIUB)  
Dhaka-1229, Bangladesh  
**Member (External)**

## Candidate's Declaration

I am hereby declaring that no portion of the work considered in this thesis has been submitted in support of an application for another degree or qualification of this or any other University or Institute either in the home or abroad.



**Debasis Kumar**

M.Phil Student

Student No. 0412093004p

Department of Mathematics

9th March 2019

## **Certificate of Research**

This is to certify that the work presented in this thesis is carried out by the author under the supervision of Dr. Md. Abdul Alim, Professor, Department of Mathematics, Bangladesh University of Engineering & Technology, Dhaka-1000, Bangladesh.

*A. Alim*

---

**Professor Dr. Md. Abdul Alim**  
(Supervisor)  
Department of Mathematics  
Bangladesh University of Engineering & Technology  
Dhaka-1000, Bangladesh

## Acknowledgment

Firstly, I would like to express my gratitude to the Almighty for His endless blessings without which it would have been impossible to accomplish the arduous job I was assigned to. I would like to state my heartfelt appreciation to my supervisor **Prof. Dr. Md. Abdul Alim**, Professor, Department of Mathematics, Bangladesh University of Engineering and Technology (BUET) and express my heartfelt gratitude to him for his perceptive supervision, continuous support, and encouragement. I feel very privileged to have his precious advice, guidance, and leadership. He has encouraged always since he took over the supervision of this thesis work.

I am thankful from the core of my heart to the faculty members of the Department of Mathematics, Bangladesh University of Engineering and Technology, especially, to **Prof. Dr. Mustafizur Rahman**, Head, Department of Mathematics, **Prof. Dr. Md. Abdul Hakim Khan**, **Prof. Dr. Md. Manirul Alam Sarker**, **Prof. Dr. Md. Elias**, **Prof. Dr. Khandker Farid Uddin Ahmed**, **Prof. Dr. Nazma Parvin**, and **Prof. Dr. Salma Parvin** and all other teachers of this department for their guidance and support.

In Addition, I would like to express my deep-felt gratitude to my dearest **parents** for their sincere support of my decisions at every step of my life. At this point, it is so much momentous than ever to have them by my side. I will always be indebted to them.

Finally, I am grateful to my **colleagues** for their sincere help and technical support throughout the thesis period. The thesis period has become extremely consequential with their cooperation. I am grateful to the **BUET authorities** for providing me with all the infrastructural, internet and other necessary facilities.

**Dedicated**

**to**

**Prof. Dr. Md. Abdus Samad**

**Department of Applied Mathematics**

**University of Dhaka**

## Abstract

In this study, the numerical solutions of a wedge flow of bio-nanofluid with Stefan blowing and different slip effects at the boundary were investigated. The governing equations were formed by using a system of partial differential equations and appropriate boundary conditions. Then those equations were transformed to governing ordinary differential equations using suitable similarity variables. The ordinary differential equations were solved numerically with the help of numerical differential equations solver package named “NDSolve” in Mathematica. Then those solutions were plotted with the variation of the different parameter and different slip phenomena. The influences of the Stefan blowing, the velocity, thermal, the concentration and microorganism slips, the magnetic number, the Lewis number, the bioconvection Lewis number, the wedge parameter, the bioconvection Péclet number, thermophoresis and Brownian motion on the dimensionless velocity, temperature, nanoparticle volume fraction, microorganisms concentration, the local skin friction coefficient, the local Nusselt number and the local Sherwood number and local density number of the motile microorganisms were analyzed and discussed. Tabular solutions were included for numerical values of the skin friction coefficients, local heat transfer rate, local mass transfer rate and the microorganisms transfer rate at the wall. Numerical solutions were compared with the published results and found an excellent agreement.

# Contents

<b>Board of Examiners .....</b>	<b>ii</b>
<b>Candidate's Declaration .....</b>	<b>iii</b>
<b>Certificate of Research .....</b>	<b>iv</b>
<b>Acknowledgment .....</b>	<b>v</b>
<b>Dedicated.....</b>	<b>vi</b>
<b>Abstract.....</b>	<b>vii</b>
<b>Contents .....</b>	<b>viii</b>
<b>List of Figures .....</b>	<b>xi</b>
<b>List of Tables .....</b>	<b>xii</b>
<b>Nomenclature.....</b>	<b>xiii</b>
<b>Literature Review.....</b>	<b>xv</b>
<b>CHAPTER 1: INTRODUCTION.....</b>	<b>1</b>
1.1 Classification of fluids.....	1
1.1.1 Newtonian fluids and non-Newtonian fluids .....	1
1.1.2 Viscous and non-viscous or inviscid fluids.....	1
1.1.3 Compressible and incompressible fluids.....	1
1.2 Some basic properties of fluids .....	2
1.2.1 Density .....	2
1.2.2 Viscosity.....	2
1.2.3 Kinematic viscosity.....	3
1.2.4 Pressure .....	3
1.2.5 Temperature .....	3
1.2.6 Thermal conductivity .....	4
1.2.7 Stefan blowing .....	4
1.2.8 Heat flux.....	4
1.2.9 Nanofluids.....	5
1.2.10 Bioconvection .....	5
1.3 Types of flow.....	5
1.3.1 Steady flow .....	5
1.3.2 Unsteady flow .....	6
1.3.3 Laminar flow.....	6
1.3.4 Turbulent flow.....	6
1.3.5 Rotational flow.....	7
1.3.6 Irrotational flow .....	7
1.3.7 Wedge flow .....	7



1.4	Magnetohydrodynamics .....	8
1.5	Boundary layer concept.....	9
1.5.1	The velocity boundary layer .....	10
1.5.2	The thermal boundary layer .....	10
1.5.3	Concentration boundary layer .....	11
1.5.4	Microorganism boundary layer .....	12
1.5.5	Slip and no-slip boundary conditions.....	12
1.6	Some dimensionless numbers .....	13
1.6.1	Prandtl number .....	13
1.6.2	Nusselt number .....	14
1.6.3	Bioconvection Péclet number .....	15
1.6.4	Lewis number.....	15
1.6.5	Bioconvection Lewis number .....	15
1.6.6	Magnetic number .....	16
1.6.7	Brownian motion parameter.....	16
1.6.8	Thermophoresis parameter.....	17
1.6.9	Skin friction.....	17
1.6.10	Sherwood number .....	18
1.6.11	Density number of motile microorganisms.....	18
<b>CHAPTER 2: MATHEMATICAL FORMULATION .....</b>		<b>19</b>
2.1	Basic equations .....	19
2.2	Physical quantities .....	22
2.3	Numerical methods and validation.....	23
<b>CHAPTER 3: RESULTS AND DISCUSSIONS .....</b>		<b>25</b>
3.1	Effects of slip and no-slip boundary conditions .....	25
3.2	Effects of velocity slip boundary condition.....	28
3.3	Effects of temperature slip boundary condition .....	30
3.4	Effects of mass slip boundary condition .....	32
3.5	Effects of microorganism slip boundary condition .....	35
3.6	Effects of Lewis number .....	37
3.7	Effects of the magnetic fields .....	40
3.8	Effects of bioconvection Lewis number.....	42
3.9	Effects of Péclet number .....	45
3.10	Effects of wedge parameter .....	47
3.11	Engineering designed quantities.....	49
<b>CHAPTER 4: CONCLUSIONS.....</b>		<b>54</b>
4.1	Conclusions .....	54
4.2	Possible future works .....	55

<b>CHAPTER 5: REFERENCES .....</b>	<b>56</b>
<b>CHAPTER 6: APPENDICES .....</b>	<b>62</b>
6.1 Appendix one .....	62
6.1.1 Momentum equation: .....	62
6.1.2 Energy equation: .....	63
6.1.3 Concentration equation: .....	64
6.1.4 Microorganism equation: .....	64
6.2 Appendix two .....	65
6.2.1 Momentum equation: .....	67
6.2.2 Energy equation: .....	68
6.2.3 Concentration equation: .....	68
6.2.4 Microorganism equation: .....	69
6.2.5 Boundary conditions .....	69
6.3 Appendix three .....	72
6.3.1 Skin friction coefficient.....	72
6.3.2 Local Nusselt number .....	72
6.3.3 Local Sherwood number .....	72
6.3.4 Local density number of the motile microorganisms.....	72

## List of Figures

<b>Fig. 1.1:</b> Boundary layer flow over a wedge .....	7
<b>Fig. 1.2:</b> The velocity boundary layer.....	10
<b>Fig. 1.3:</b> The thermal boundary layer .....	11
<b>Fig. 1.4:</b> The concentration boundary layer.....	11
<b>Fig. 1.5:</b> The microorganism boundary layer .....	12
<b>Fig. 2.1:</b> Physical model of the forced convective flow of bio-nanofluid along a wedge.....	19
<b>Fig. 3.1(a):</b> Variation of $f'(\eta)$ with different values of $S$ in the presence and absence of slip boundary conditions.....	25
<b>Fig. 3.1(b):</b> Variation of $\theta(\eta)$ with different values of $S$ in the presence and absence of slip boundary conditions.....	26
<b>Fig. 3.1(c):</b> Variation of $\phi(\eta)$ with different values of $S$ in the presence and absence of slip boundary conditions.....	27
<b>Fig. 3.1(d):</b> Variation of $\chi(\eta)$ with different values of $S$ in the presence and absence of slip boundary conditions.....	27
<b>Fig. 3.2(a):</b> Variation of $f'(\eta)$ for different values of $S$ and $a$ .....	28
<b>Fig. 3.2(b):</b> Variation of $\theta(\eta)$ for different values of $S$ and $a$ .....	28
<b>Fig. 3.2(c):</b> Variation of $\phi(\eta)$ for different values of $S$ and $a$ .....	29
<b>Fig. 3.2(d):</b> Variation of $\chi(\eta)$ for different values of $S$ and $a$ .....	30
<b>Fig. 3.3(a):</b> Variation of $f'(\eta)$ for different values of $S$ and $b$ .....	30
<b>Fig. 3.3(b):</b> Variation of $\theta(\eta)$ for different values of $S$ and $b$ .....	31
<b>Fig. 3.3(c):</b> Variation of $\phi(\eta)$ for different values of $S$ and $b$ .....	31
<b>Fig. 3.3(d):</b> Variation of $\chi(\eta)$ for different values of $S$ and $b$ .....	32
<b>Fig. 3.4(a):</b> Variation of $f'(\eta)$ for different values of $S$ and $d$ .....	33
<b>Fig. 3.4(b):</b> Variation of $\theta(\eta)$ for different values of $S$ and $d$ .....	33
<b>Fig. 3.4(c):</b> Variation of $\phi(\eta)$ for different values of $S$ and $d$ .....	34
<b>Fig. 3.4(d):</b> Variation of $\chi(\eta)$ for different values of $S$ and $d$ .....	34
<b>Fig. 3.5(a):</b> Variation of $f'(\eta)$ for different values of $S$ and $e$ .....	35
<b>Fig. 3.5(b):</b> Variation of $\theta(\eta)$ for different values of $S$ and $e$ .....	36
<b>Fig. 3.5(c):</b> Variation of $\phi(\eta)$ for different values of $S$ and $e$ .....	36
<b>Fig. 3.5(d):</b> Variation of $\chi(\eta)$ for different values of $S$ and $e$ .....	37
<b>Fig. 3.6(a):</b> Variation of $f'(\eta)$ for different values of $S$ and $Le$ .....	38
<b>Fig. 3.6(b):</b> Variation of $\theta(\eta)$ for different values of $S$ and $Le$ .....	38

<b>Fig. 3.6(c):</b> Variation of $\phi(\eta)$ for different values of $S$ and $Le$ .....	39
<b>Fig. 3.6(d):</b> Variation of $\chi(\eta)$ for different values of $S$ and $Le$ .....	39
<b>Fig. 3.7(a):</b> Variation of $f'(\eta)$ for different values of $S$ and $M$ .....	40
<b>Fig. 3.7(b):</b> Variation of $\theta(\eta)$ for different values of $S$ and $M$ . ....	41
<b>Fig. 3.7(c):</b> Variation of $\phi(\eta)$ for different values of $S$ and $M$ . ....	41
<b>Fig. 3.7(d):</b> Variation of $\chi(\eta)$ for different values of $S$ and $M$ . ....	42
<b>Fig. 3.8(a):</b> Variation of $f'(\eta)$ for different values of $S$ and $Lb$ .....	42
<b>Fig. 3.8(b):</b> Variation of $\theta(\eta)$ for different values of $S$ and $Lb$ . ....	43
<b>Fig. 3.8(c):</b> Variation of $\phi(\eta)$ for different values of $S$ and $Lb$ . ....	43
<b>Fig. 3.8(d):</b> Variation of $\chi(\eta)$ for different values of $S$ and $Lb$ . ....	44
<b>Fig. 3.9(a):</b> Variation of $f'(\eta)$ for different values of $S$ and $Pe$ .....	45
<b>Fig. 3.9(b):</b> Variation of $\theta(\eta)$ for different values of $S$ and $Pe$ . ....	45
<b>Fig. 3.9(c):</b> Variation of $\phi(\eta)$ for different values of $S$ and $Pe$ . ....	46
<b>Fig. 3.9(d):</b> Variation of $\chi(\eta)$ for different values of $S$ and $Pe$ . ....	47
<b>Fig. 3.10(a):</b> Variation of $f'(\eta)$ for different values of $S$ and $m$ .....	47
<b>Fig. 3.10(b):</b> Variation of $\theta(\eta)$ for different values of $S$ and $m$ . ....	48
<b>Fig. 3.10(c):</b> Variation of $\phi(\eta)$ for different values of $S$ and $m$ . ....	48
<b>Fig. 3.10(d):</b> Variation of $\chi(\eta)$ for different values of $S$ and $m$ . ....	49
<b>Fig. 3.11(a):</b> Variation of the skin friction factor $f''(0)$ for different values of $S, M$ and $a$ . ..	49
<b>Fig. 3.11(b):</b> Variation of $-\theta'(0)$ for different values of $S, Nt, Nb$ and $b$ . ....	50
<b>Fig. 3.11(c):</b> Variation of $-\phi'(0)$ for different values of $S, Le$ and $d$ .....	51
<b>Fig. 3.11(d):</b> Variation of $-\chi'(0)$ for different values of $S, Lb$ and $e$ .....	52

## List of Tables

<b>Table 1:</b> Comparison of analytical solutions (Fang and Jing [36]) and numerical solutions (present study) of surface concentration gradient $-\phi'(0)$ and surface temperature gradient $-\theta'(0)$ . ....	24
<b>Table 2:</b> Values of the skin friction factor, local heat transfer rate, local mass transfer rate and the local microorganisms transfer rate at the wall.....	53

## Nomenclature

$a$	velocity slip parameter (–)
$a_0$	arbitrary constant ( $s^{-1}$ )
$b$	thermal slip parameter (–)
$\bar{b}$	chemotaxis constant ( $m$ )
$B$	variable magnetic field ( $(kg)A^{-1}s^{-2}$ )
$B_0$	constant magnetic field ( $(kg)A^{-1}s^{-2}$ )
$C$	nanoparticle volume fraction (–)
$C_w$	wall nanoparticle volume fraction (–)
$C_\infty$	ambient nanoparticle volume fraction (–)
$d$	mass slip parameter (–)
$D_1$	variable thermal slip factor ( $m$ )
$(D_1)_0$	constant thermal slip factor ( $m$ )
$D_B$	Brownian diffusion coefficient ( $m^2 s^{-1}$ )
$D_n$	diffusivity of microorganisms ( $m^2 s^{-1}$ )
$D_T$	thermophoretic diffusion coefficient ( $m^2 s^{-1}$ )
$e$	microorganism slip parameter (–)
$E_1$	variable concentration slip factor ( $m$ )
$(E_1)_0$	constant concentration slip factor ( $m$ )
$f(\eta)$	dimensionless stream function (–)
$F_1$	variable microorganism slip factor ( $m$ )
$(F_1)_0$	constant microorganism slip factor ( $m$ )
$k$	thermal conductivity ( $Wm^{-1} K^{-1}$ )
$K$	arbitrary constant (–)
$Lb$	bioconvection Lewis number (–)
$Le$	Lewis number (–)
$m$	wedge parameter (–)
$M$	magnetic number (–)
$N$	volume fraction of motile microorganisms (–)
$N_1$	variable velocity slip factor ( $s m^{-1}$ )
$(N_1)_0$	constant velocity slip factor ( $s m^{-1}$ )
$Nb$	Brownian motion parameter (–)
$Nn_x$	local density number of the motile microorganisms (–)

$Nt$	thermophoresis parameter (–)
$Nu_x$	local Nusselt number (–)
$N_w$	wall microorganisms (–)
$N_\infty$	ambient microorganisms (–)
$Pe$	bioconvection Péclet number (–)
$Pr$	Prandtl number (–)
$S$	Stefan blowing parameter (–)
$Sh_x$	local Sherwood number (–)
$T$	nanofluid temperature (K)
$T_w$	wall temperature (K)
$T_\infty$	ambient temperature (K)
$u, v$	velocity components along the $x$ - and $y$ - axes ( $m s^{-1}$ )
$\tilde{v}$	microorganisms swimming velocity ( $m s^{-1}$ )
$u_e$	ambient velocity ( $m s^{-1}$ )
$W_c$	maximum cell swimming speed ( $m s^{-1}$ )
$x, y$	Cartesian coordinates ( $x$ -axis is aligned along and $y$ -axis is normal to the wedge) ( $m$ )

### **Greek symbols**

$\alpha$	effective thermal diffusivity ( $m^2 s^{-1}$ )
$\eta$	similarity variable (–)
$\theta(\eta)$	dimensionless temperature (–)
$\mu$	dynamic viscosity ( $(kg)m^{-1} s^{-1}$ )
$\nu$	kinematic viscosity of the fluid ( $m^2 s^{-1}$ )
$\rho$	the density of the base fluid ( $(kg) m^{-3}$ )-
$\sigma$	electric conductivity ( $(kg)^{-1} m^{-3} s^3 A^2$ )
$\chi(\eta)$	the rescaled density of motile microorganisms (–)
$\tau$	ratio between the effective heat capacity of the nanoparticle material and heat capacity of the fluid (–)
$\phi(\eta)$	rescaled nanoparticle volume fraction (–)
$\psi$	stream function (–)

### **Subscripts/superscripts**

$w$	condition at the wall
$\infty$	free stream condition
'	differentiation with respect to $\eta$

## Literature Review

Thermal properties of liquids play an important role in heating as well as cooling applications in many industrial processes. Conventional heat transfer fluids have a poor thermal conductivity which makes them inadequate for ultra-high cooling applications. Scientists, applied mathematician, and engineers have tried to enhance the inherently poor thermal conductivity of these conventional heat transfer fluids using solid additives following the classical effective medium theory Maxwell [1] for effective properties of mixtures. Fine-tuning of the dimensions of these solid suspensions to the millimeter and micrometer ranges for getting better heat transfer performance has failed because of the drawbacks such as still low thermal conductivity, particle sedimentation, corrosion of components of machines, particle clogging, excessive pressure drops, etc. Downscaling of particle sizes continued in the search for new types of fluid suspensions having enhanced thermal properties as well as heat transfer performance. Modern nanotechnology offers physical and chemical routes to prepare nanometer-sized particles or nanostructure materials engineered on the atomic or molecular scales with enhanced thermo-physical properties compared to their respective bulk forms. Choi [2] and Lee [3] have shown that it is possible to break down the limits of conventional solid particle suspensions by conceiving the concept of nanoparticle-fluid suspensions.

According to published papers, nanoparticles are made from various materials, namely oxide ceramics ( $\text{Al}_2\text{O}_3$ ,  $\text{CuO}$ ), nitride ceramics ( $\text{AlN}$ ,  $\text{SiN}$ ), carbide ceramics ( $\text{SiC}$ ,  $\text{TiC}$ ), metals ( $\text{Cu}$ ,  $\text{Ag}$ ,  $\text{Au}$ ), semiconductors ( $\text{SiC}$ ), carbon nanotubes and composite materials such as alloyed nanoparticles or nanoparticle core-polymer shell composites. Nanofluid consists of the base fluid and ultrafine nanoparticles. It aims to achieve the maximum possible thermal properties at the minimum possible concentrations (preferably  $< 1\%$  by volume) by uniform dispersion and stable suspension of nanoparticles (preferably  $< 10$  nm) in base fluids (Murshed et al. [4] and Kakac et al. [5]). Nanofluids are able to enhance thermophysical properties such as thermal conductivity, thermal diffusivity, viscosity, and convective heat transfer coefficients compared to those of base fluids like oil or water (Kaufui and Omar [6]). Nanobiofluids have many applications. Examples include electronics cooling, vehicle cooling, transformer cooling, computers cooling, electronic devices cooling, materials and chemicals, detergency, food and drink, oil and gas, paper and printing, and textiles. Ultra-high-performance cooling is necessary for many industrial technologies.

Firstly, Falkner and Skan [7] worked on wedge flow to explain the application of the Prandtl boundary layer theory. He used the similarity variable to convert the set of partial differential equations to ordinary differential equations. Recently Atalik and Sonmezler [8] and [9] have worked on their two papers to investigate boundary layer flow over a wedge by using electric forces and fields. Seddeek et al. [10] studied Steady MHD Falkner-Skan flow by using wedge geometry with the effects of variable viscosity and thermal conductivity. Hayat et al. [11] analyzed Falkner-Skan wedge flow with mixed convection and porous medium by the power-law fluid. Also, Falkner-Skan flow with nanofluid for a static or moving wedge are investigated by Yacob et al. [12]. Prasad et al. [13] discussed MHD mixed convection flow over a permeable non-isothermal wedge. And unsteady MHD accelerating flow with thermal radiation and internal heat generation /absorption past over a wedge studied by Ashwini et al. [14].

The microorganism is heavier and denser than water, so they are swimming upward and tending to swim in a particular direction. When the upper surface is too dense, microorganisms fall down to cause bioconvection. Some oxytactic bacteria such as *Bacillus subtilis* organized by their consumption of oxygen and oxygen is refilled by diffusion from the surface (Lee and Kim [15]). The formulation of species transfer is similar to the heat transfer equation. Kuznetsov [16], [17] and [18] worked furthermore about nanoparticles and microorganisms, such as the onset of nanofluid bioconvection in a suspension, simultaneous effects of gyrotactic and oxytactic micro-organisms over nanofluid bio-thermal convection and nanofluid bioconvection in water-based suspensions. Khan et al. [19] worked with gyrotactic microorganisms for free convection of non-Newtonian nanofluids in porous media. Tham et al. [20] studied steady mixed convection flow by using nanofluid with gyrotactic microorganisms on a horizontal circular cylinder embedded in a porous medium. Bég et al. [21] analyzed numerically about mixed bioconvection in porous media with nanofluid which containing oxytactic microorganisms. Shaw et al. [22] also used nanofluid with gyrotactic microorganisms to investigate MHD and sores effects on bioconvection in a porous medium. Zaimi et al. [23] considered the stagnation-point flow of nanofluid containing both gyrotactic microorganisms and nanoparticles toward a stretching/shrinking sheet. Also, nanofluid containing both nanoparticles and gyrotactic microorganisms developed by Xu and Pop [24] with mixed convection flow in a horizontal channel. Raees et al. [25] analyzed mixed convection of gravity-driven nano liquid with nanoparticles and gyrotactic microorganisms. Magnetic field analysis in a suspension of gyrotactic microorganisms and nanoparticles are



also investigated by Akbar and Khan [26] over a stretching surface. Mutuku and Makinde [27] computed the effect of gyrotactic microorganisms and Hydromagnetic bioconvection of nanofluid with a permeable vertical plate geometry. Xu [28] considered an outer power-law stream of a nanofluid bioconvection over a vertical flat surface by Lie group analysis. Amirsom et al. [29] analyzed variable transport properties of three-dimensional stagnation point flow of bio-nanofluid. Latiff [30] used a solid rotating stretchable disk to show Stefan blowing effect on the bioconvective flow of nanofluid. Babu and Sandeep [31] investigated the effect of nonlinear thermal radiation over a stretching sheet using non-aligned bioconvective stagnation point flow of a magnetic-nanofluid. Makinde and Animasaun [32] worked on thermophoresis and Brownian motion effects on MHD bioconvection of nanofluid past on the upper horizontal surface with nonlinear thermal radiation and quartic chemical reaction.

Species transfer or mass transfer is said to occur due to the water content in the wet paper sheet and the temperature difference. These species transfer can produce blowing effect what is related to the Stefan species transfer called Stefan blowing (Nellis and Klein [33]). The blowing effect of the species transfer creates the extra motion of fluid flows and generates an extra correction factor between habitual results without blowing effects (Lienhard iv and Lienhard v [34]). There is some difference between blowing due to transpiration or mass injection and Stefan blowing effect. The flow field is affected by mass blowing and due to the flow field, all these effects generate dependency between concentration and momentum fields (Fang [35]). Fang and Jing [36] worked on flow, heat, and species transfer over a stretching plate considering coupled Stefan blowing effects from species transfer and Latiff et al. [37] showed Stefan blowing effect on the bioconvective flow of nanofluid over a solid rotating stretchable disk. Uddin et al. [38] used a spinning cone in an anisotropic porous medium to show Stefan blowing, Navier slip, and radiation effects on thermo-solutal convection. Amirsom et al. [39] investigated melting heat transfer and Stefan blowing effects of electromagnetoconvective stagnation point flow of bio-nanofluid. Faisal et al. [40] submerged Stefan blowing with microorganisms and analyzed the effect on nanofluid flow with leading-edge accretion or ablation. In the presence of gyrotactic microorganisms, Stefan blowing effects on MHD bioconvection flow of a nanofluid investigated by Giri et al. [41] with active and passive nanoparticles flux. Recently, Zohra et al. [42] showed the effect of Stefan blowing from a rotating cone with anisotropic slip magneto-bioconvection flow to a nanofluid.

Nanofluid slip flow model for bio-nano-materials processing was studied by Uddin et al. [43]. Further velocity, thermal, and solutal slip boundary conditions for MHD boundary layer flow and heat transfer of a nanofluid past a permeable stretching sheet developed by Ibrahim and Shankar [44]. Uddin et al. [45] examined G-Jitter mixed convective slip in a Darcian porous media with variable viscosity. Zheng and Zhang [46] worked on velocity slip and temperature jump in a porous medium for nanofluid over a stretching sheet. Magneto-convective non-Newtonian nanofluid slip flow from a permeable stretching sheet studied by Uddin et al. [47]. Hamad et al. [48] investigated numerically the hydrodynamic slip effects by Lie group analysis with variable diffusivity. Thermal slip boundary condition effects over a permeable shrinking cylinder investigated by Mishra and Singh [49]. Crane and McVeigh [50] studied the boundary layer development about slip flow on a body of revolution. Hettiarachchi et al. [51] worked on temperature-jump boundary condition with laminar slip-flow in a rectangular microchannel. Further slip flow in rectangular microchannels for all versions of constant wall temperature developed by Kuddusi [52]. For rarefied electrically conducting gas, unsteady magnetic low-speed slip flow examined by Djukic [53]. Slip flow in circular microchannels for non-Newtonian fluids studied by Barkhordari and Etemad [54]. Further work on the slip in the flow of power-law liquids past smooth spherical particles with Navier linear slip model done by Kishore and Ramteke [55]. Shateyi and Mabood [56] considered MHD mixed convection slip flow in the presence of viscous dissipation on a nonlinearly vertical stretching sheet near a stagnation-point. Khan et al. [57] analyzed multiple slip effects of nanofluids in a Darcian porous medium on unsteady MHD rear stagnation point flow. Basir et al. [58] showed Schmidt and Péclet number effects on nanofluid slip flow over a stretching cylinder. Rosca et al. [59] focused on velocity slip using Buongiorno's mathematical model using a semi-analytical solution method for the flow of a nanofluid over a permeable stretching/shrinking sheet. Uddin et al. [60] computed multiple-slip and Stefan blowing effects on buoyancy-driven bioconvection nanofluid flow with microorganisms.

Transport problem can be governed by a set of PDE with relevant boundary conditions (Fang and Jing [36] and Uddin et al. [60]). However, no-slip boundary conditions provide unrealistic results. In this work, multiple slips boundary conditions were incorporated to get physically realistic and practically applicable results for Stefan blowing effects along a wedge.

# CHAPTER 1: INTRODUCTION

---

## 1.1 Classification of fluids

Fluids can be classified in different ways based on various characteristics and properties.

### 1.1.1 Newtonian fluids and non-Newtonian fluids

**(i) Newtonian fluids:** A fluid for which the coefficient of viscosity ( $\mu$ ) does not change with the rate of deformation is said to be Newtonian fluid and represented by a straight line. In other words, fluids which obey the Newtonian law of viscosity are known as Newtonian fluids. Fluids like water, air, and mercury are all Newtonian fluids.

**(ii) Non-Newtonian fluids:** A fluid for which the coefficient of viscosity ( $\mu$ ) changes with the rate of deformation, then it is said to be Non-Newtonian fluid. In other words, the fluids which do not obey Newton's law of viscosity are known as Non-Newtonian fluids. Fluid like paints, colter, and polymer solutions are all non-Newtonian fluids.

### 1.1.2 Viscous and non-viscous or inviscid fluids

**(i) Viscous Fluids:** A fluid is said to be viscous fluid when the normal, as well as shearing stresses, exist. Coulter, Molasses, and heave oil are treated as a viscous fluid.

**(ii) Non-viscous Fluids:** A fluid is said to be non-viscous when it does not exert any shearing stress, whether at rest or in motion. Clearly, the pressure exerted by an inviscid fluid on any surface is always along the normal to the surface at the point. All gases are treated as inviscid fluids.

### 1.1.3 Compressible and incompressible fluids

**(i) Compressible fluids:** A compressible fluid is one when a fixed mass of fluid undergoes changes in volume, its density also changes. Gasses are extremely compressible and expand infinity when all external forces are removed. In other word, fluid is compressible if it can be easily compressed. The compressible fluid has a variable density.

**(ii) Incompressible fluids:** An incompressible fluid is one whose elements undergo no changes in volume or density. In other words, fluid is said to be incompressible if it cannot be compressed easily. Liquids are relatively incompressible. There exist no fluid which can be classified as perfectly compressed.

## 1.2 Some basic properties of fluids

Some important basic properties of the fluid are given below.

### 1.2.1 Density

The density of a material is defined as its mass per unit volume. The symbol of density is  $\rho$

Mathematically,

$$\rho = \lim_{\delta v \rightarrow 0} \frac{\delta m}{\delta v},$$

where,

$\rho$  density of the fluid ( $(kg) m^{-3}$ ),

$\delta v$  elementary volume ( $m^3$ ),

$m$  mass within  $\delta v$  ( $m$ ).

Different materials usually have different densities, so density is an important concept regarding buoyancy, metal purity and packaging. In some cases, density is expressed as the dimensionless quantities specific gravity (SG) or relative density (RD), in which case it is expressed in multiples of the density of some other standard material, usually water or air/gas.

### 1.2.2 Viscosity

The normal force per unit area is called normal stress and the tangential force per unit area is called shearing stress. Due to shearing stress, a viscous fluid produces resistance to the body moving through it as well as between the particles of the fluid and itself. We know that the flow of water and air are much easier than the coater and heavy oil. This demonstrates the existence of a property in the fluid. This controls its rate of flow. This property of fluids is said to be viscosity or internal friction, i.e. viscosity is a property of a fluid which demonstrates its resistance to shearing stress. When the shearing stress  $\tau$  is increased by increasing the force, the rate of shearing stress is increased in direct proportion that

$$\tau \propto \frac{du}{dy}.$$

This result indicates that for common fluids such as water, oil, gasoline, and airs, the shearing stress and the rate of shearing stress can be related to a relation of the form

$$\tau = \mu \frac{du}{dy},$$

where the constant of proportionality is designated by the Greek symbol  $\mu$  and is called the dynamic viscosity or simply the viscosity of the fluid. An ideal fluid has no viscosity. In reality, there is no fluid which can be classified as a perfectly ideal fluid. However, the fluids with very little viscosity are sometimes considered as ideal fluids. The viscosity of a fluid is due to chosen and interaction between particles. The viscosity of a gas increases with temperature, but the viscosity of a liquid decreases with temperature.

### 1.2.3 Kinematic viscosity

The ratio of dynamic viscosity and fluid density is known as kinematic viscosity, defined as follows

$$\nu = \frac{\mu}{\rho},$$

where,

$\mu$  dynamic viscosity  $((kg)m^{-1}s^{-1})$ ,

$\rho$  fluid density  $((kg)m^{-3})$ .

The kinematic viscosity sometimes referred to as diffusivity of momentum because it is comparable to and has some unit  $(m^2s^{-1})$  as diffusivity of heat and diffusivity of mass.

### 1.2.4 Pressure

The pressure is the force per unit area applied in a direction perpendicular to the surface of an object. The pressure is an effect which occurs when a force is applied on a surface. The symbol of pressure is  $p$ . Mathematically,

$$p = \lim_{\delta A \rightarrow 0} \frac{\delta F}{\delta A},$$

where,

$p$  pressure  $((kg)m^{-1}s^{-2})$ ,

$\delta A$  elementary area  $(m^2)$ ,

$\delta F$  normal force due to fluid on  $\delta A$   $((kg)ms^{-2})$ .

The pressure is a tensor quantity and has SI units of Pascal,  $1 Pa = 1 Nm^{-2}$ .

### 1.2.5 Temperature

When two bodies are in thermal equilibrium then they are said to have a common property, known as temperature  $T$ .

### 1.2.6 Thermal conductivity

The well-known Fourier's heat conduction law states that the conductive heat flow per unit area (or heat flux)  $q_n$  is proportional to the temperature decrease per unit distance in a direction normal to the area through the heat is flowing.

Thus, mathematically

$$q_n \propto -\frac{\partial T}{\partial A}$$

So,  $q_n = -k \frac{\partial T}{\partial A}$ ,

where,

$$k \quad \text{thermal conductivity } (Wm^{-1}k^{-1}) .$$

### 1.2.7 Stefan blowing

Species transfer is said that the performance that blowing of the fluid from the boundary to ambient or from free stream to wall, i.e. condensation or mass diffusion at the wall. The blowing effect by Stefan blowing is different from general mass injection or suction, where wall behaves as the permeable surface. Stefan blowing considered for impermeable surface and species flux transferred from ambient to surface or surface to ambient. Stefan problem for species transfer first introduced this blowing effect called "Stefan blowing". This blowing effect cause of correction in conservation equations and produce a blowing factor in the boundary condition. Flow field influenced by mass diffusion and make a strong coupling between momentum and concentration equations. An especial example of Stefan blowing is the paper drying process where the mass transfer is related to transformation by evaporation.

### 1.2.8 Heat flux

Heat flux or thermal flux sometimes also referred to as heat flux density or heat flow rate intensity is a flow of energy per unit of area per unit of time. In SI units, it is measured in  $[Wm^{-2}]$ . It has both a direction and a magnitude, so it is a vector quantity. To define the heat flux at a certain point in space, one takes the limiting case where the size of the surface becomes infinitesimally small ([https://en.wikipedia.org/wiki/Heat\\_flux](https://en.wikipedia.org/wiki/Heat_flux)). Heat flux is often denoted  $\vec{\phi}_q$ , the subscript  $q$  specifying heat flux, as opposed to mass or momentum flux. The most important appearance of heat flux in physics is in Fourier's law, describing heat conduction.

### 1.2.9 Nanofluids

A nanofluid is said to be a fluid containing nanometer-sized particles called nanoparticles. These fluids are engineered colloidal suspensions of nanoparticles in a base fluid. The nanoparticles used in nanofluids are typically made of metals, carbides, or carbon nanotubes. Nanofluids are two-phase systems with one phase (solid phase) in another (liquid phase). Nanofluids have been found to possess enhanced thermophysical properties such as thermal conductivity, thermal diffusivity, viscosity, and convective heat transfer coefficient compared to those of base fluids like oil or water. For a two-phase system, one of the most important issues is the stability of the nanofluid and it is a big challenge to achieve the desired stability of nanofluids. The potentials of nanofluids in heat transfer have attracted more and more attention. Due to the high density of chips, the design of electronic components with more compact makes heat dissipation more difficult. Recent Researchers illustrated that nanofluids could increase the heat transfer coefficient by increasing the thermal conductivity of a coolant.

### 1.2.10 Bioconvection

Microorganisms, which are usually denser than water and swim upward create bioconvection. By gathering microorganisms, the upper surface becomes unstable and produce bioconvection. Typically, two types of microorganisms are oxytactic bacteria and bottom alga. Due to asymmetric mass distribution, microorganisms with bottom-heavy properties swim upward. Although, microorganisms are acting on the cell and cell tends to swim toward the downwelling fluid region is called gyro taxis. On another hand, oxytactic bacteria consume oxygen and performed in a chamber with an upper level of open suspension (Uddin et. al. [60]).

## 1.3 Types of flow

### 1.3.1 Steady flow

The flow is said to be steady when the flow characteristics, such as velocity, density, pressure, and temperature do not change with time. The flow will be steady when the rate of change in these characteristics is zero.

For example, if  $v$  is the velocity at any point, the flow will be steady if

$$\frac{dv}{dt} = 0.$$

Water flowing through a tap at a constant rate is an example of steady flow. In fact, the steady flow is possible only when the flow is laminar. However, even in the case of turbulent flow when the mean velocity and mean values of other characteristics do not change with time, then the flow becomes steady.

### 1.3.2 Unsteady flow

The flow is said to be unsteady when the flow characteristics such as velocity, density, pressure and temperature change with respect to time.

For example, if  $v$  is the velocity at any point, the flow will be unsteady if

$$\frac{dv}{dt} \neq 0.$$

It has been seen that water flowing through a tap at a changing rate is an example of unsteady flow. When the tap is just opened, the flow is unsteady. After some time, the flow in the pipe becomes constant and the flow becomes steady.

### 1.3.3 Laminar flow

A flow in which each fluid particle traces out a definite curve and the curves traced out by any two different fluid particles do not intersect is said to be laminar flow. The fluid will be laminar when one or more of the following conditions occur:

- (i). Viscosity is very high
- (ii). Velocity is very low
- (iii). The passage is very narrow

Laminar flow occurs in a pipe when the Reynolds number is less than 2300 ([https://en.wikipedia.org/wiki/Reynolds\\_number](https://en.wikipedia.org/wiki/Reynolds_number)).

### 1.3.4 Turbulent flow

Fluid flow in which the fluid undergoes irregular fluctuations or mixing. The speed of the fluid at a point is continuously undergoing changes in magnitude and direction, which results in swirling and eddying as the bulk of the fluid moves in a specific direction. A common example of turbulent flow includes atmospheric and ocean, blood flows in arteries, oil transport in the pipeline, lava flow, flow-through pump and turbines, and the flow in boat wakes and around aircraft wingtips.



### 1.3.5 Rotational flow

The flow of a fluid in which the curl of the fluid viscosity is not zero. So that each minute particles of fluid rotate about its own axis. It is also known as rotational motion.

### 1.3.6 Irrotational flow

The flow of a fluid in which the curl of the fluid viscosity is zero everywhere so that the circulation of velocity about any closed curved vanishes. It is also known as a cyclic motion or irrotational motion.

### 1.3.7 Wedge flow

The flow along a wedge geometry called wedge flow. Fig shows the geometry of the wedge flow. Raisinghania [62] explains the geometry and mathematical formulation of boundary layer flow over a wedge as follows. Let us consider the flow around a wedge submerged in a fluid of very small viscosity. At the leading stagnation point, the thickness of the boundary layer is zero and it grows slowly towards, the rear of the wedge. Within a very thin boundary layer of thickness  $\delta$ , a large velocity gradient exists, i.e. the velocity increases from zero at the wall to the value of potential flow at the edge of the boundary layer. This geometry leads the boundary-layer equations for plane steady incompressible flow to well-known Falkner-Skan equation as  $f''' + ff'' + \beta(1 - f'^2) = 0$ . Where,  $\pi\beta$  is the wedge angle,  $\beta = \frac{2m}{m+1}$  and  $m$  is the power-law index of the velocity  $u = ax^m$ .

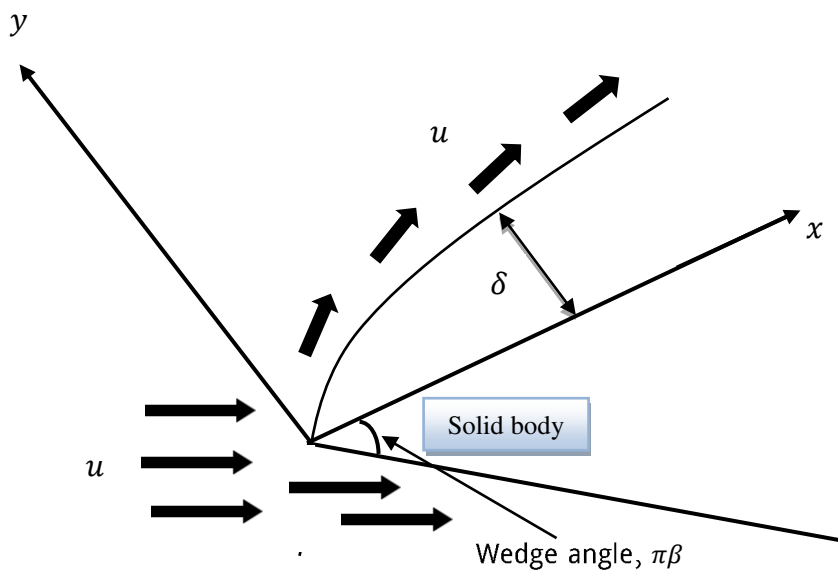


Fig. 1.1: Boundary layer flow over a wedge.

## 1.4 Magnetohydrodynamics

Magnetohydrodynamics [MHD] is a physical-mathematical framework that concerns the dynamics of magnetic fields in electrically conducting fluids, e.g. in plasmas and liquid metals and most commonly saline solutions. The word magneto hydrodynamic is comprised of the words magneto meaning magnetic, hydro meaning water (or liquid) and dynamics referring to the movement of an object by force. Less frequently used synonyms of MHD are the terms ‘magnetohydrodynamics’ and ‘hydromagnetic’. Hanne’s Alfvén was among the first scientist who initiated the MHD theory and received Nobel Prize in physics (1970) for fundamental research in magnetohydrodynamics and it has useful applications in plasma physics.

The magnetohydrodynamics fluid being conductive can be affected by the magnetic field. This idea plays a key role in MHD theory. The magnetic field induces currents in the fluid and as a consequence affecting the magnetic field itself. A key point for a particular MHD fluid is the relative strength of the advective motion in the fluid, compared to the diffusive effects caused by the electrical resistivity. In MHD theory the fluid may be treated as a continuum, without mean-free-path effects. Since MHD theory is non-relativistic and microscopic, the governing equations may be derived from Boltzmann’s equation assuming space and time scales to be larger than all inherent scale-lengths such as Debye length or the gyro-radii of the charged particles. It is, however, more convenient to obtain the MHD equations in a phenomenological way as the electromagnetic extension of the Navier-Stokes equations for ordinary fluid, where the prime assumption is to neglect the displacement current for an ideal MHD, the magnetic field is tightly coupled in the fluid, and said to be frozen into the fluid, the main parameters in the MHD theory are magnetic Reynolds number and the plasma beta. The magnetic Reynolds number is the ratio of advective and diffusive terms in the ordinary fluid flows, the plasma beta is defined as the ratio of the gas pressure to magnetic pressure.

Topics studied within MHD include typical computational astrophysics topics, such as magneto-convection, MHD turbulence, and hydromagnetic dynamo action. Typically, a multitude of intermittent magnetic structures are generated in such and other stellar objects, these magnetic structures may take the form of cool spots (sunspots) and magnetic bright points.

As the only conducting fluids available for laboratory experiments are mercury and liquid sodium, both are inconvenient for different reasons. It is very difficult to reach large magnetic Reynolds number in laboratory experiments, and so to verify important theoretical results with accuracy. There is another MHD laboratory plasma where the magnetic Reynolds number is very large. So, the magnetic field is well and truly frozen into this fluid. However, we cannot change the experimental parameters, and we do not know what is going on below the level that we can see, so it is less than perfect laboratory nevertheless, there are many other interesting a varied phenomenon that shows the influence of MHD very well.

### 1.5 Boundary layer concept

The boundary layer was first defined by Ludwig Prandtl in a paper presented on August 12, 1904, at the third International Congress of Mathematicians in Heidelberg, Germany. It allows aerodynamicists to simplify the equations of fluid flow by dividing the flow field into two areas: one inside the boundary layer, where viscosity is dominant and the majority of the drag experienced by a body immersed in a fluid is created and one outside the boundary layer where viscosity can be neglected without significant effects on the solution. This allows a closed-form solution for the flow in both areas, which is a significant simplification over the solution of the full Navier–Stokes equations. The majority of the heat transfer to and from a body also takes place within the boundary layer, again allowing the equations to be simplified in the flow field outside the boundary layer. The thickness of the velocity boundary layer is normally defined as the distance from the solid body at which the flow velocity is 99% of the freestream velocity, that is, the velocity that is calculated at the surface of the body in an inviscid flow solution. An alternative definition, the displacement thickness, recognizes the fact that the boundary layer represents a deficit in mass flow compared to an inviscid case with slip at the wall. It is the distance by which the wall would have to be displaced in the inviscid case to give the same total mass flow as the viscous case. The no-slip condition requires the flow velocity at the surface of a solid object be zero and the fluid temperature be equal to the temperature of the surface. The flow velocity will then increase rapidly within the boundary layer, governed by the boundary layer equations. The thermal boundary layer thickness is similarly the distance from the body at which the temperature is 99% of the temperature found from an inviscid solution. The ratio of the two thicknesses is governed by the Prandtl number. If the Prandtl number is 1, the two boundary layers are the same thickness. If the Prandtl number is greater than 1, the thermal boundary layer is thinner than

the velocity boundary layer. If the Prandtl number is less than 1, which is the case for air at standard conditions, the thermal boundary layer is thicker than the velocity boundary layer.

### 1.5.1 The velocity boundary layer

In case of fluid motions for which the measured pressure distribution nearly agrees with the perfect fluid theory, such as the fluid past the streamline or aerofoil, the influence of viscosity at high Reynolds numbers is confined to a very thin layer in the immediate neighborhood of the solid wall. The fact that at the wall fluid adheres to it means that frictional forces retard the motion of the fluid increases from zero at the wall (no-slip) to its full value which corresponds to external frictionless flow. This thin layer is called the velocity boundary layer. In short, the boundary layer is the thin fluid layer adjacent to the surface of a body in which a strong viscous effect exists. The quantity  $\delta_u$  is termed as the thickness, and it is typically defined as the value of  $y$  for which  $u = 0.99U$ , where  $U$  is the free stream velocity. This boundary layer profile refers to the manner in which  $u$  varies with  $y$  through the boundary layer and that's why referred to the velocity boundary layer. It develops whenever there is fluid flow over a surface, and it is of fundamental importance to problems involving convection transport.

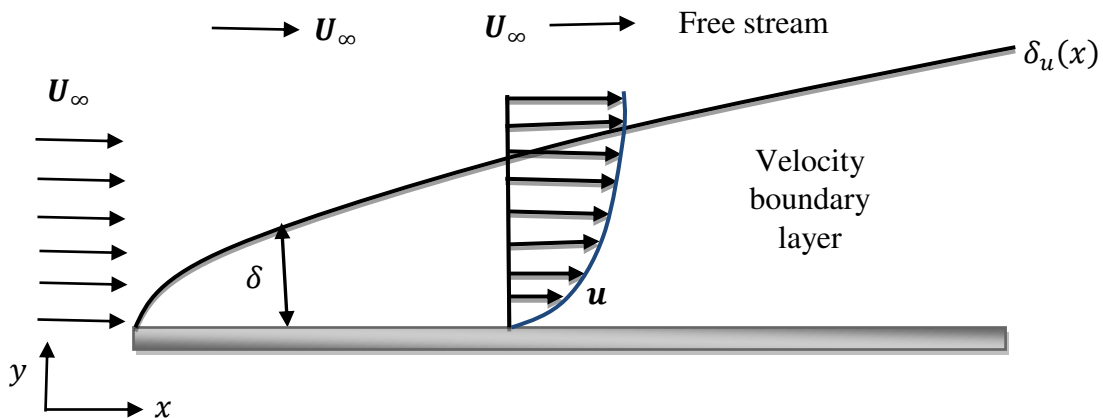


**Fig. 1.2:** The velocity boundary layer.

### 1.5.2 The thermal boundary layer

A thermal boundary layer develops if the fluid stream and surface temperature differ. We consider a flow over an isothermal plate. The fluid particle that comes into contact with the plate achieves thermal equilibrium at the plate's surface temperature. In turn, these particles

exchange energy with those in the adjacent fluid layer, and temperature gradients developed in the fluid. The region of the fluid in which these temperature gradients exist is the thermal boundary layer and its thickness  $\delta_T$  is typically defined as the value of  $y$  for which the ratio  $\frac{(T_w - T)}{(T_w - T_\infty)} = 0.99$ , with increasing distance from the leading edge, the effects of heat transfer penetrate further into the free stream and the thermal boundary layer grows.

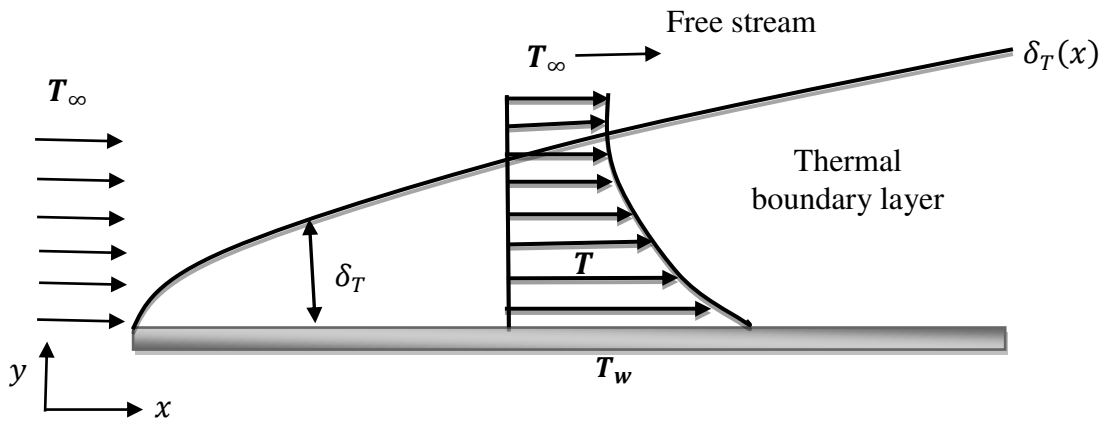


Fig. 1.3: The thermal boundary layer.

### 1.5.3 Concentration boundary layer

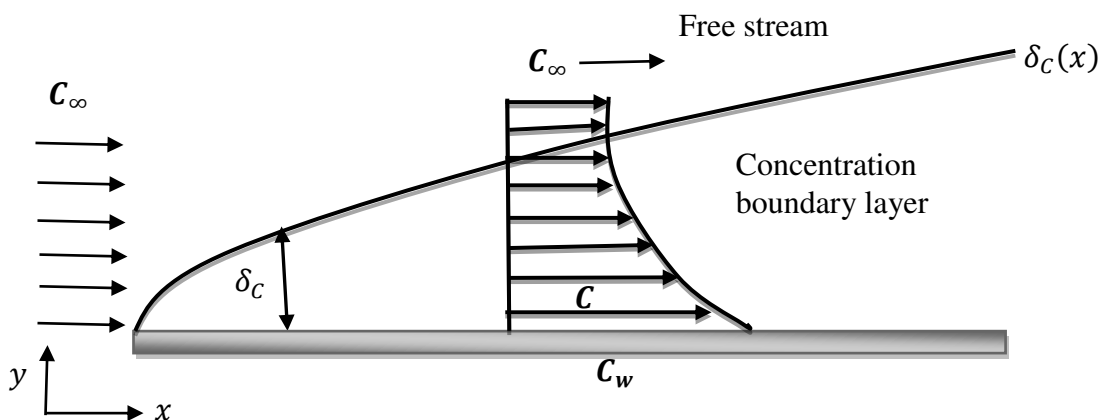


Fig. 1.4: The concentration boundary layer.

Species transfer by convection between the surface and the free stream fluid is determined by conditions in the boundary layer. Concentration boundary layer and convection mass transfer

will exist if the fluid's species concentration at the surface differs from its species concentration in the free stream. The concentration boundary layer is the region of the fluid in which concentration gradients exist and its thickness  $\delta_C$  is typically defined as the value of  $y$  for which  $\frac{(C_w - C)}{(C_w - C_\infty)} = 0.99$ . With increasing distance from the wall, the effects of species transfer penetrate farther into the free stream and the concentration boundary layer grows.

#### 1.5.4 Microorganism boundary layer

Development of microorganism boundary layer is similar to the velocity and thermal boundary layers. The microorganism boundary layer occurs due to the number of microorganisms difference between wall and fluid stream. In fluid flow, for adhesion, microorganisms are attached to the surface and make a microorganism difference. This instance constructs a thin layer called the microorganism boundary layer. The boundary layer thickness denoted as  $\delta_N$  and it indicates that the distance from the wall, till where the number of microorganisms is 99% of microorganisms present in free stream.

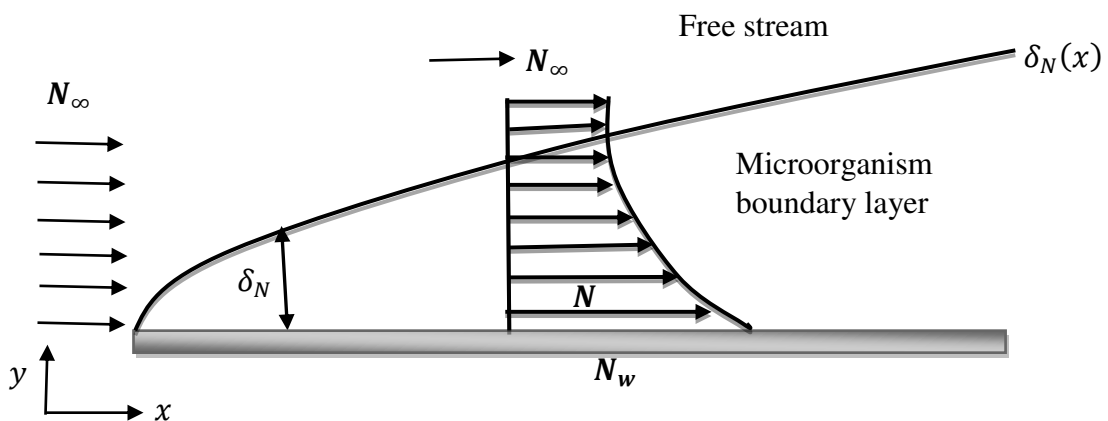


Fig. 1.5: The microorganism boundary layer.

#### 1.5.5 Slip and no-slip boundary conditions

For fluid flow when it is considered that flow has zero velocity at solid boundary then it is called no-slip boundary condition. It is a conceptual property that when adhesion is stronger than cohesion, fluid-particle stuck in the wall and retards motion at the boundary. On the other hand, the no-slip condition refers to a surface where the effect of shear stress is considered zero. In reality, velocity is not actually zero in the wall and slip phenomenon occurs at the boundary. So, we consider there are some nonzero values in velocity boundary

condition at the wall. Mathematically, it can be written as  $u = u_w + N_1(x) \nu \frac{\partial u}{\partial y}$ , where,  $u_w$  denotes wall velocity which is generally considered as zero and  $N_1(x)$  considered as a slip factor. On another hand, when fluid particles contracted with the wall it has considered that fluid has gained the same temperature with the boundary wall. It is called the isothermal boundary condition. But, when fluid particles are getting equilibrium state in temperature with boundary wall, there is some temperature difference between wall and fluid near the boundary. This temperature gap is considered as temperature slip boundary condition. It can be expressed as a summation of wall temperature and a correction factor called temperature slip as,  $T = T_w + D_1(x) \frac{\partial T}{\partial y}$ ,  $D_1(x)$  is the thermal slip factor. Similarly, slip phenomenon is added for the concentration boundary layer. For the no-slip concentration boundary condition, the concentration of fluid adjacent to boundary considered the same as the concentration of the fluid at the boundary wall. Due to flow variation like negative or positive blowing or suction/injection, the concentration at the wall differs and concentration of fluid may not the same near the wall. This concentration variation at wall consequences concentration slip. Wall concentration and slip phenomena can be expressed as  $C = C_w + E_1(x) \frac{\partial C}{\partial y}$ , where  $E_1(x)$  act as a slip factor with dimension meter ( $m$ ). In the same way, motile microorganisms difference between the solid wall and very near wall implies slip boundary condition of the motile microorganisms. Basically, it has been considered that microorganisms trapped at the wall and the number of microorganisms became same near the wall, this called no-slip microorganism boundary condition. But always some dissimilarity happens between streamline and the solid wall. For example, it can be expressed as a summation of slip factor and wall microorganism as,  $N = N_w + F_1(x) \frac{\partial N}{\partial y}$ ,  $F_1(x)$  is the microorganism slip factor. Certain slip conditions are used in hydrophobic fuel cell design, polishing of artificial heart valves and hydrophobic walls in fuel cells. When the slip phenomena occur, modification of boundary conditions is required.

## 1.6 Some dimensionless numbers

### 1.6.1 Prandtl number

The ratio between momentum diffusivity to thermal diffusivity is a dimensionless number called Prandtl number. It is named after the German physicist Ludwig Prandtl who introduced the concept of the boundary layer in 1904 and made significant contributions to boundary layer theory. Mathematically,

$$Pr = \frac{v}{\alpha} = \frac{\text{viscous diffusion rate}}{\text{thermal diffusion rate}} = \frac{\mu/\rho}{k/\rho C_p} = \frac{\mu C_p}{k},$$

where,

- $v$  momentum diffusivity or kinematics viscosity ( $m^2s^{-1}$ ),
- $\alpha$  thermal diffusivity ( $m^2s^{-1}$ ),
- $\mu$  dynamics viscosity ( $Nsm^{-2}$ ),
- $k$  thermal conductivity ( $Wm^{-1}k^{-1}$ ),
- $C_p$  specific heat ( $J(kg)^{-1}k^{-1}$ ),
- $\rho$  density ( $(kg)m^{-3}$ ).

Higher Prandtl number implies that viscous diffusion much more dominance compared to thermal diffusion. Heavy oil is the example of those types of fluids with Prandtl number near 100000. On the other hand, lower Prandtl number means that the thermal diffusion rate is much higher than viscous diffusion. Prandtl number for liquid metals is less than 0.01. It also be noted that for gas, Prandtl number is near 1 and for water it's 7. If  $Pr = 1.0$  then the thermal and momentum boundary layers have the same thickness. If it is less than 1.0 then the thermal boundary layer is thicker than the momentum boundary layer as in the case of air. Conversely, if  $Pr$  is greater than 1.0 then the momentum boundary layer is thicker.

### 1.6.2 Nusselt number

The Nusselt number  $Nu$  is the ratio of convective heat transfer across (normal) to conductive heat transfer. The conductive component is measured under the same condition as the heat convection but with a (hypothetically) stagnant fluid. The Nusselt number is defined as the ratio of these two measures of heat. Mathematically,

$$Nu = \frac{\text{convective heat transfer}}{\text{conductive heat transfer}} = \frac{hL}{k},$$

where,

- $L$  characteristic length ( $m$ ),
- $k$  thermal conductivity of the fluid ( $Wm^{-1}k^{-1}$ ),
- $h$  heat transfer coefficient ( $Wm^{-2}k^{-1}$ ).

If we consider the length to be the distance from the surface boundary to the local point, then it called local Nusselt number, and mathematically,

$$Nu_x = \frac{\text{convective heat transfer}}{\text{conductive heat transfer}} = \frac{h_x x}{k},$$



where,  $x$  is the local point of interest ( $m$ ).

If convective heat transfer and conductive heat transfer are the same magnitudes, so Nusselt number close to the unit is laminar flow and large Nusselt number corresponds to turbulent flow.

### 1.6.3 Bioconvection Péclet number

Bioconvection Péclet number is a dimensionless number which determines the relation between cell swimming speed to microorganisms diffusivity is,

$$Pe = \frac{\bar{b}W_c}{D_n},$$

where,

$\bar{b}$  chemotactic constant ( $m$ ),

$W_c$  maximum cell swimming speed ( $ms^{-1}$ ),

$D_n$  diffusivity of microorganisms ( $m^2 s^{-1}$ ).

Cell swimming speed maximizes the value of bioconvection Péclet number, on the other hand, microorganisms diffusivity lowered it. Here chemotactic constant indicates the tendency to flow of organism to a chemical stimulus.

### 1.6.4 Lewis number

Lewis number is defined as the ratio between thermal diffusivity to mass diffusivity,

$$Le = \frac{\alpha}{D_B},$$

where,

$\alpha$  effective thermal diffusivity ( $m^2 s^{-1}$ ),

$D_B$  Brownian diffusion coefficient ( $m^2 s^{-1}$ ).

It is named after the scientist Warren K. Lewis (1882–1975) who first use it. When Lewis number become 1 then thermal diffusivity and Brownian diffusion coefficient are identical and for higher thermal diffusivity compared to Brownian diffusion gives  $Pe > 1$  and  $Pe < 1$  for higher Brownian diffusion.

### 1.6.5 Bioconvection Lewis number

The dimensionless number called bioconvection Lewis number defined by the ratio of kinematic viscosity and diffusivity of microorganisms, mathematically,

$$Lb = \frac{\nu}{D_n},$$

where,

- $\nu$  kinematics viscosity ( $m^2 s^{-1}$ ),
- $D_n$  diffusivity of microorganisms ( $m^2 s^{-1}$ ).

Higher bioconvection Lewis number depends on a fluid with higher kinematic viscosity compared to microorganisms diffusion, conversely higher microorganisms diffusion dropped bioconvection Lewis number.

### 1.6.6 Magnetic number

Dimensionless parameter magnetic number depends on magnetic flux and electric conductivity of the fluid. It is directly proportional to these phenomena and inversely proportional to the density of the base fluid. Mathematically it is defined as,

$$M = \frac{\sigma B_0^2}{\rho a_0},$$

where,

- $\sigma$  electrical conductivity ( $(kg)^{-1}m^{-3}s^3A^2$ ),
- $B_0$  constant magnetic flux ( $(kg)s^{-2}A^{-1}$ ),
- $\rho$  the density of the base fluid ( $(kg) m^{-3}$ ),
- $a_0$  arbitrary constant ( $s^{-1}$ ).

Higher magnetic number interpret that fluid with properties that higher magnetic flux and higher electric conductivity, and higher density reduce the magnetic number.

### 1.6.7 Brownian motion parameter

Brownian motion named after Robert Brown (1773-1858), which random motion of fluid-particle within the fluid volume. It has a significant effect on fluid internal energy. Mathematically Brownian motion parameter defined as,

$$N_b = \frac{\tau D_B \Delta C}{\alpha},$$

where,

- $\tau$  ratio between the effective heat capacity of the nanoparticle material and heat capacity of the fluid (-),
- $D_B$  Brownian diffusion coefficient ( $m^2 s^{-1}$ ),
- $\alpha$  effective thermal diffusivity ( $m^2 s^{-1}$ ),
- $\Delta C$  difference between wall nanoparticle volume fraction and ambient nanoparticle volume fraction (-).

Brownian motion parameter mainly ratio between the Brownian diffusion coefficient and effective thermal diffusivity. Brownian diffusion rises Brownian motion parameter and higher thermal diffusivity reduced it.

### 1.6.8 Thermophoresis parameter

Thermophoresis is a physical phenomenon that different fluid particle shows a different response to the temperature gradient force within the fluid. It depends on the thermophoretic diffusion coefficient and thermal diffusivity. Symbolically,

$$N_t = \frac{\tau D_T \Delta T}{T_\infty \alpha},$$

where,

- $\tau$  ratio between the effective heat capacity of the nanoparticle material and heat capacity of the fluid (-),
- $D_T$  thermophoretic diffusion coefficient ( $m^2 s^{-1}$ ),
- $\Delta T$  difference between wall temperature  $T_w$  and ambient temperature  $T_\infty$  of the fluid ( $T$ ),
- $\alpha$  effective thermal diffusivity ( $m^2 s^{-1}$ ).

So, thermophoresis is directly proportional to the thermophoretic diffusion coefficient and inversely proportional to thermal diffusivity. In range 0.1 to 0.5 states that fluid with higher thermal diffusivity and lower thermophoretic diffusion. Although, temperature and  $\tau$  have also a significant effect on thermophoresis.

### 1.6.9 Skin friction

Skin friction is said to be a physical property of the fluid which resistant force due to viscosity and retards the motion of a flow. Skin friction depends on the Reynolds number, which is the ratio of inertial force and viscous force. When fluid past in contract with a wall it produces friction and obstruct the forward movement of fluid, this is known as skin friction, defined as,

$$C_f = \frac{\tau_w}{\frac{1}{2}\rho v^2},$$

where,

- $\tau_w$  skin shear stress on a surface ( $(kg) m^{-1}s^{-2}$ ),
- $\rho$  density of the fluid ( $(kg) m^{-3}$ ),
- $v$  free stream speed of fluid ( $m s^{-1}$ ).

### 1.6.10 Sherwood number

Sherwood number is a dimensionless physical number named after Thomas Kilgore Sherwood (1903 –1976) and well used in mass transfer calculation. It calculated by the ratio between convective mass transfer and the rate of diffusive mass transport. Defined as

$$Sh = \frac{h}{D/L},$$

where,

$h$  convective mass transfer rate( $ms^{-1}$ ),

$L$  characteristic length ( $m$ ),

$D$  mass diffusivity ( $m^2 s^{-1}$ ).

With the increase of mass diffusion, Sherwood number becomes smaller and greater Sherwood number depend on higher convective mass transfer rate.

### 1.6.11 Density number of motile microorganisms

Density number of motile microorganisms is a dimensionless parameter and the ratio between convective microorganisms transfer and the rate of diffusive microorganisms transport.

$$Nn = \frac{h_n}{D_n/L},$$

where,

$h_n$  convective microorganisms transfer rate( $ms^{-1}$ ),

$L$  characteristic length ( $m$ ),

$D_n$  microorganisms diffusivity ( $m^2 s^{-1}$ ).

So,  $Nn$  can be inversely proportional to microorganisms diffusivity and density number lowered due to higher microorganisms diffusivity. On the other hand, convective microorganisms transfer increases the density number of motile microorganisms.

## CHAPTER 2: MATHEMATICAL FORMULATION

---

### 2.1 Basic equations

The steady two-dimensional gyrotactic bioconvection boundary layer flow of Newtonian water-based nanofluid over a wedge was considered. The flow model with the appropriate coordinate system can be seen from Fig. 2.1. In the energy equation, viscous dissipation was neglected, and thermal stratification and thermal dispersion were also neglected. The nanoparticle suspension was assumed to be stable. It was also assumed that the presence of nanoparticles had no effect on the direction of microorganism's swimming, so microorganism's swimming was independent and their swimming velocity also independent. It was prescribed that the surface temperature, nanoparticle volume fraction and density of motile microorganisms were  $T_w, C_w$  and  $N_w$ , while the ambient values were denoted as  $T_\infty, C_\infty$  and  $N_\infty$  respectively.

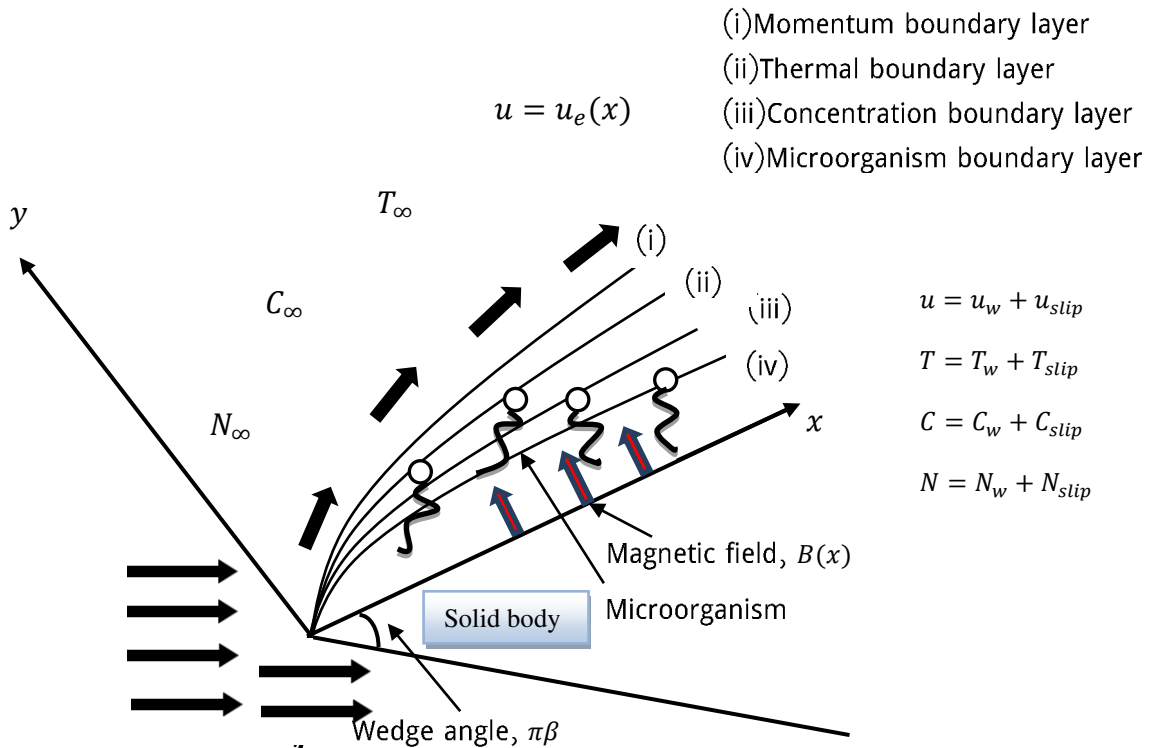


**Fig. 2.1:** Physical model of the forced convective flow of bio-nanofluid along a wedge.

Under the above assumptions, the governing equations in vector form were (Uddin et. al. [60]).

$$\text{Continuity equation: } \nabla \cdot \vec{V} = 0, \quad (2.1.1)$$

$$\text{Momentum equation: } \rho(\vec{V} \cdot \nabla) \vec{V} = -\nabla p + \mu \nabla^2 \vec{V} + \sigma(\vec{V} \times \vec{B}) \times \vec{B}, \quad (2.1.2)$$

$$\text{Energy equation: } (\vec{V} \cdot \nabla) T = \alpha \nabla^2 T + \tau \left[ D_B \nabla C \cdot \nabla T + \left( \frac{D_T}{T_\infty} \right) \nabla T \cdot \nabla T \right], \quad (2.1.3)$$

$$\text{Volume fraction equation : } (\vec{V} \cdot \nabla) C = D_B \nabla^2 C + \left( \frac{D_T}{T_\infty} \right) \nabla^2 T, \quad (2.1.4)$$

$$\text{Microorganism equation: } \nabla \cdot (N \vec{V} + N \vec{\tilde{V}} - D_n \nabla N) = 0. \quad (2.1.5)$$

Here,  $\vec{V} = (u, v, 0) = u \hat{x} + v \hat{y}$  denotes flow velocity,  $\nabla = \frac{\partial}{\partial x} \hat{x} + \frac{\partial}{\partial y} \hat{y}$  denotes vector differential operator,  $\vec{B}$  denotes the magnetic field. The magnetic field  $\vec{B}$  was applied perpendicular to the flow,  $\therefore \vec{B} = (0, B(x), 0)$ .  $u, v$  denote the velocity components along the  $x$ - and  $y$ -axes,  $T$  denotes the temperature,  $C$  denotes the concentration,  $N$  denotes the microorganisms,  $\nu$  denotes the kinematic viscosity,  $\rho$  denotes the density of the base fluid,  $D_B$  denotes the Brownian diffusion coefficient,  $D_T$  denotes the thermophoretic diffusion coefficient,  $D_n$  denotes the diffusivity of microorganisms,  $\tau$  denotes the ratio between the effective heat capacity of the nanoparticle material and heat capacity of the fluid,  $\alpha$  denotes the thermal diffusivity of the fluid,  $\mu$  denotes the dynamic viscosity,  $\sigma$  denotes the electric conductivity, and  $\vec{\tilde{V}} = \frac{bW_c}{\Delta C} \nabla C$  denotes the microorganism's swimming velocity.

The following governing equations were transformed to dimensional form given below (see appendix one, 6.1).

$$\frac{\partial u}{\partial x} + \frac{\partial v}{\partial y} = 0, \quad (2.1.6)$$

$$u \frac{\partial u}{\partial x} + v \frac{\partial u}{\partial y} = Ku_e \frac{du_e}{dx} + \nu \frac{\partial^2 u}{\partial y^2} - (u - Ku_e) \frac{\sigma B^2(x)}{\rho}, \quad (2.1.7)$$

$$u \frac{\partial T}{\partial x} + v \frac{\partial T}{\partial y} = \alpha \frac{\partial^2 T}{\partial y^2} + \tau \left[ D_B \frac{\partial C}{\partial y} \frac{\partial T}{\partial y} + \left( \frac{D_T}{T_\infty} \right) \left( \frac{\partial T}{\partial y} \right)^2 \right], \quad (2.1.8)$$

$$u \frac{\partial C}{\partial x} + v \frac{\partial C}{\partial y} = D_B \frac{\partial^2 C}{\partial y^2} + \left( \frac{D_T}{T_\infty} \right) \frac{\partial^2 T}{\partial y^2}, \quad (2.1.9)$$

$$u \frac{\partial N}{\partial x} + v \frac{\partial N}{\partial y} + \frac{\partial}{\partial y} (N \tilde{v}) = D_n \frac{\partial^2 N}{\partial y^2}. \quad (2.1.10)$$

Subject to the boundary conditions (Uddin et. al. [60]),

$$\begin{aligned} u &= N_1(x) \nu \frac{\partial u}{\partial y}, \quad v = -\frac{D_B}{1-C_w} \frac{\partial C}{\partial y}, \quad T = T_w + D_1(x) \frac{\partial T}{\partial y}, \\ C &= C_w + E_1(x) \frac{\partial C}{\partial y}, \quad N = N_w + F_1(x) \frac{\partial N}{\partial y} \quad \text{at } y = 0. \end{aligned} \quad (2.1.11)$$

$$u = Ku_e(x) = Ka_0x^m, T = T_\infty, C = C_\infty, N = N_\infty = 0 \text{ as } y \rightarrow \infty. \quad (2.1.12)$$

Here,  $u_e$  denotes the ambient velocity,  $T_\infty$  denotes the ambient temperature,  $C_\infty$  denotes the ambient concentration,  $N_\infty$  denotes the ambient microorganisms,  $T_w$  denotes the wall temperature,  $C_w$  means the wall concentration,  $N_w$  denotes the wall microorganisms,  $N_1$ ,  $D_1$ ,  $E_1$ , and  $F_1$  denote the variable velocity slip factor, thermal slip factor, mass slip factor, and microorganism slip factor respectively,  $\tilde{v}$  denotes the microorganism's swimming velocity component, and  $K, m$  and  $a_0$  are constants.

By substituting these following similarity variables (Uddin et. al. [60]),

$$\begin{aligned} \psi &= \sqrt{u_e(x)vx} f(\eta), \quad \eta = \sqrt{\frac{u_e(x)}{vx}} y, \quad \theta(\eta) = \frac{T-T_\infty}{\Delta T}, \quad \phi(\eta) = \frac{C-C_\infty}{\Delta C}, \quad \chi(\eta) = \frac{N-N_\infty}{\Delta N}, \quad u = \\ &u_e(x) f'(\eta), \quad v = -\frac{m+1}{2} \sqrt{\frac{u_e(x)v}{x}} \left[ f(\eta) + \frac{m-1}{m+1} \eta f'(\eta) \right], \quad \tilde{v} = \left( \frac{\bar{b}W_c}{\Delta C} \right) \frac{\partial C}{\partial y}, \quad \Delta T = T_w - T_\infty, \\ &\Delta C = C_w - C_\infty, \quad \Delta N = N_w - N_\infty, \end{aligned}$$

into equations (2.1.7)-(2.1.12), the following ordinary differential equations were found.

Here,  $\psi$  is the stream function defined as  $u = \frac{\partial \psi}{\partial y}$  and  $v = -\frac{\partial \psi}{\partial x}$ ,  $\Delta T$  is the characteristic temperature,  $\Delta C$  is the characteristic concentration,  $\Delta N$  is the characteristic density motile microorganisms (see appendix two, 6.2).

$$f''' + mK^2 - mf'^2 + \left(\frac{m+1}{2}\right)ff'' - M(f' - K) = 0, \quad (2.1.13)$$

$$\theta'' + Pr \left(\frac{m+1}{2}\right) f\theta' + Nb\phi'\theta' + Nt\theta'^2 = 0, \quad (2.1.14)$$

$$\phi'' + \left(\frac{m+1}{2}\right) LePrf\phi' + \frac{Nt}{Nb}\theta'' = 0, \quad (2.1.15)$$

$$\chi'' + \left(\frac{m+1}{2}\right) Lbf\chi' - Pe[\phi'\chi' + \chi\phi''] = 0. \quad (2.1.16)$$

Subject to the boundary conditions,

$$\begin{aligned} f(0) &= \frac{2S}{(m+1)PrLe} \phi'(0), \quad f'(0) = af''(0), \quad \theta(0) = 1 + b\theta'(0), \quad \phi(0) = \\ &1 + d\phi'(0), \quad \chi(0) = 1 + e\chi'(0), \quad f'(\infty) = K, \quad \theta(\infty) = \phi(\infty) = \chi(\infty) = 0. \end{aligned} \quad (2.1.17)$$

Here the prime denotes differentiation with respect to  $\eta$ .

$$\text{Here, } a = (N_1)_0 \sqrt{va_0}, \quad (N_1)_0 = N_1(x)x^{\frac{m-1}{2}}, \quad b = (D_1)_0 \sqrt{\frac{a_0}{v}}, \quad (D_1)_0 = D_1(x)x^{\frac{m-1}{2}},$$

$$d = (E_1)_0 \sqrt{\frac{a_0}{v}}, \quad (E_1)_0 = E_1(x)x^{\frac{m-1}{2}}, \quad e = (F_1)_0 \sqrt{\frac{a_0}{v}}, \quad \text{and } (F_1)_0 = F_1(x)x^{\frac{m-1}{2}}.$$

The dimensionless parameters were appeared in the equations (2.1.13)-(2.1.17),

$$\text{Magnetic number } M = \frac{\sigma B_0^2}{\rho a_0},$$

$$\text{Prandtl number } Pr = \frac{\nu}{\alpha},$$

$$\text{Brownian motion parameter } Nb = \frac{\tau D_B \Delta C}{\alpha},$$

$$\text{Thermophoresis parameter } Nt = \frac{\tau D_T \Delta T}{T_\infty \alpha},$$

$$\text{Bioconvection Lewis number } Lb = \frac{\nu}{D_n},$$

$$\text{Lewis number } Le = \frac{\alpha}{D_B},$$

$$\text{and Bioconvection Péclet number } Pe = \frac{\bar{b} W_c}{D_n}.$$

## 2.2 Physical quantities

The main physical quantities of this study were the skin friction  $C_{fx}$ , the local Nusselt number  $Nu_x$ , the local Sherwood number  $Sh_x$ , and the local density number of the motile microorganisms  $Nn_x$  were defined as

$$C_{fx} = \frac{\nu}{u_e^2(x)} \left( \frac{\partial u}{\partial y} \right)_{y=0} = \left( \sqrt{\frac{\nu}{xu_e(x)}} f''(\eta) \right)_{y=0}, \quad (2.2.1)$$

$$Nu_x = -\frac{x}{\Delta T} \left( \frac{\partial T}{\partial y} \right)_{y=0} = -\left( \sqrt{\frac{xu_e(x)}{\nu}} \theta'(\eta) \right)_{y=0}, \quad (2.2.2)$$

$$Sh_x = -\frac{x}{\Delta C} \left( \frac{\partial C}{\partial y} \right)_{y=0} = -\left( \sqrt{\frac{xu_e(x)}{\nu}} \phi'(\eta) \right)_{y=0}, \quad (2.2.3)$$

$$Nn_x = -\frac{x}{\Delta N} \left( \frac{\partial N}{\partial y} \right)_{y=0} = -\left( \sqrt{\frac{xu_e(x)}{\nu}} \chi'(\eta) \right)_{y=0}. \quad (2.2.4)$$

By substituting the similarity variables into (2.2.1)-(2.2.4), (see appendix three, 6.3)

$$C_{fx} Re_x^{\frac{1}{2}} = f''(0), \quad Nu_x Re_x^{-\frac{1}{2}} = -\theta'(0), \quad (2.2.5)$$

$$Sh_x Re_x^{-\frac{1}{2}} = -\phi'(0), \quad Nn_x Re_x^{-\frac{1}{2}} = -\chi'(0),$$

$$\text{where, } Re_x = \frac{xu_e(x)}{\nu}.$$



### 2.3 Numerical methods and validation

In this dissertation, a well-known built-in command `NDSolve` in Mathematica was used to find the numerical solutions and plotted to corresponding profiles. `NDSolve` has solved the system of ordinary differential equations with the boundary conditions and produced numerical values and figures of the dimensionless velocity, temperature, concentrations, and the motile microorganism profiles with the help of internal method using finite element methods. This method was very useful and explained by many researchers (Fang and Jing [36]). But new technique added here, with the help of version Mathematica 11, it can use very well established finite element method as an internal solution processing method. To use this, it required to download the package `Needs["NDSolve`FEM`"]` and add this option as `NDSolve[....., Method -> {"FiniteElement"}]`. The converging procedure of this method was also satisfactory and obtain the accuracy with seven orders of local accuracy of convergence. The most important thing is, it can improve the accuracy of the solution with the option as an example `Evaluate[Abs[f'[a - 1] - f'[a]]/.solution], a}], {a, 1, 30, 1}]`, from where it can decide the best accuracy of solution for boundary condition at infinity as a value of infinity which behaves like tends to infinity.

For the code verification, the present study was compared with the existing paper of Fang and Jing [36].  $M = Nt = Nb = Pe = K = Lb = b = d = e = 0$ . Also  $f'(0) = a = m = 1, Pr = 5$  with various case  $Le = 2$ , and  $0.4$ .  $S = 4, 40, 8$ , and  $20$  to adjust the values of the series at the referred paper as  $Pr = 5, \gamma = 4$ , and  $Sc = 1, 2, 5$ , and  $10$  were considered. Here, the corresponding values and comparing table were showed in Fang and Jing [36]. More importantly, the values of comparing table perfectly matched with published results investigated by Fang and Jing [36].

Table 5. of Fang and Jing [36] were considered  $Pr = 5$  and Stefan blowing parameter  $\gamma = 4$  as fixed and values of  $Sc$  varies. For comparing these values,  $Pr = 5$  was fixed and varied the values of  $Le$  and  $S$ . Since  $Sc = Le * Pr$  and how first boundary condition relates Fang and Jing [36] blowing parameter  $\gamma$  to Stefan blowing parameter  $S$ . The values of corresponding physical parameters from the present study were perfectly matched with analytical solutions and here boundary conditions at infinity were converged at  $\eta \rightarrow 25$ .

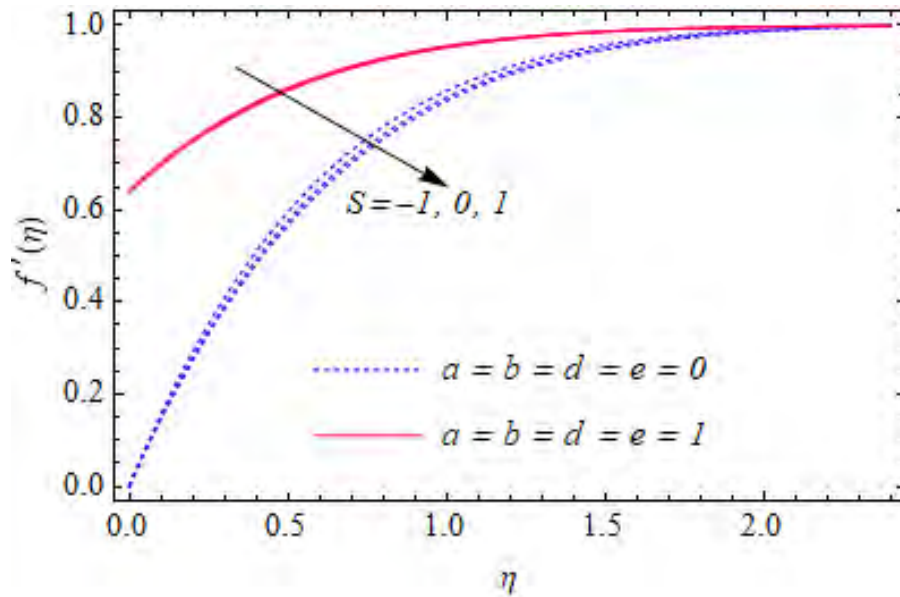
**Table 1:** Comparison of analytical solutions (Fang and Jing [36]) and numerical solutions (present study) of surface concentration gradient  $-\phi'(0)$  and surface temperature gradient  $-\theta'(0)$ .

Fang and Jing [36] $Pr = 5,$ $\gamma = 4.$	Present study $Pr = 5$ (numerical)	Fang and Jing [36] $-\phi'(0)$ (analytical)	Present study $-\phi'(0)$	Fang and Jing [36] $-\theta'(0)$ (analytical)	Present study $-\theta'(0)$
$Sc = 1$	$Le = 0.2, S = 4$	0.194923	0.194923	0.0915398	0.0915398
$Sc = 2$	$Le = 0.4, S = 8$	0.192341	0.192341	0.0972581	0.097258
$Sc = 5$	$Le = 1, S = 20$	0.167467	0.167467	0.167467	0.167467
$Sc = 10$	$Le = 2, S = 40$	0.142111	0.142111	0.271687	0.271687

## CHAPTER 3: RESULTS AND DISCUSSIONS

Generally, the variations of the dimensionless velocity profiles, temperature profiles, concentration profiles, and the microorganism profiles under the different values of slip parameters, and Stefan blowing parameter were considered. To plot the behavior patterns of these profiles  $a = b = d = e = M = m = Pe = K = 1, Pr = 6.8, Nb = 0.1, Nt = 0.1, Le = 2$ , and  $Lb = 2$  were considered as default values. Now, the results and profiles due to the variation of different parameters are described below.

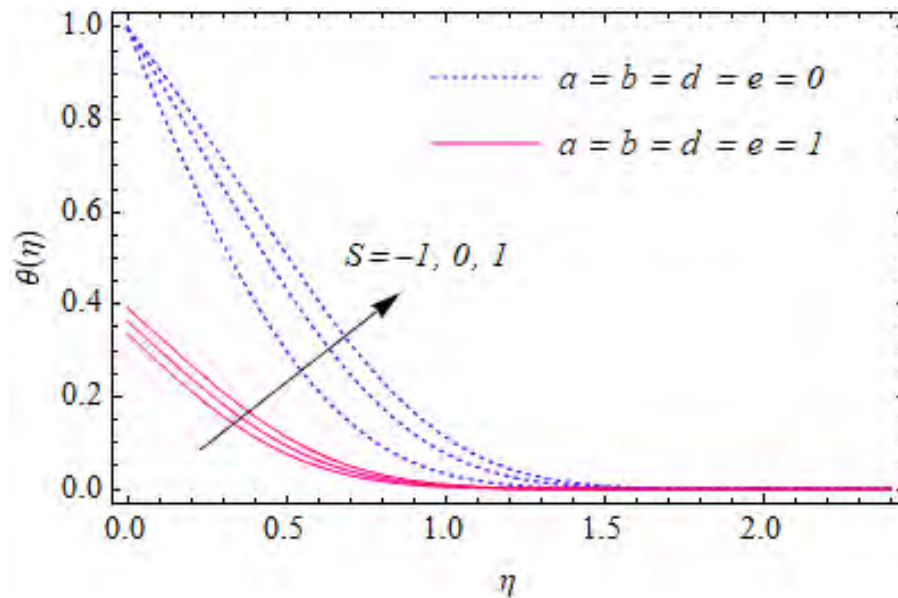
### 3.1 Effects of slip and no-slip boundary conditions



**Fig. 3.1(a):** Variation of  $f'(\eta)$  with different values of  $S$  in the presence and absence of slip boundary conditions.

Fig. 3.1(a) indicates the effects of the Stefan blowing on the velocity profiles with slip and no-slip boundary conditions as a function of similarity variable. Here, the dotted lines and solid lines stand for no-slip and slip boundary conditions respectively. Interestingly the velocity profiles with slip boundary conditions were provided similar results at different Stefan blowing effects, while the velocity profiles for no-slip boundary condition were decreased with the increasing of blowing parameter. For the case of slip boundary conditions, velocity profiles were reached a self-similarity state. These results were illustrated that when the slip condition applied to the velocity field there was a negligible effect of  $S$ , whether blowing occurs to the wall. At  $\eta = 0$ , the values of the dimensionless velocity profiles were

found about 0.6 for the slip boundary condition whereas velocity profiles were zero for the case of no-slip boundary condition. Furthermore, for  $\eta \geq 2$ , the velocity profiles were collapsed for both with and without slip boundary conditions.



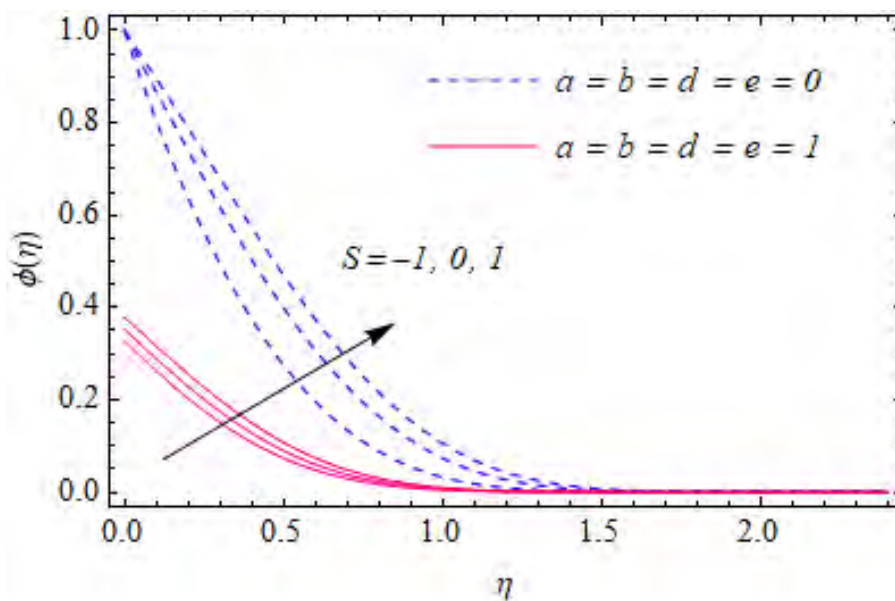
**Fig. 3.1(b):** Variation of  $\theta(\eta)$  with different values of  $S$  in the presence and absence of slip boundary conditions.

Fig. 3.1(b) describes the dimensionless temperature profiles under different values of the Stefan blowing parameter, considered with slip and without slip boundary conditions. Here, temperature profiles were lifted upward as increasing of the value of Stefan blowing parameter. For the case of both slip and no-slip boundary conditions, temperature profiles were showed significant effects of Stefan blowing. At  $\eta = 0$ , the values of the dimensionless temperature profiles were found near about 0.4 for the slip boundary conditions, whether for no-slip boundary conditions those values were nearly 1 as defined in boundary conditions.

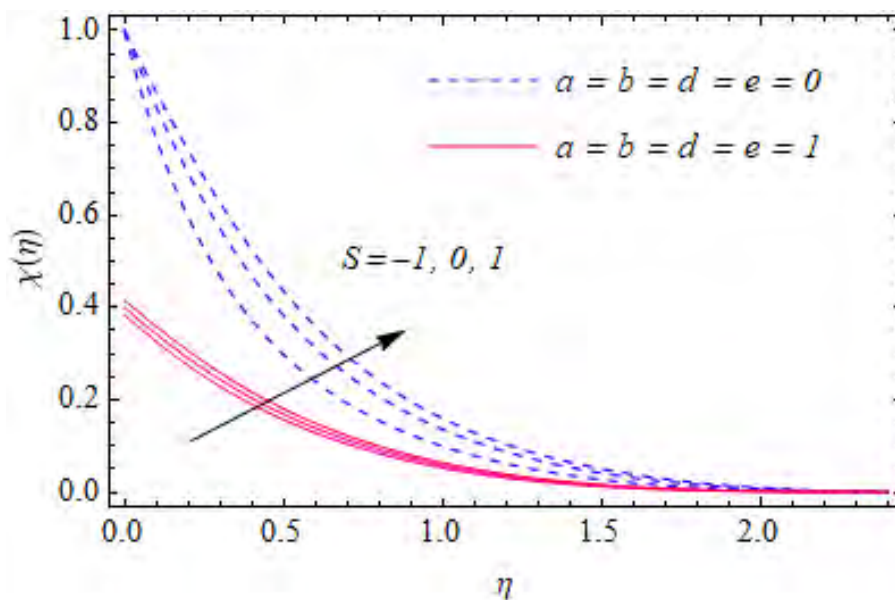
Fig. 3.1(c) illustrates the variation of the dimensionless concentration profiles with the change of Stefan blowing for both slip and no-slip boundary conditions. The concentration profiles were quite similar to previously described temperature profiles under similar conditions. Boundary layer thickness got thicker and caused a strong elevation with the increasing of blowing parameter. It is also noticeable that these profiles were well converged most rapidly for slip boundary conditions in comparison with no-slip boundary conditions.

Fig. 3.1(d) presents the response of the dimensionless motile microorganism profiles due to the Stefan blowing under with slip and without slip boundary conditions. Microorganism profiles were boosted with strong blowing from the wall and produced maximum profiles and

consequently, strong blowing from the ambient to the wall was decreased the microorganism profiles. Also, a variety of profiles were more noticeable at no-slip conditions whereas profiles were elevated slowly as slip condition presents. In addition, the microorganism profiles were converged slowly compared to the concentration and the temperature profiles.



**Fig. 3.1(c):** Variation of  $\phi(\eta)$  with different values of  $S$  in the presence and absence of slip boundary conditions.



**Fig. 3.1(d):** Variation of  $\chi(\eta)$  with different values of  $S$  in the presence and absence of slip boundary conditions.

### 3.2 Effects of velocity slip boundary condition

Fig. 3.2(a) shows the effects of the Stefan blowing parameter on the dimensionless velocity profiles for with and without velocity slip boundary conditions. Here the effects of Stefan blowing on the velocity profiles under with and without velocity slip were provided almost single line i.e., there was very small depletion in the velocity profiles. A similar result also observed in figure 3.1(a) except for no-slip boundary conditions. So, it can conclude that strong blowing at the wall did not affect the velocity profiles.

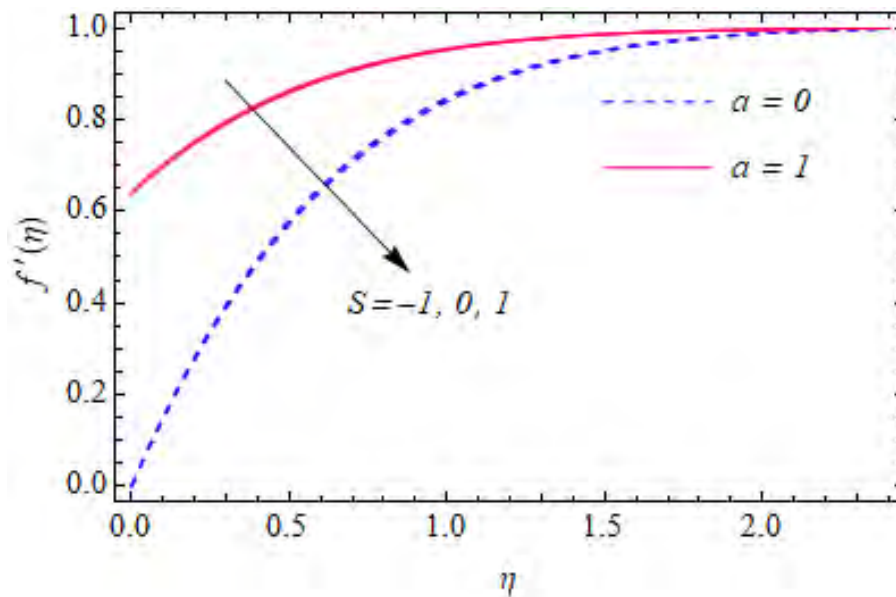


**Fig. 3.2(a):** Variation of  $f'(\eta)$  for different values of  $S$  and  $a$ .

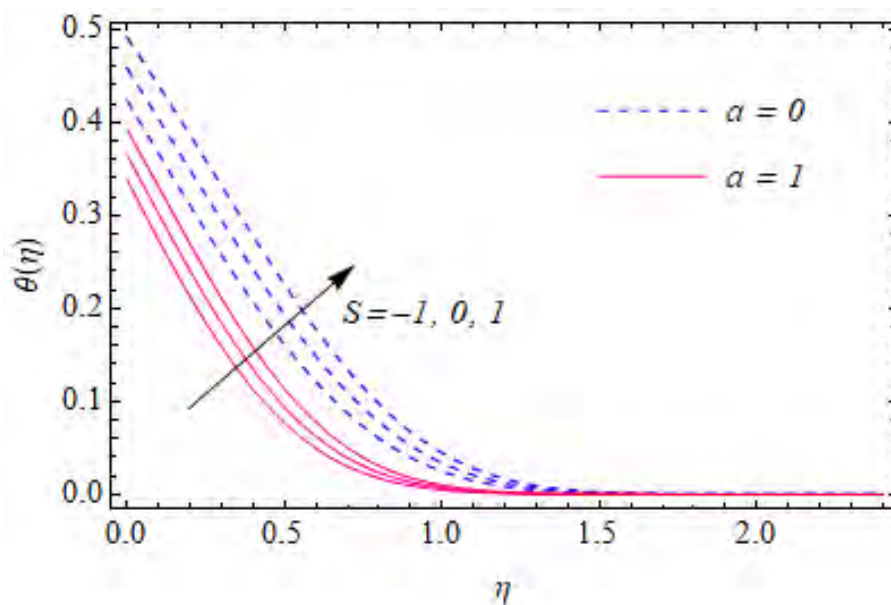


**Fig. 3.2(b):** Variation of  $\theta(\eta)$  for different values of  $S$  and  $a$ .

Fig 3.2(b) establishes the effects of Stefan blowing parameter with both conditions of with velocity slip and without velocity slip boundary conditions. The increasing trend of the temperature profiles as increasing of the Stefan blowing parameter was found. For the initial value of  $\eta$ , values of the temperature profiles given about 0.5 for the case of no-slip velocity boundary condition while the values of these parameters were nearly 0.4 for the slip velocity boundary condition. So, increasing the velocity slip factor were induced a reduction of the temperature profiles for both solid wedge and permeable wedge.

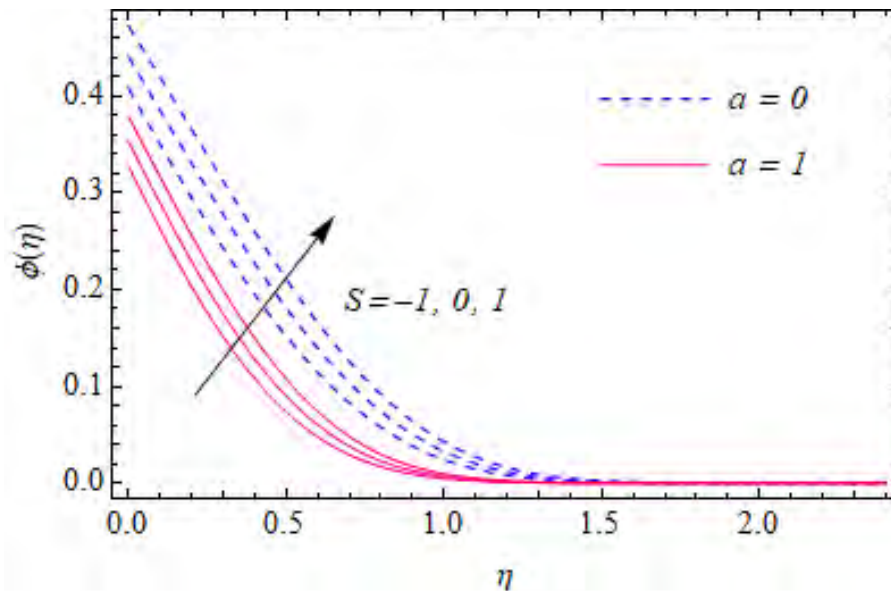


**Fig. 3.2(c):** Variation of  $\phi(\eta)$  for different values of  $S$  and  $a$ .

Fig. 3.2(c) determines the concentration profiles under the variation of the Stefan blowing parameter with the presence of velocity slip and without velocity slip. The values of the concentration profiles were decreased as decreasing of blowing parameters. Blowing from the wall were enhanced the profiles and trend became maximum with the case that absence of velocity slip factor whereas the trend was reversed for blowing to the wall and produced minimum concentration profiles with the presence of velocity slip.

Fig. 3.2(d) represents the effects of the Stefan blowing parameter on the motile microorganism profiles with the presence of velocity slip and without velocity slip factor. The blowing parameter was enhanced the microorganism profiles and produced thicker microorganism boundary layer. Profiles became minimum for blowing to the wall with the presence of velocity slip and contrarily became maximum for blowing from the wall when slip factor becomes zero. It is also noticeable that the microorganism profiles were decreased significantly in the presence of the velocity slip factor. Furthermore, microorganism and



velocity profiles were not rapidly converging in comparison with the temperature and concentration profiles.

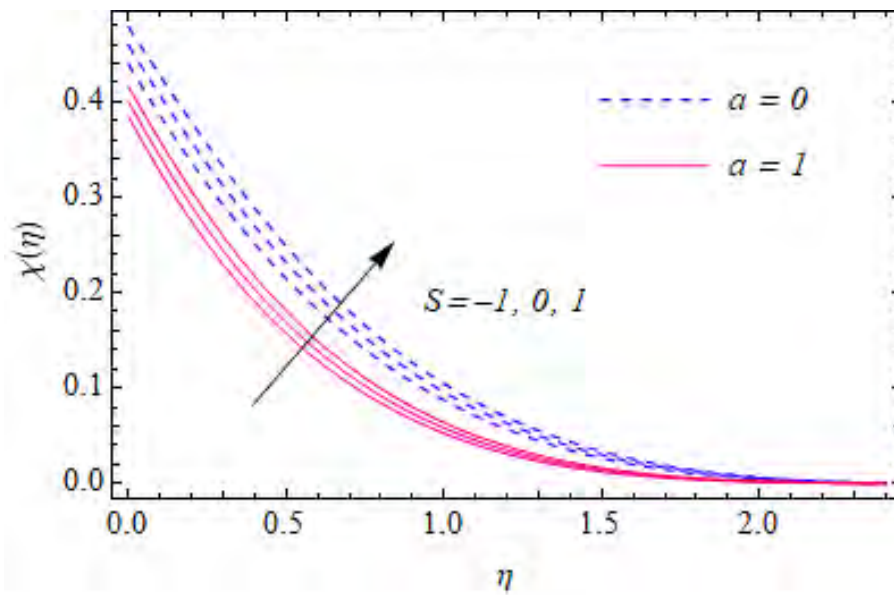


Fig. 3.2(d): Variation of  $\chi(\eta)$  for different values of  $S$  and  $a$ .

### 3.3 Effects of temperature slip boundary condition

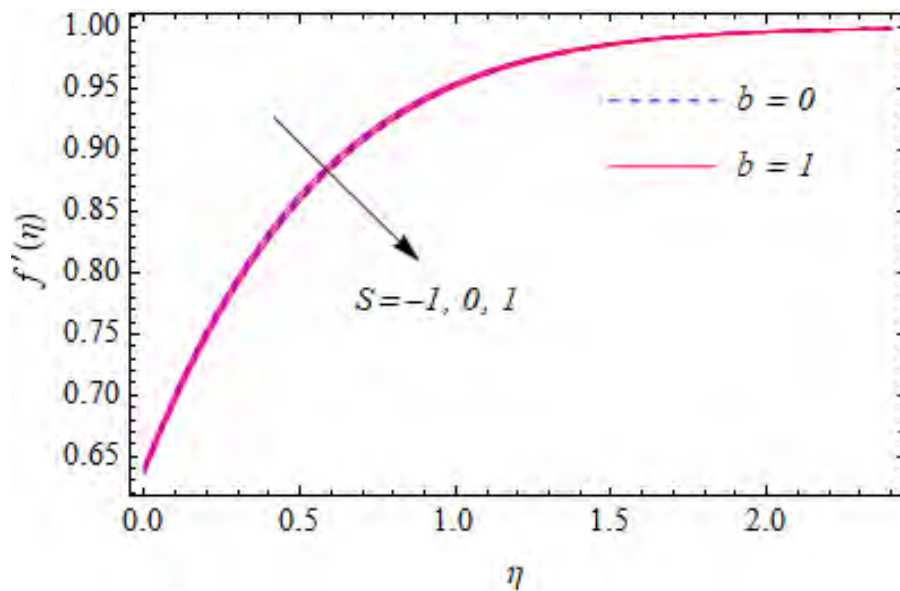
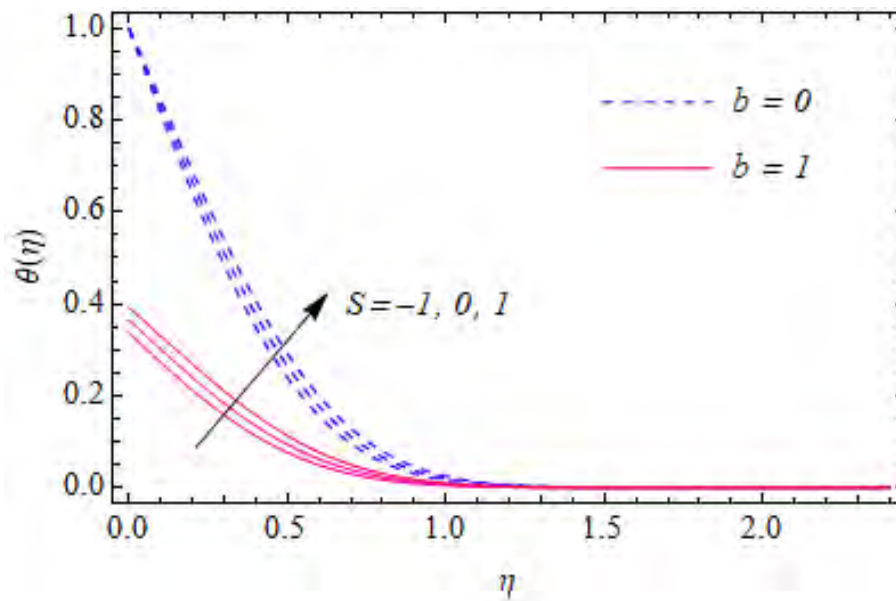


Fig. 3.3(a): Variation of  $f'(\eta)$  for different values of  $S$  and  $b$ .

Fig. 3.3(a) describes the Stefan blowing effects along with temperature slip and no-slip boundary conditions. It was observed that, for the Stefan blowing, the velocity profiles were almost collapsed for the variation of temperature slip boundary condition. So, the velocity remains unaffected with strong blowing at the wall. The profiles were very slowly decreased



with the increasing of blowing parameter. Effects of the temperature slip also ignorable for the velocity profiles.



**Fig. 3.3(b):** Variation of  $\theta(\eta)$  for different values of  $S$  and  $b$ .

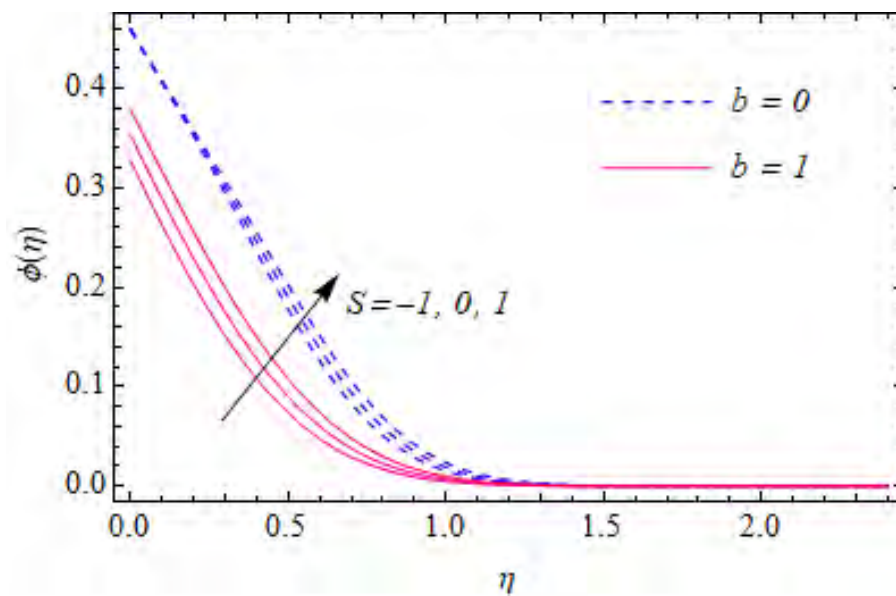


**Fig. 3.3(c):** Variation of  $\phi(\eta)$  for different values of  $S$  and  $b$ .

Fig. 3.3(b) reveals the temperature profiles with the variation of the Stefan blowing and temperature boundary slip condition in the presence of velocity, concentration, and microorganism slip condition. Due to negative values of the blowing, the temperature profiles became minimum whereas upward increasing phenomena were noticed for the temperature profiles as a strong blowing from the wall. Furthermore, in the presence of

temperature slip boundary condition the temperature profiles were retarded and produced thinner boundary layer thickness compared to the condition of no temperature slip at the wall.

Fig. 3.3(c) shows the effects of the Stefan blowing parameter on the concentration profiles, where, with and without temperature slip boundary conditions were considered. The more interesting thing was, in the case of no-slip temperature boundary condition, the starting value of the concentration profiles were not varying as different values of blowing parameter, despite that for in presence of concentration slip. However, increasing in blowing parameter were implied increasing behavior of the concentration profiles. Additionally, temperature slip factor was strongly reduced the concentration profiles.

Fig. 3.3(d) determines the dimensionless motile microorganism profiles under the variation of the Stefan blowing parameter with temperature slip and no temperature slip conditions. The microorganism profiles were poorly elevated with the increase of the blowing parameter. However, temperature slip factor was induced a slight reduction on microorganism profiles.

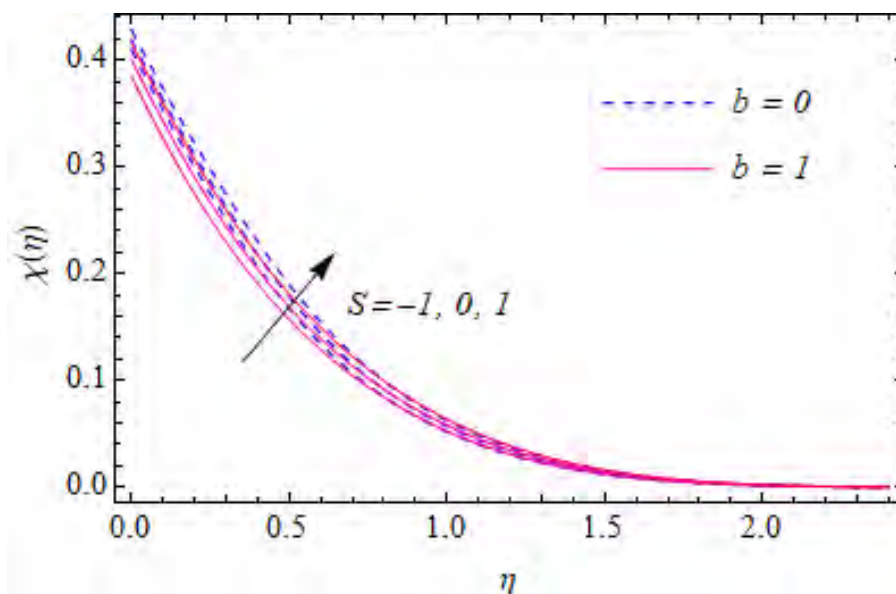
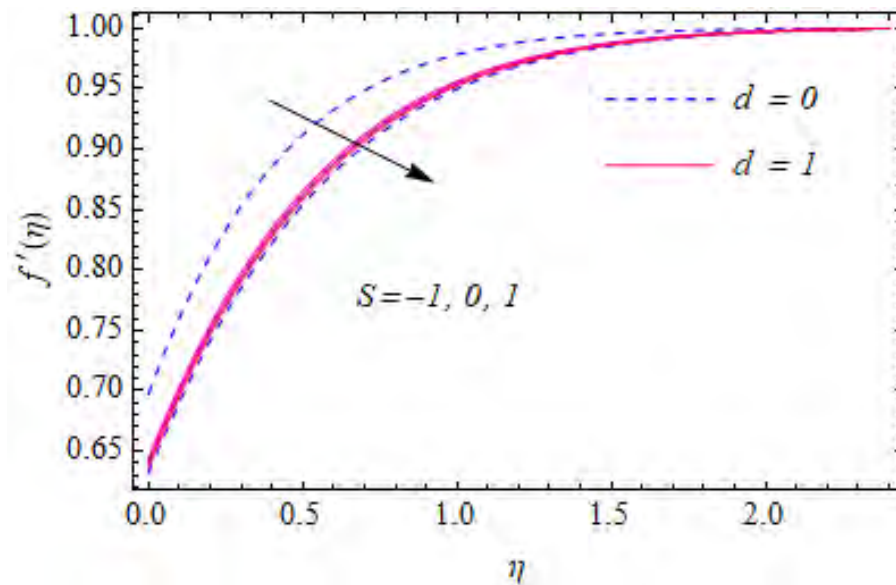


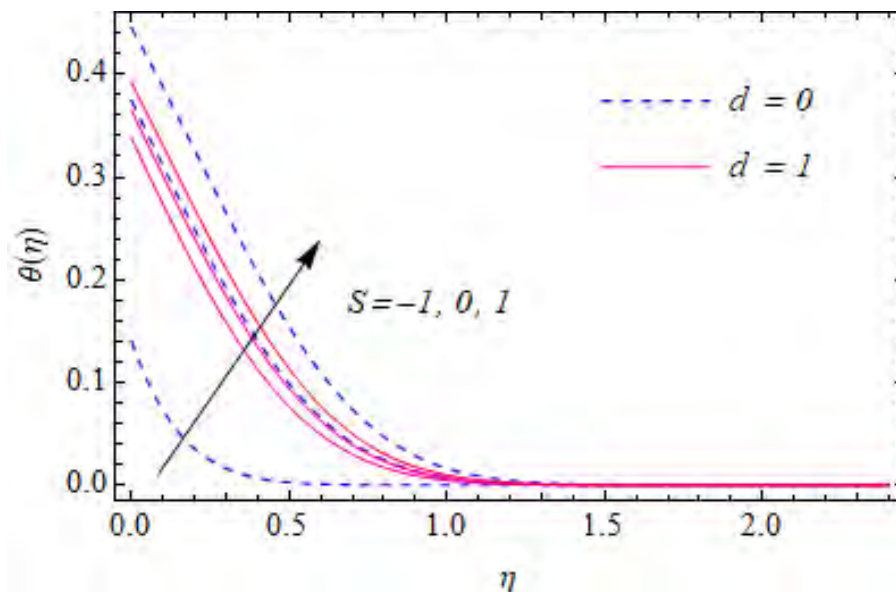
Fig. 3.3(d): Variation of  $\chi(\eta)$  for different values of  $S$  and  $b$ .

### 3.4 Effects of mass slip boundary condition

Fig. 3.4(a) displays the effects of the concentration slip and the Stefan blowing parameter on the dimensionless velocity distributions. Effect of the Stefan blowing parameter was showed a very slight reduction in velocity for both cases. The variation of concentration slip was showed a little change in the dimensionless velocity profiles for mass blowing in both direction and solid wedge.



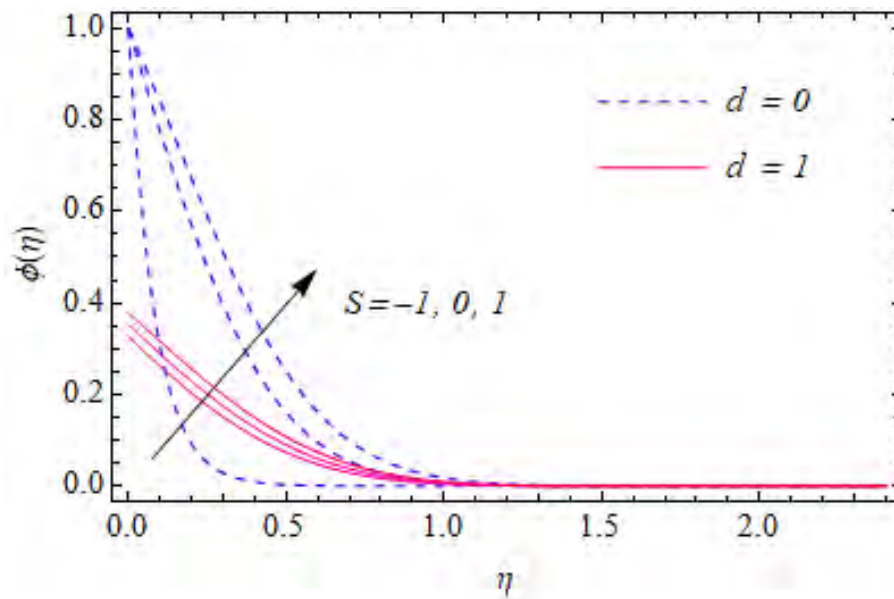
**Fig. 3.4(a):** Variation of  $f'(\eta)$  for different values of  $S$  and  $d$ .



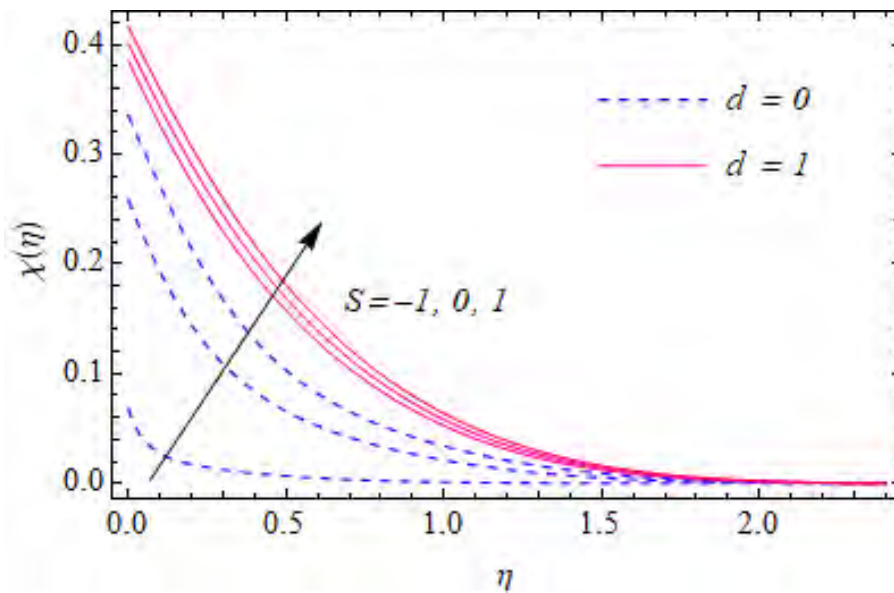
**Fig. 3.4(b):** Variation of  $\theta(\eta)$  for different values of  $S$  and  $d$ .

Fig. 3.4(b) portrays the effects of the Stefan blowing and concentration slip on the temperature profiles. For temperature distributions, variations were presented strong contrary effects from the previous figure, with an elevation of blowing parameter, especially when concentration slip was zero. In the presence of concentration slip wall, the temperature profiles were increased slowly with the increase of mass flux parameter but those were boosted in the absence of mass slip parameter. So, blowing to the wall was enhanced temperature while blowing from the wall lessened it. However, the temperature profiles were minimized for strong blowing to the wall and maximized for strong blowing from the wall

and both opposite cases were performed when the concentration slip was zero. Another noticeable situation to declare that it converged very rapidly, nearby after  $\eta = 1.1$  for both cases.



**Fig. 3.4(c):** Variation of  $\phi(\eta)$  for different values of  $S$  and  $d$ .



**Fig. 3.4(d):** Variation of  $\chi(\eta)$  for different values of  $S$  and  $d$ .

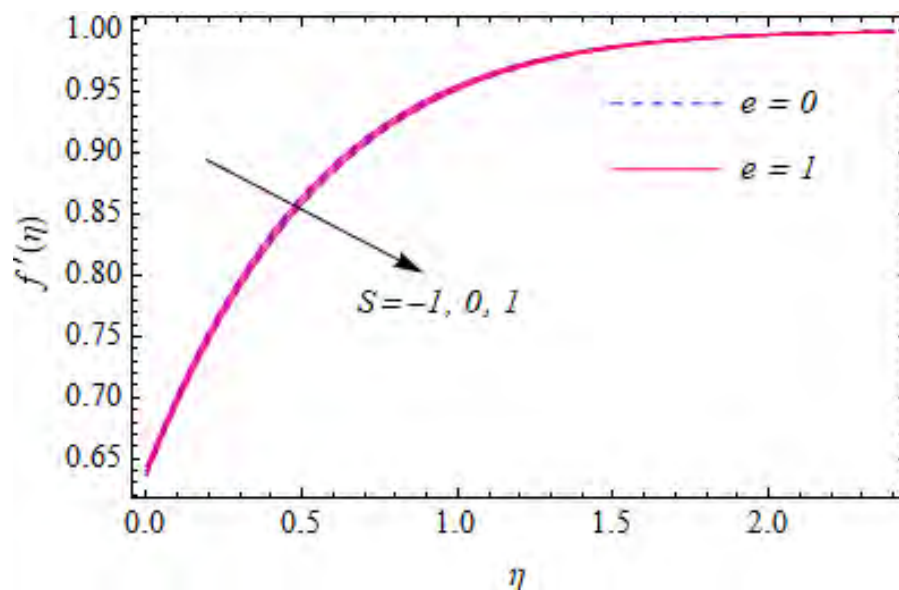
Fig. 3.4(c) presents the Stefan blowing effects on the nanoparticle concentration profiles for different values of mass slip parameter. In the existence of mass slip, concentration function significantly elevated whereas it strongly elevated for the no-slip condition with the growth of Stefan blowing parameter. Changes of concentration profiles were more noticeable for the absence of concentration slip, particularly for negative blowing, those were fallen suddenly

near the wall and profiles have represented the minimum values of the concentration parameter whereas concentration profiles were maximum for blowing from the wall.

Fig. 3.4(d) presents the distribution of the motile microorganisms density number for variation of the Stefan blowing and concentration slip parameter. In the presence of the concentration slip, the microorganism profiles were maximized for both directions of blowing as well as for solid wall although profiles were minimized for the absence of slip factor. Increasing of microorganism slip parameter caused a strong raising of microorganism profiles and trends were more remarkable for zero concentration slip. The microorganism profiles were strongly fallen near the wall when blowing performed ambient to wall whereas contrary effects achieved for solid wall and for blowing performed wall to ambient.

### 3.5 Effects of microorganism slip boundary condition

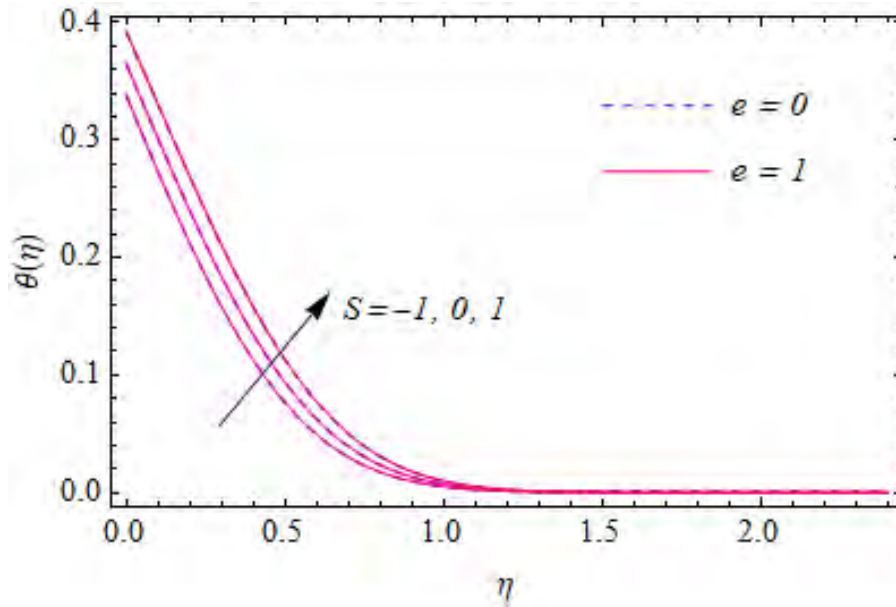
Fig. 3.5(a) determines the effects of the microorganism slip and the Stefan blowing parameter on the dimensionless velocity profiles. For the strong blowing and solid wall, velocity differed very slowly. The dimensionless velocity profiles behave stable situation according to the change of microorganism slip. It can be revealed due to weak coupling between microorganisms species number density equation and momentum equation, the consequence of both parameters was not effective for the velocity domination.



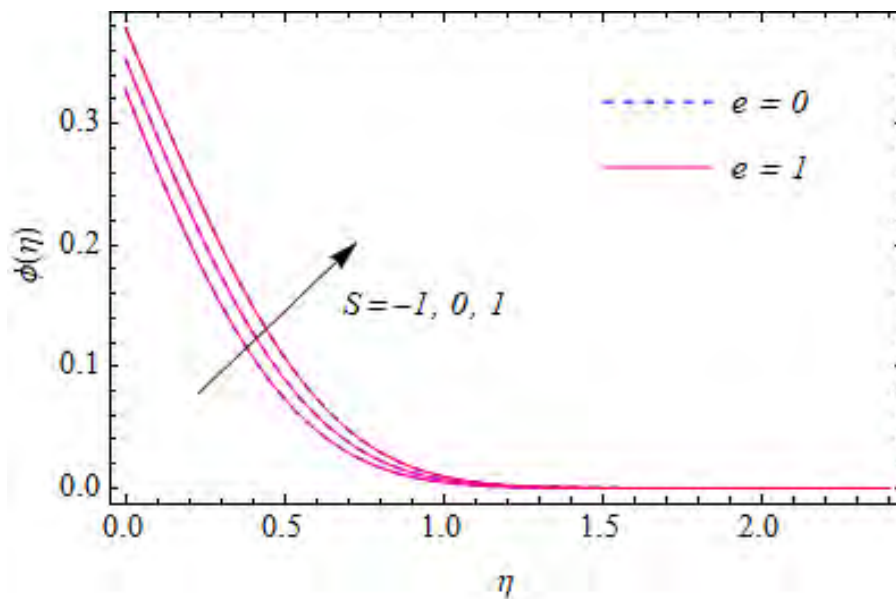
**Fig. 3.5(a):** Variation of  $f'(\eta)$  for different values of  $S$  and  $e$ .

Fig. 3.5(b) establishes the changes of temperature rate by the variation of the blowing parameter and microorganism slip. Temperature profiles were enhanced with blowing from

the wall and reduced for the blowing to the wall. The increasing Stefan blowing were enhanced temperature profiles for both with and without the presence of microorganism slip. Temperature profiles were found to maximize for a positive  $S$  while to minimized for negative  $S$  at the wall. In addition, the temperature profiles remain unchanged with the variation of microorganism slip.



**Fig. 3.5(b):** Variation of  $\theta(\eta)$  for different values of  $S$  and  $e$ .



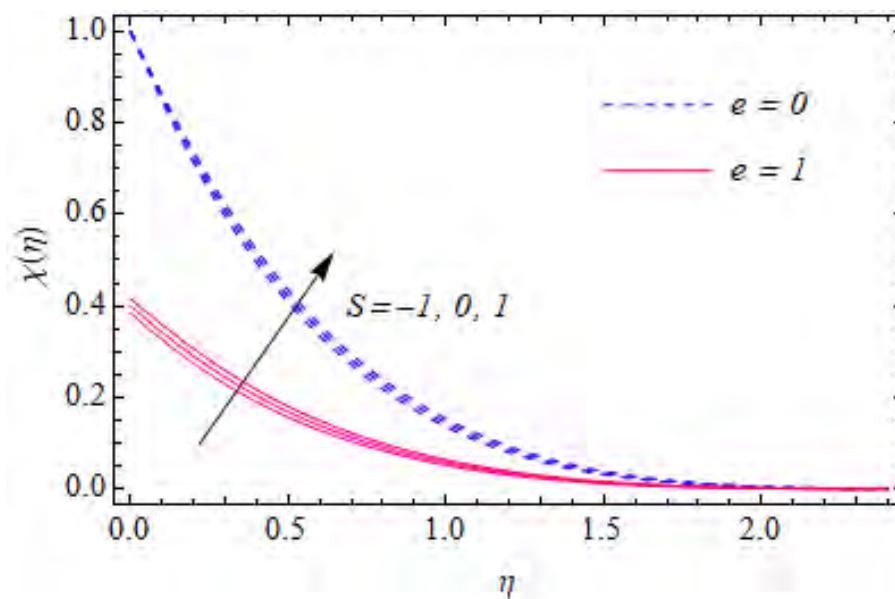
**Fig. 3.5(c):** Variation of  $\phi(\eta)$  for different values of  $S$  and  $e$ .

Fig. 3.5(c) reveals the evolution of the concentration profiles with the different values of microorganism slip and Stefan blowing parameter. The tendency of the concentration profiles



was quite similar to the temperature profiles. The concentration profiles were elevated with the blowing from the wall whereas blowing to the wall lowered it. The effects of the microorganism slip on the concentration profiles were not significant.

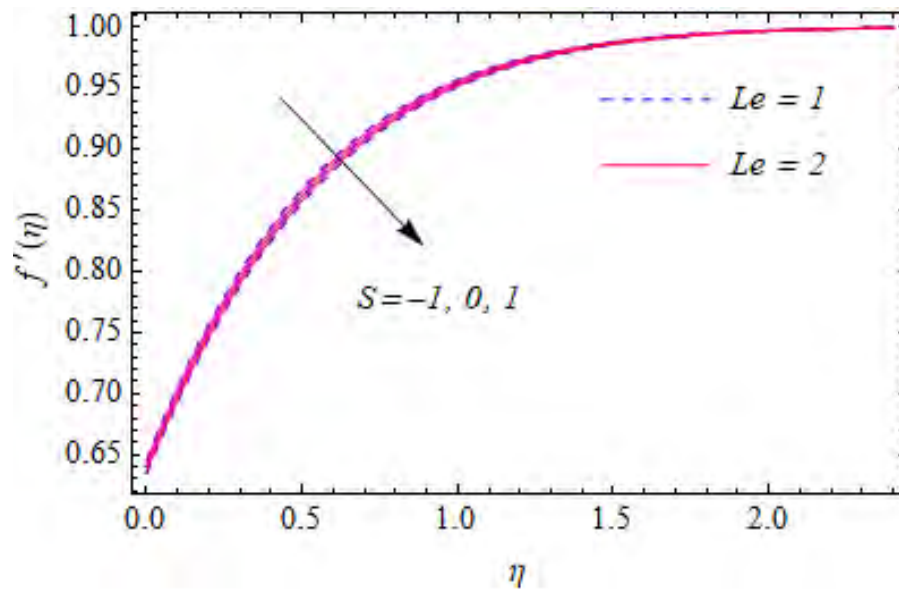
Fig. 3.5(d) prescribes the influence of the microorganism slip and the Stefan blowing parameters on the motile microorganisms density number function. The profiles of the microorganisms were increased with the blowing from the wall whereas the opposite phenomena were noticed in the presence of the strong blowing to the wall. The microorganism profiles were increased as the Stefan blowing parameter increased and the maximum values of the microorganism profiles were found for the no-slip boundary condition. However, the microorganism profiles were strongly reduced with increasing of the microorganism slip parameter. Finally, the microorganism profiles were converged slowly in comparison with the temperature and concentration profiles.



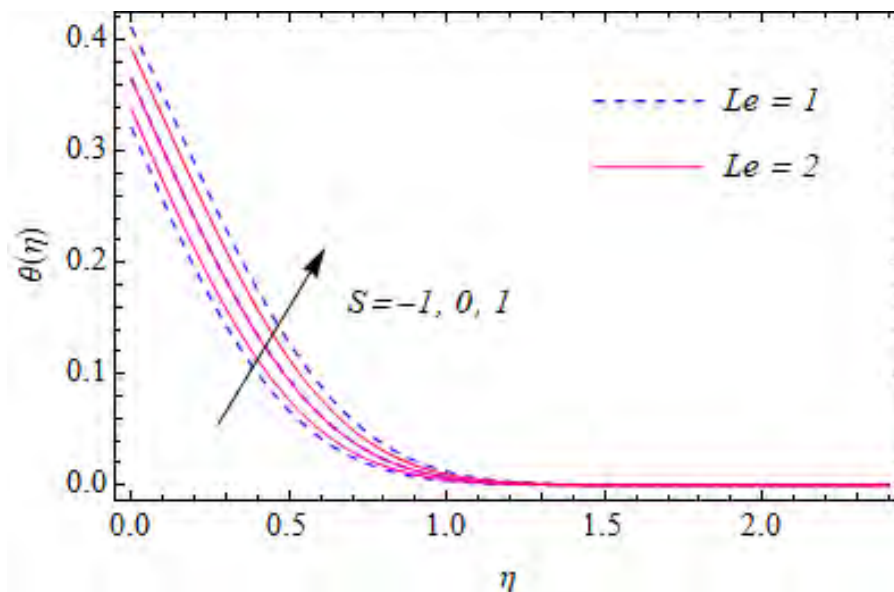
**Fig. 3.5(d):** Variation of  $\chi(\eta)$  for different values of  $S$  and  $e$ .

### 3.6 Effects of Lewis number

Fig. 3.6(a) depicts the effects of the blowing parameter for the various values of Lewis number on the dimensionless velocity profiles. Physically Lewis number relates the thermal diffusivity to the Brownian diffusion coefficient. Inspection of the momentum equation it can easily be concluded that there were no effects of Lewis number on the velocity profiles and graph also showed the same conclusion. Although, there was a very small reduction in the velocity profiles for different blowing parameter.



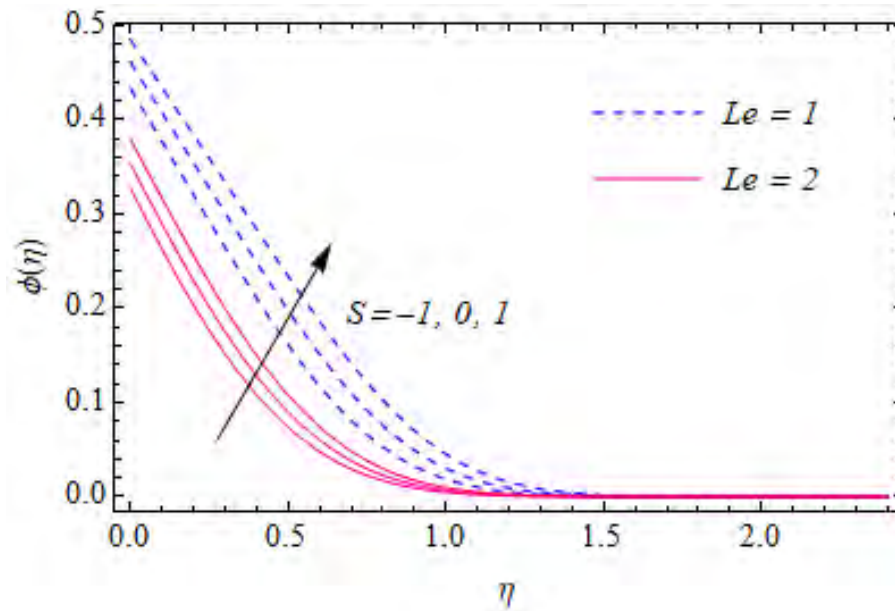
**Fig. 3.6(a):** Variation of  $f'(\eta)$  for different values of  $S$  and  $Le$ .



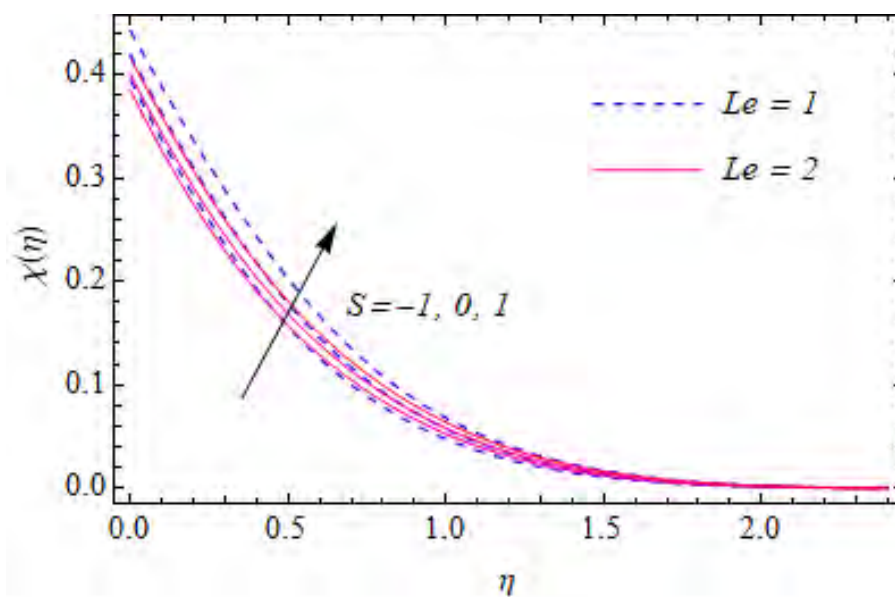
**Fig. 3.6(b):** Variation of  $\theta(\eta)$  for different values of  $S$  and  $Le$ .

Fig. 3.6(b) illustrates the influences of the Lewis number and the Stefan blowing parameter on the dimensionless temperature profiles. Here, a unique type of uplifted and dropped values of temperature profiles were observed for  $Le = 1$ . For positive Stefan blowing parameter, the temperature profiles became maximum, also minimum for the negative blowing and both impacts the described for lower Lewis number. After increasing the Lewis number, change in temperature became slower. However, the temperature has induced a reduction for blowing to the wall and enhanced for blowing from the wall. And other noticeable incidence happened that, temperature profiles conversed more rapidly.





**Fig. 3.6(c):** Variation of  $\phi(\eta)$  for different values of  $S$  and  $Le$ .



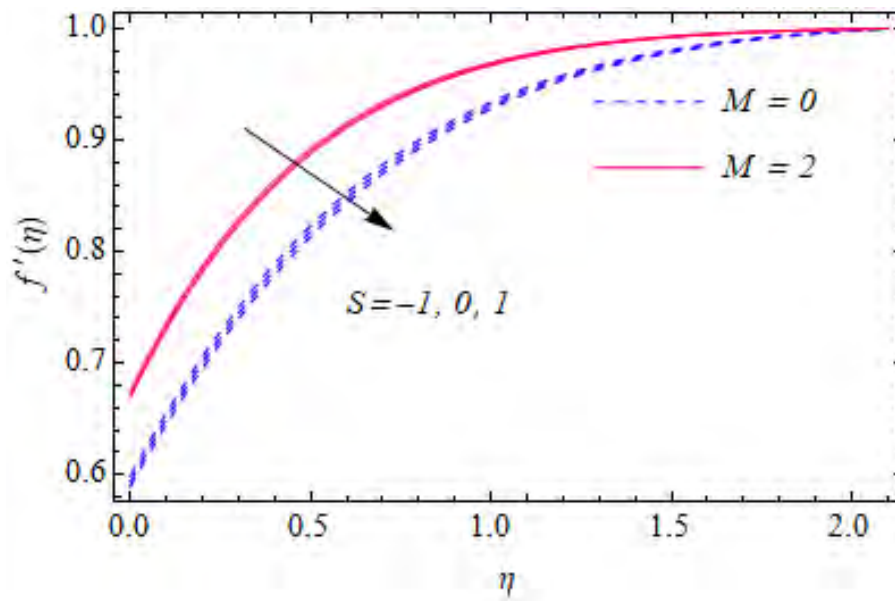
**Fig. 3.6(d):** Variation of  $\chi(\eta)$  for different values of  $S$  and  $Le$ .

Fig. 3.6(c) shows the variation of the concentration profiles with the variation of the dimension Lewis number and Stefan blowing parameter. Concentration profiles became minimum for strong blowing to the wall with higher Lewis number, on the other hand, concentration profiles became maximum for strong blowing to the wall at lower Lewis number. So, Stefan blowing parameter was enhanced the concentration profiles and decreasing of Lewis number became the cause of the strong elevation.

Fig. 3.6(d) explains the effects of the Lewis number on the dimensionless motile microorganisms. The blowing from the wall weakly accelerated microorganism profiles

whereas blowing to the wall was reduced those slowly. Profiles became maximum for lower Lewis number and it also causes strong elevation whereas the trend was reversed for higher Lewis number. Even though Stefan blowing parameter was slowly enhanced microorganisms density, but the profiles were not effectively notified for higher Lewis number.

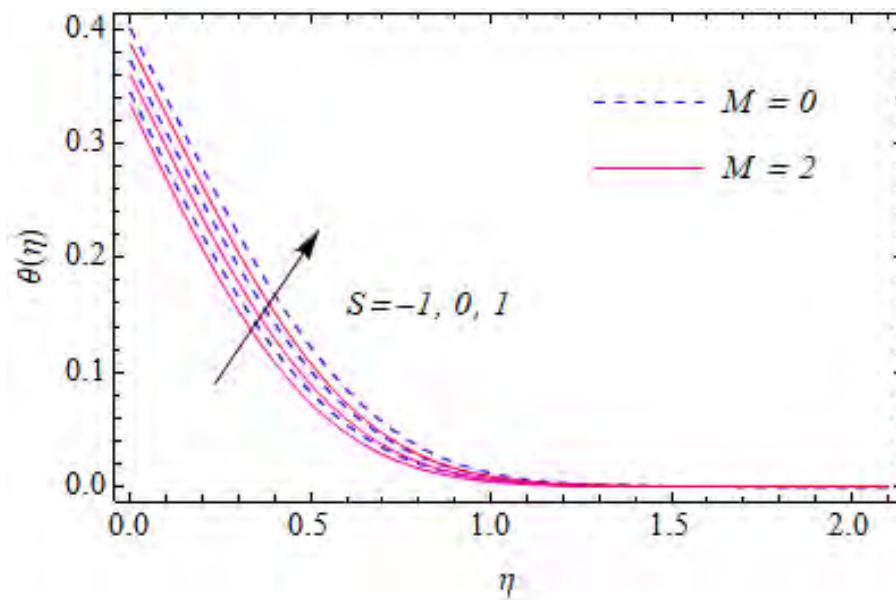
### 3.7 Effects of the magnetic fields



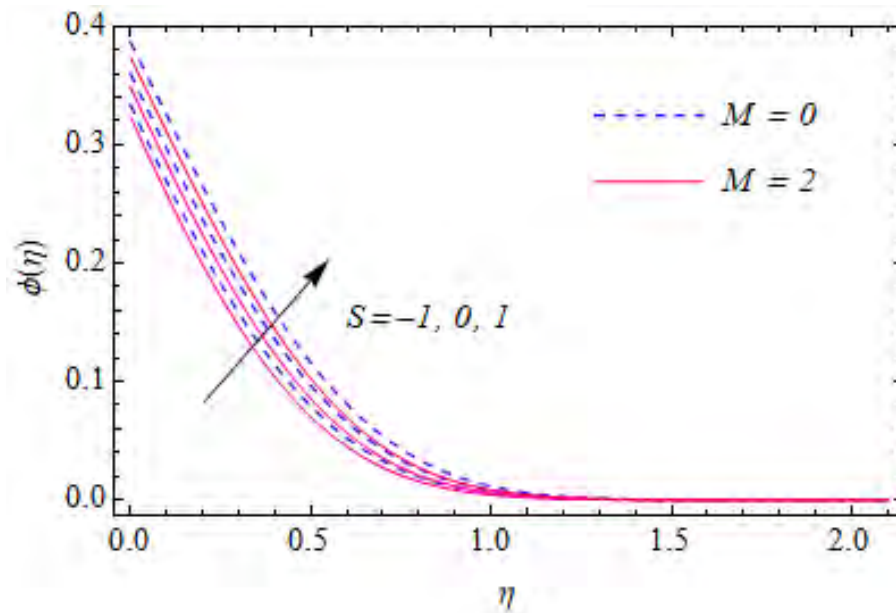
**Fig. 3.7(a):** Variation of  $f'(\eta)$  for different values of  $S$  and  $M$ .

Fig. 3.7(a) reveals the impact of the magnetic field with the presence of the Stefan blowing on the dimensionless velocity profiles. The magnetic parameter was the cause of strong elevation of the flow field near the wall and ambient flow. Since the magnetic field parameter presence in the momentum equation, the flow field was dominated by it and increased the flow velocity. Effects of blowing were trivial, velocity slightly reduced with blowing from the wall and increased conversely. However, blowing to the wall was established the maximum values of the velocity profiles with the higher magnetic number and strong blowing from the wall cause of minimum velocity in the presence of the lower magnetic field.

Fig. 3.7(b) depicts the response of the temperature profiles with combined effects of the magnetic field and Stefan blowing. Positive Stefan blowing parameter's value was strongly enhanced the temperature profiles whereas negative parameter which indicates blowing to the wall, was generated the converse trend and produced minimum temperature outlines. Increasing the magnetic field was found to reduce the dimensionless temperature.



**Fig. 3.7(b):** Variation of  $\theta(\eta)$  for different values of  $S$  and  $M$ .



**Fig. 3.7(c):** Variation of  $\phi(\eta)$  for different values of  $S$  and  $M$ .

Fig. 3.7(c) presents the distribution of the concentration profiles with the variation of the magnetic field for different values of the blowing parameter. The profiles were quite similar to the temperature profiles. The strong magnetic field was reduced concentration slightly and provided a minimum trend for blowing to the wall. Whereas, positive blowing was induced to maximum profiles with the lower magnetic field. Also, profiles conversed very quickly.

Fig. 3.7(d) illustrates the collective effects of the magnetic field and blowing parameter on the dimensionless motile microorganism profiles. Motile microorganism profiles were

slightly reduced with the increase of the magnetic field and portrayed minimum profiles with strong blowing to the wall, at flat wall profiles were elevated and for strong blowing from the wall, it became maximum. So, with the increasing of  $S$ , profiles were enhanced and with the increasing of magnetic field profiles reduced slightly.

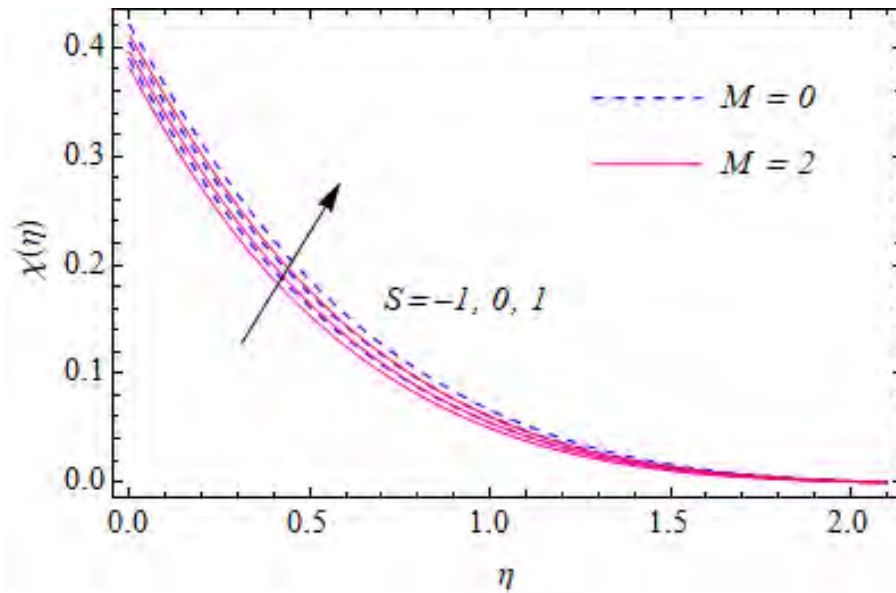


Fig. 3.7(d): Variation of  $\chi(\eta)$  for different values of  $S$  and  $M$ .

### 3.8 Effects of bioconvection Lewis number

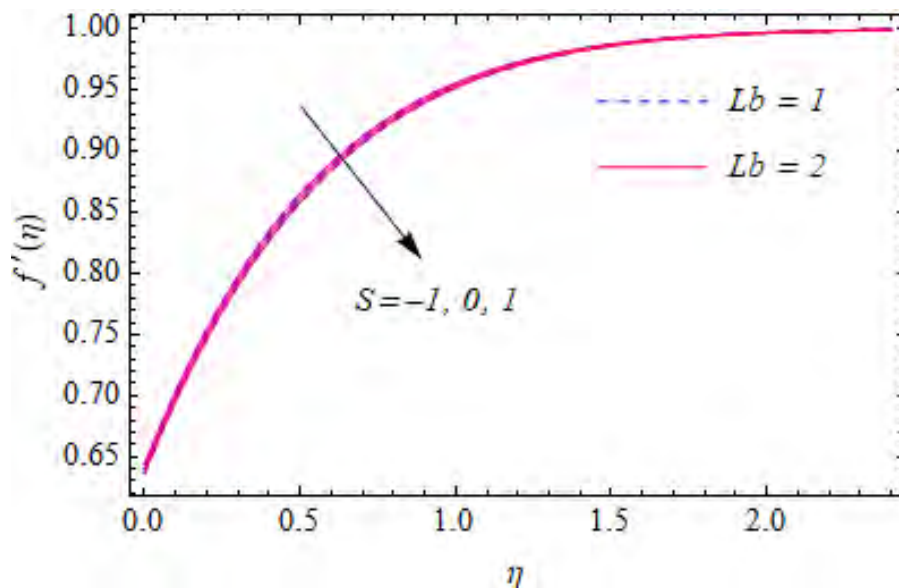


Fig. 3.8(a): Variation of  $f'(\eta)$  for different values of  $S$  and  $Lb$ .

Fig. 3.8(a) displays the effects of the blowing parameter and the bioconvection Lewis number on the velocity profiles. The blowing parameter was weakly decreased the velocity profiles as

well as the thickness of the hydrodynamic boundary layer. For the different values of bioconvection Lewis number, velocity profiles very weakly differed. So it can conclude that the parameter was a very poor effect on the velocity.

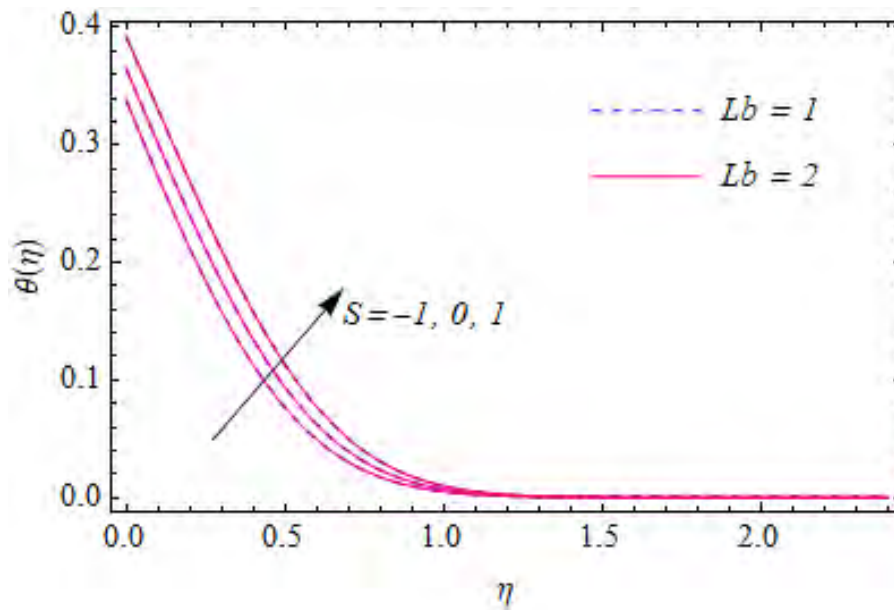


Fig. 3.8(b): Variation of  $\theta(\eta)$  for different values of  $S$  and  $Lb$ .

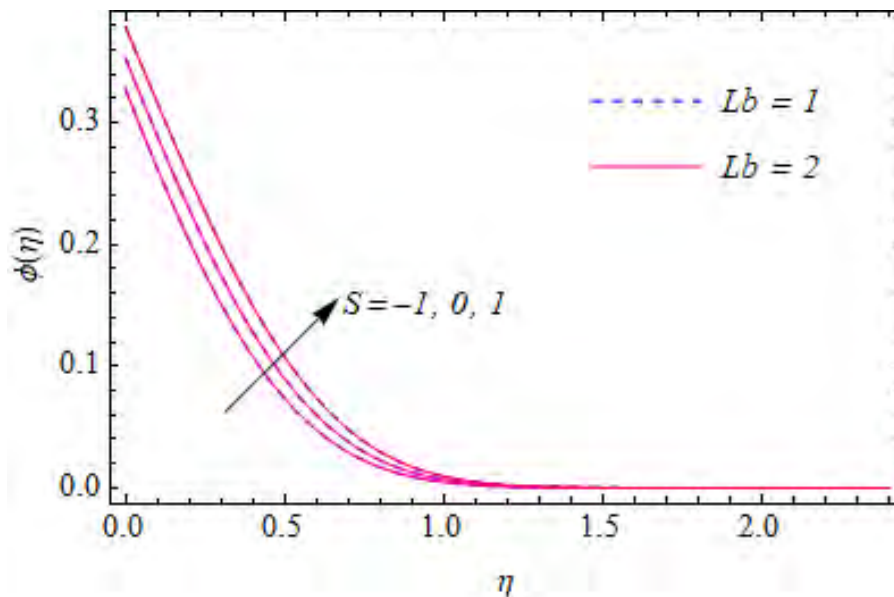


Fig. 3.8(c): Variation of  $\phi(\eta)$  for different values of  $S$  and  $Lb$ .

The temperature profiles were shown in fig. 3.8(b) with the different values of bioconvection Lewis number and Stefan blowing parameter. Regardless of the value of  $Lb$ , the blowing parameter was increased the temperature profiles significantly. But for the higher values of bioconvection Lewis number, temperature profiles were responded very poorly. Since

bioconvection Lewis number depends on kinematic viscosity and diffusivity of microorganisms, which does not relate with temperature profile directly.

The effects of the blowing parameter and the bioconvection Lewis number on dimensionless concentration profiles were shown in fig. 3.8(c). Due to the variation of the bioconvection Lewis number, concentration profiles were affected very rarely but Stefan blowing enhanced it. The thickness of the mass boundary layer was increased with the increasing of Stefan blowing parameter. So, it can be concluded that positive blowing was enhanced concentration profiles whereas negative blowing reduced it.

Fig. 8(d) describes the effects of the Stefan blowing parameter and bioconvection Lewis number on the dimensionless motile microorganism profiles. Generally, bioconvection Lewis number is the ratio of kinematic viscosity and diffusivity of microorganisms. So, increasing of the diffusivity of microorganisms consequences that decreasing of bioconvection Lewis number. Therefore, motile microorganism profiles were enhanced with the decreasing of bioconvection Lewis number. On another hand, Stefan blowing parameter elevated the thickness of microorganism boundary layer. So strong blowing from the wall with lower bioconvection Lewis number was produced maximum profiles and contrary effects were portrayed by strong blowing to the wall with higher  $Lb$ , so profiles became minimum.

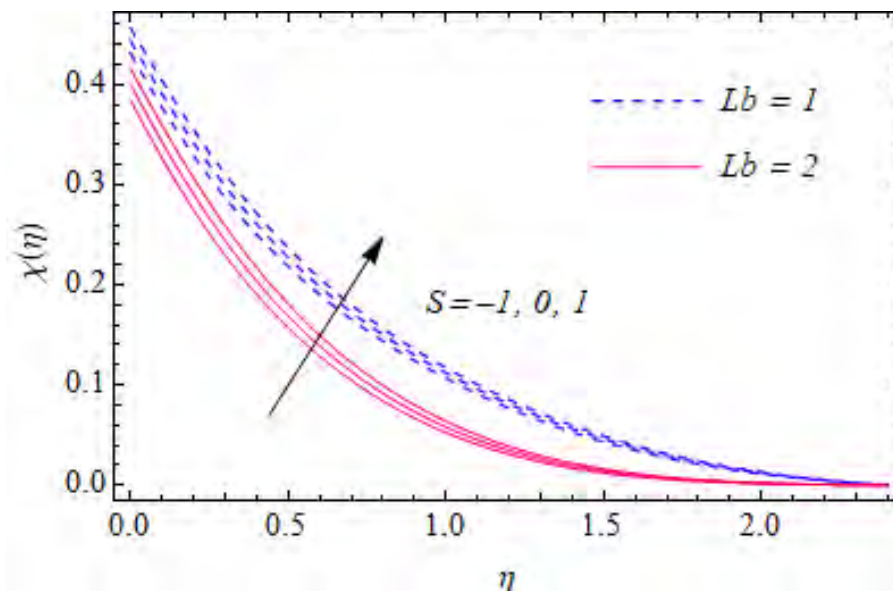


**Fig. 3.8(d):** Variation of  $\chi(\eta)$  for different values of  $S$  and  $Lb$ .



### 3.9 Effects of Péclet number

The velocity profiles were plotted in fig. 3.9(a) under the different values of the Péclet number and Stefan blowing parameter. Péclet number, as well as blowing parameter, did not affect the velocity profiles as much as other profiles were described earlier. Dimensionless Péclet number related to constant maximum cell swimming speed and diffusivity of microorganisms. So, velocity profiles remain similar by changing it but slightly reduced with increasing of blowing parameter.

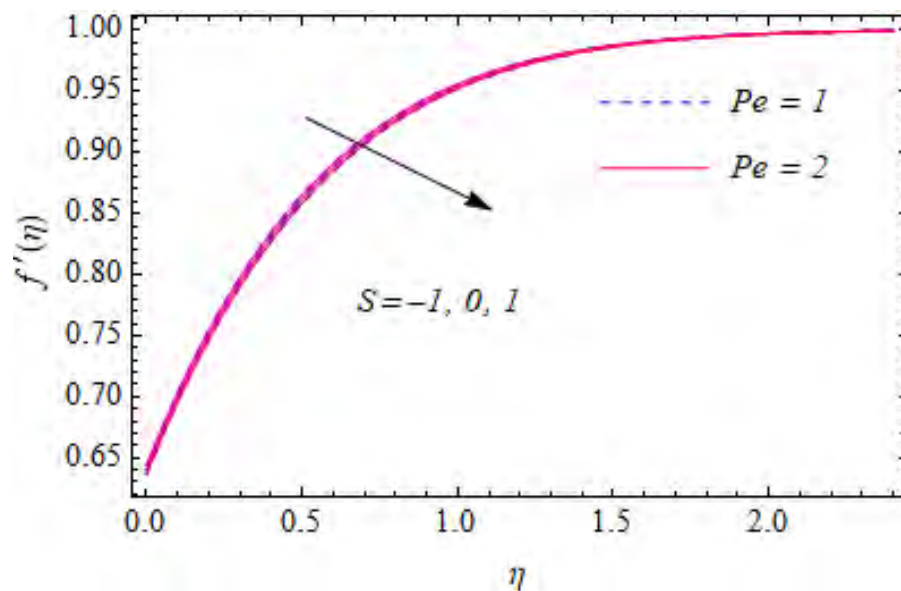


**Fig. 3.9(a):** Variation of  $f'(\eta)$  for different values of  $S$  and  $Pe$ .

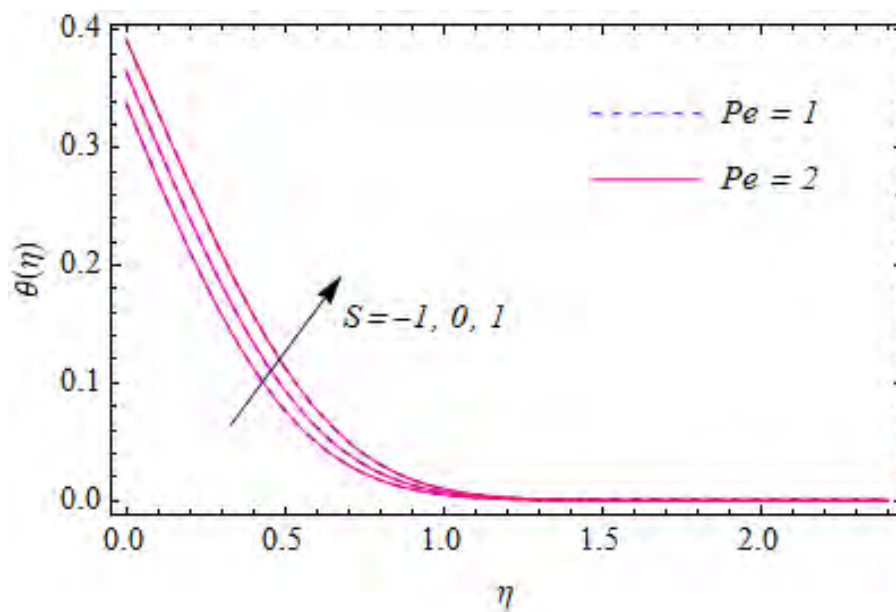


**Fig. 3.9(b):** Variation of  $\theta(\eta)$  for different values of  $S$  and  $Pe$ .

Fig. 3.9(b) specifies the variation in the temperature profiles with the variation of Péclet number and the blowing parameter. In the reformed energy equation, there was no interaction between the Péclet number and the dimensionless temperature profiles. So, temperature profiles remain unchanged due to the variation of the Péclet number. But with the increase of the blowing parameter, temperature profiles were blown further away from the wall with the thicker boundary layer.

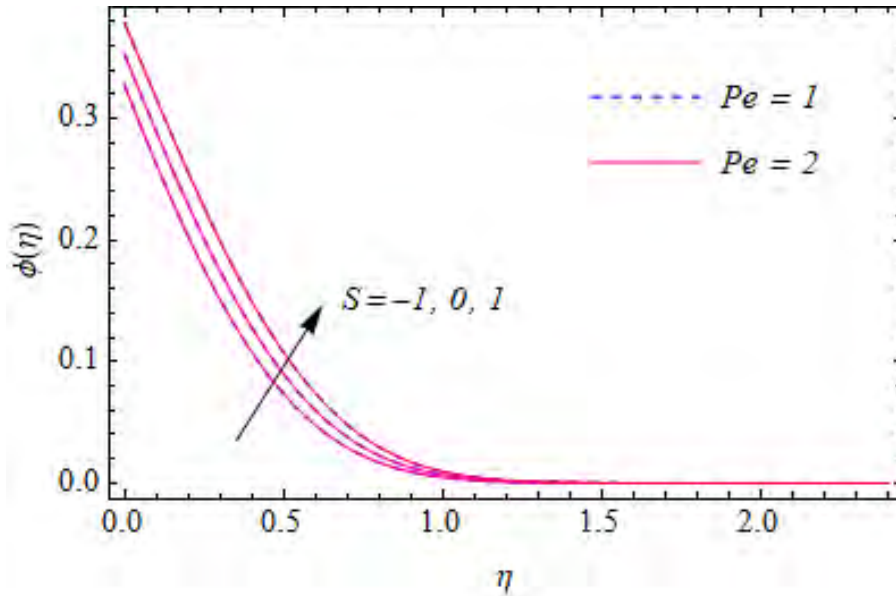


**Fig. 3.9(c):** Variation of  $\phi(\eta)$  for different values of  $S$  and  $Pe$ .

Concentration profiles illustrated in fig 3.9(c) under the variation of blowing parameter and different values of Péclet numbers. The concentration profiles behave like previously described temperature profiles under the same variations. It can be explained as declared previously there was no coupling between the dimensionless concentration profiles and the Péclet number.

Fig 3.9(d) shows the variation of the dimensionless motile microorganism profiles with the changes of the Péclet number and blowing parameters. As explained earlier that the Péclet number is related to the ratio between constant maximum cell swimming speed and diffusivity of microorganisms. So, Péclet number has had pronounced effects on the dimensionless motile microorganism profiles. Microorganism profiles became thinner with the increase in the Péclet number and it became minimum for blowing to the wall. Whereas profiles became thicker with the increasing of Stefan blowing and produced maximum values for blowing from the wall with lower Péclet number.



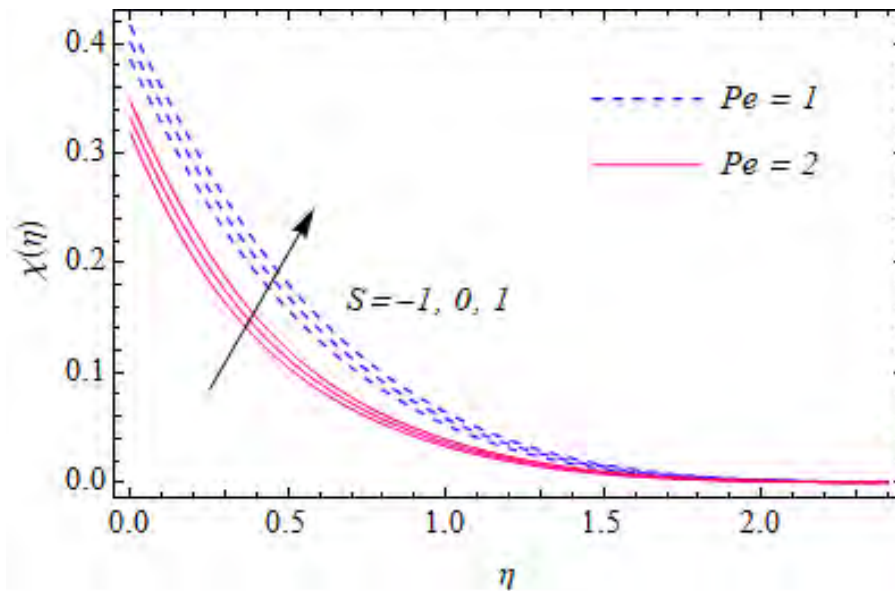


Fig. 3.9(d): Variation of  $\chi(\eta)$  for different values of  $S$  and  $Pe$ .

### 3.10 Effects of wedge parameter

Fig. 3.10(a) explains the effects of the wedge parameter and the Stefan blowing parameter on the dimensionless velocity profiles. Here, two different velocity profiles for with the presence of wedge parameter and without the presence of it. The absence of wedge parameter was decreased the velocity profiles whereas wedge parameter enhanced it. As usually Stefan blowing lower the velocity profiles, and it became minimum for blowing to the wall with the case of without wedge parameter.

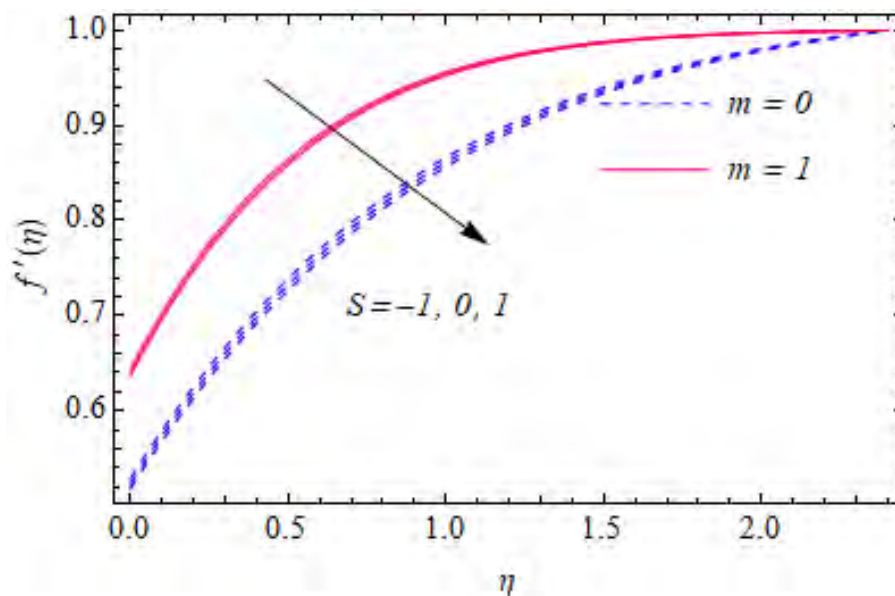
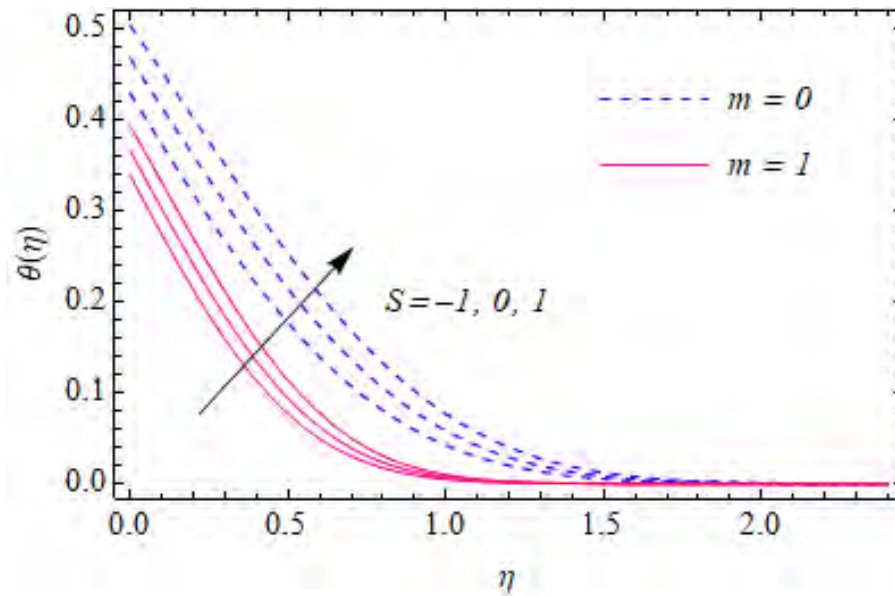


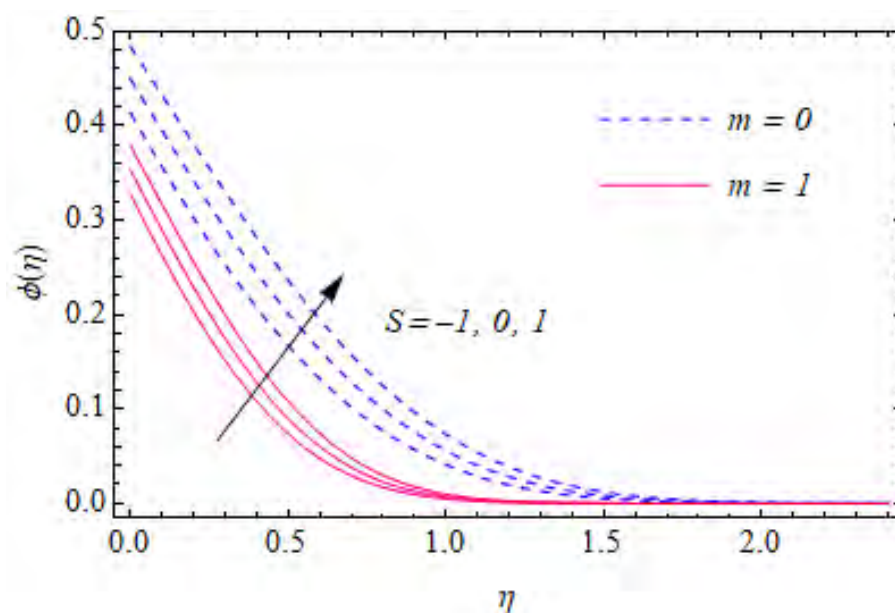
Fig. 3.10(a): Variation of  $f'(\eta)$  for different values of  $S$  and  $m$ .

Fig. 3.10(b) portrays the response of the wedge parameter and the blowing parameter on the dimensionless temperature profiles. When  $m = 1$ , the temperature profiles were reduced with the increase of wedge parameter for both direction of blowing.



**Fig. 3.10(b):** Variation of  $\theta(\eta)$  for different values of  $S$  and  $m$ .

Fig. 3.10(c) determines the effects of the wedge parameter with the blowing parameter on the dimensionless concentration profiles. Wedge parameter was made thinner the mass boundary layer and lowered the concentration profiles. The Stefan blowing parameter also enhanced the concentration profiles and made it maximum with the absence of wedge parameter and profiles were reversed for blowing to the wall with the presence of wedge parameter.



**Fig. 3.10(c):** Variation of  $\phi(\eta)$  for different values of  $S$  and  $m$ .

Fig. 3.10(d) reveals the motile microorganism profiles with the variation of Stefan blowing parameters and different conditions of wedge parameter. The motile microorganism profiles were enhanced with the condition that the absence of wedge parameter and reduction of profiles were produced with the presence of wedge parameter. So, this parameter was made thinner the microorganism boundary layer and retarded the profiles. Also, blowing from the wall were boosted the dimensionless motile microorganism profiles whereas negative blowing depressed it and the boundary layer became thinner.

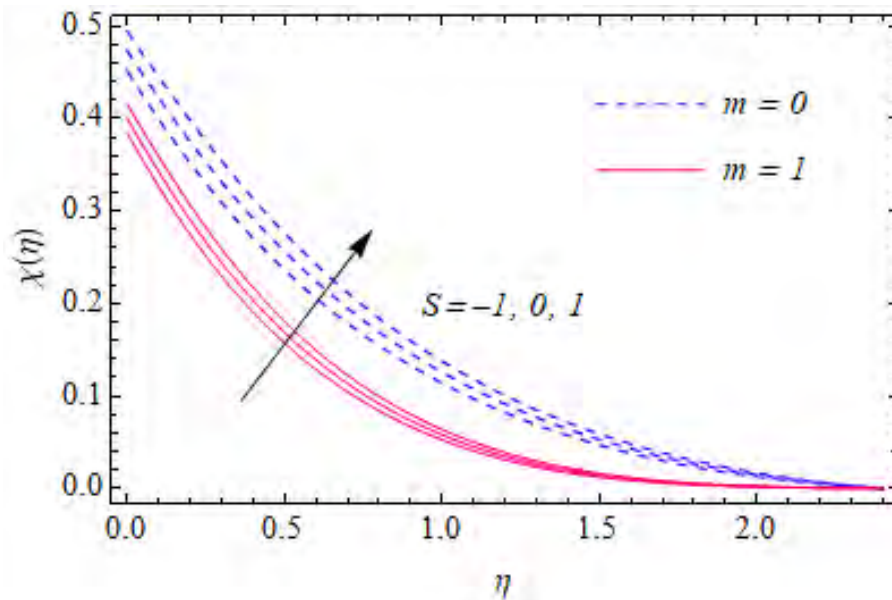


Fig. 3.10(d): Variation of  $\chi(\eta)$  for different values of  $S$  and  $m$ .

### 3.11 Engineering designed quantities

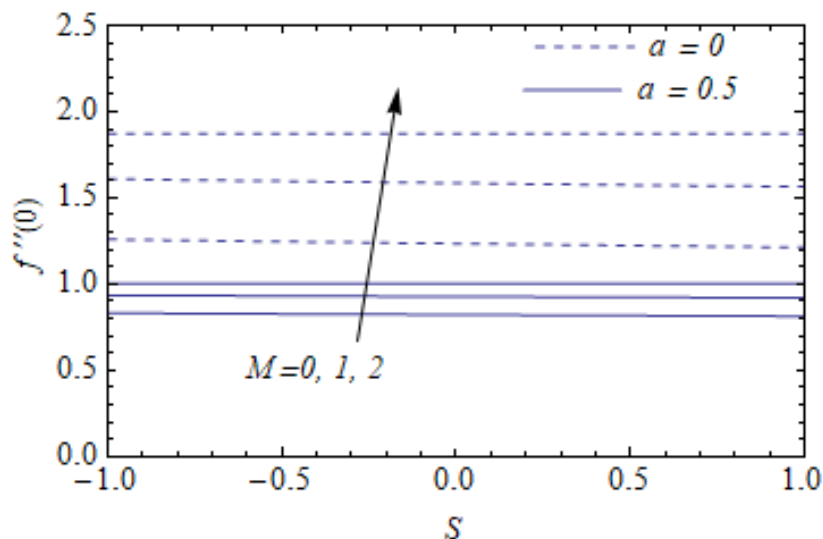
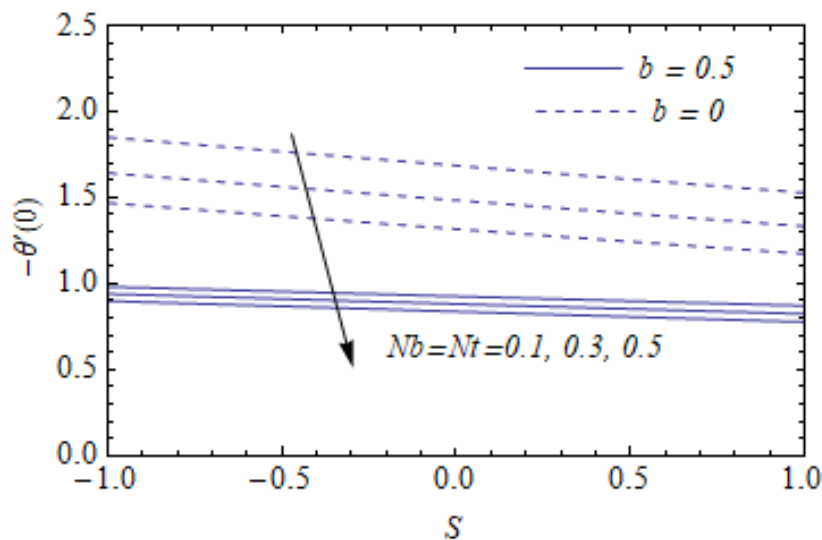


Fig. 3.11(a): Variation of the skin friction factor  $f''(0)$  for different values of  $S$ ,  $M$ , and  $a$ .

Fig. 3.11(a) illustrates the behavior of the skin friction factor  $f''(0)$  for the variation of the Stefan blowing parameter, magnetic field, and velocity slip parameters. Skin friction observed to remain same with the increasing of blowing parameter which also consistent with previous results that were investigated earlier, velocity profiles very slightly decreased with the increasing of blowing parameter which was almost ignorable, and consequence of that results generated weak shear variation at the wedge face. On the other hand, the magnetic field parameter was created thicker velocity boundary layer and accelerated flow, also generated higher shear at the wedge face. So, skin frictions were enhanced with the increasing of the magnetic field and those produced maximum values when flows were considered without velocity slip condition. Variation of the skin frictions was more pronounced with the absence of slip factor whereas variation was reduced with the increase of velocity slip. Furthermore, the slip factor has induced a reduction in skin friction coefficient. Since, the velocity slip factor lowering shear at the wall, therefore skin friction was depressed.



**Fig. 3.11(b):** Variation of  $-\theta'(0)$  for different values of  $S, Nt, Nb$  and  $b$ .

Fig. 3.11(b) establishes the characteristics of the heat transfer rate  $-\theta'(0)$  at the wedge's wall due to change of the Stefan blowing, thermal slip, Brownian motion, and thermophoresis parameters. The Stefan blowing parameter induced a reduction in the heat transfer rate at the edge surface. Strong blowing from the wall made thicker the temperature boundary layer whereas strong blowing to the wall made it thinner. Negative blowing generated greater local Nusselt number at wall face and positive blowing lowered it. As a result wall heat transfer rate slightly fell with the increasing of the Stefan blowing parameter. Temperature slip enhanced heat transfer rate. Variation in values of  $-\theta'(0)$  due to Brownian motion parameter

and thermophoresis parameter were much considerable when temperature slip factor was zero as assumed there was no temperature slip at wedge surface. Also, the heat transfer rates were lowered according to temperature slip factor imposed. Temperature slip at the wall was retarded temperature profiles and the heat transfer rate was also depressed. In addition, the variation for Brownian motion parameter and thermophoresis parameter also significant. Local Nusselt numbers were depleted with rising of the values of Brownian motion parameter and thermophoresis parameter. Both parameters had a significant effect on the heat transfer rate and induced a reduction with uplifting Brownian motion and thermophoresis.

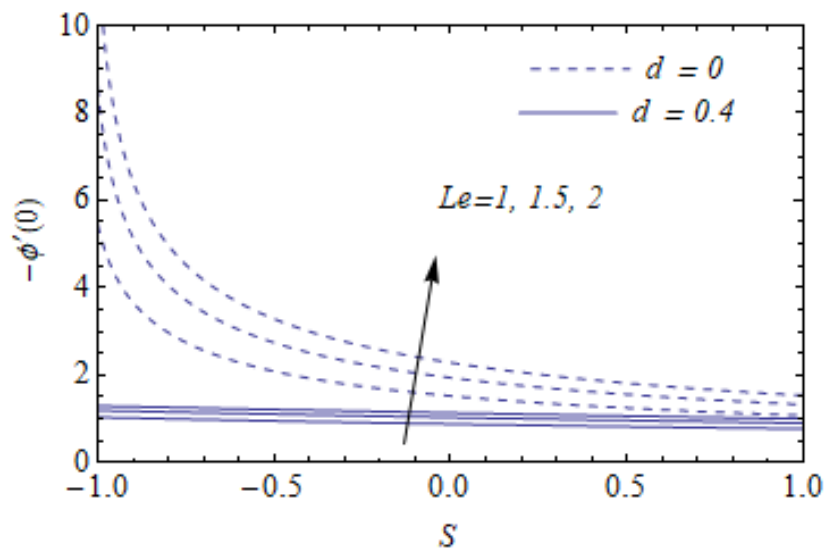


**Fig. 3.11(c):** Variation of  $-\phi'(0)$  for different values of  $S$ ,  $Le$  and  $d$ .

Fig. 3.11(c) demonstrates the behavior of the local mass transfer rate  $-\phi'(0)$  near the wedge surface with the variation of the Stefan blowing parameter, Lewis number, in absence of concentration slip and with the presence of concentration slip boundary condition. In the boundary condition, Stefan blowing parameter and mass transfer rate factor  $-\phi'(0)$  closely related to each other. So, blowing factor was strongly effected to the behavior of local mass transfer profiles. It observed that for strong blowing to the wall, the mass transfer rates were massively boosted and became maximum. With the imposed condition as Lewis number  $Le = 2$  and absence of mass slip boundary condition, the local mass transfer rate was increased to 10. It is clear from the first boundary condition, the negative value of blowing parameter and for the higher values of Lewis number, maximum values of local Sherwood number were produced. In that consequence, strong blowing to the wedge wall with the help of higher Lewis number was boosted the local mass transfer rate. But for the blowing from the wedge wall with the same conditions were created a contrary effect on mass transfer, it

strongly fell with the increasing of blowing parameter. Interestingly, all those phenomena happened only for the absence of concentration boundary slip condition. Whereas, in the presence of slip condition, the local mass transfer variation tends to steady-state, trends were reduced very slowly. So, mass slip parameter strongly depressed the mass transfer rate at the wall. Although, local Sherwood number was enhanced with the higher Lewis number. We know that Lewis number directly proportional to thermal diffusivity and inversely proportional to the Brownian diffusion coefficient and higher Lewis number lowered concentration profiles. Due to the fact, local mass transfer rates were elevated for higher Lewis number.

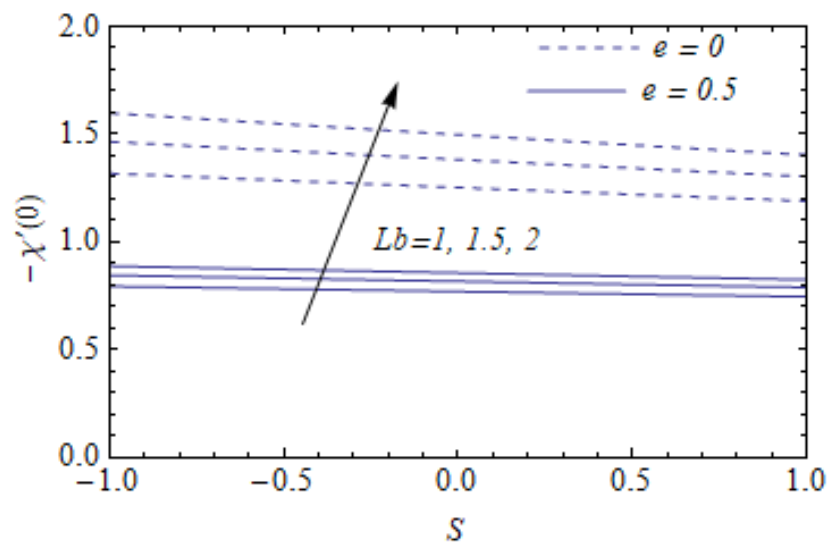


**Fig. 3.11(d):** Variation of  $-\chi'(0)$  for different values of  $S$ ,  $Lb$  and  $e$ .

Fig. 3.11(d) describes that the increasing of bioconvection Lewis number was hoisted the local microorganisms transfer rate  $-\chi'(0)$  and increasing of Stefan blowing parameter and microorganism slip factor depleted microorganisms transfer rate. From the previous study, it severally noticed that the blowing factor was induced slight elevation into the motile microorganism profiles. So physically, higher blowing parameter made the microorganism boundary layer thicker and it retarded microorganisms transfer rate at the wall. The variation was not so strong, but negative blowing can produce higher microorganisms transfer compared to blowing from the wall. As for similarity with previous physical quantity trends, microorganism slip factor also reduced microorganisms transfer rate at the wedge wall. Transfer rate enhanced when no microorganism slip boundary condition was imposed. Again, bioconvection Lewis number directly proportional to kinematic viscosity and inversely proportional to the diffusivity of microorganisms. Increasing of bioconvection Lewis number

was lowered diffusivity of microorganisms and enhanced microorganisms transfer rate at the surface of the wedge.

**Table 2:** Values of the skin friction factor, local heat transfer rate, local mass transfer rate and the local microorganisms transfer rate at the wall.

$S$	$a$	$b$	$d$	$e$	$f''(0)$	$-\theta'(0)$	$-\phi'(0)$	$-\chi'(0)$
-1					1.609800	0.576574	0.591809	0.560495
0	0	1	1	1	1.585870	0.542044	0.559185	0.540774
1					1.564780	0.508702	0.527499	0.521317
-1					0.935103	0.643629	0.655026	0.603011
0	0.5	1	1	1	0.927304	0.614819	0.627828	0.586494
1					0.920135	0.585760	0.600373	0.569828
-1					0.643178	1.850440	0.539861	0.589965
0	1	0	1	1	0.640320	1.686000	0.540507	0.581027
1					0.637441	1.528040	0.540218	0.571627
-1					0.643683	0.981652	0.635578	0.560180
0	1	0.5	1	1	0.640320	0.926230	0.616679	0.549313
1					0.637134	0.871244	0.597601	0.538375
-1					0.697588	0.859694	11.70810	0.932002
0	1	1	0	1	0.640320	0.625756	2.284460	0.741832
1					0.632113	0.554679	1.530940	0.664935
-1					0.646200	0.676213	1.114650	0.669724
0	1	1	0.5	1	0.640320	0.633025	1.008330	0.641813
1					0.635454	0.591990	0.911094	0.614194
-1					0.643876	0.661825	0.672235	1.598490
0	1	1	1	0	0.640320	0.635062	0.646950	1.498150
1					0.637008	0.607810	0.621202	1.404060
-1					0.643876	0.661825	0.672235	0.888423
0	1	1	1	0.5	0.640320	0.635062	0.646950	0.856539
1					0.637008	0.607812	0.621202	0.824934

## CHAPTER 4: CONCLUSIONS

---

### 4.1 Conclusions

This investigation was focused on the effects of Stefan blowing with multiple slips boundary conditions. Here, the forced convective flow of bio-nanofluid with wedge geometry was considered. Appropriate similarity transformation variables were used to convert system of PDEs to system of ordinary differential equations with slip boundary conditions. A built-in MATHEMATICA command was used to solve the system numerically and present those results graphically. The effects of foremost parameters on the velocity, temperature, concentration, and microorganism profiles were described graphically and engineering designed quantities were also discussed graphically and with the table. A comparing table with the related previous investigation was also arranged. Based on the results, the main findings are highlighted briefly as

- (i) The Stefan blowing effects on velocity profiles were very weakly decreased but strongly elevated temperature, concentration, and microorganism profiles in the presence of both slip and without slip boundary conditions.
- (ii) Velocity slip boundary condition was enhanced the velocity profiles, but temperature, concentration, and microorganism profiles were enhanced by no velocity slip condition.
- (iii) The temperature slip weakened temperature, and concentration profiles but had no effect on velocity and microorganism profiles.
- (iv) Strong blowing from the wall was boosted temperature, concentration, and microorganism profiles and blowing to the wall was shown opposite behavior for no mass slip boundary, but Stefan blowing effected slowly with mass slip boundary condition.
- (v) The microorganism slip boundary condition had lowered microorganism profiles.
- (vi) The Lewis number had strongly dropped concentration profiles.
- (vii) The magnetic field was strongly uplifted velocity profiles but insignificantly depressed other profiles.
- (viii) The bioconvective Lewis number had reduced microorganism profiles only.
- (ix) The Péclet number was also lessened microorganism profiles only and other profiles were unaffected.



- (x) The wedge parameter improved velocity profiles but decreased other profiles.
- (xi) The Stefan blowing parameter was slowly reduced skin friction parameter and strong magnetic field hoisted it quickly.
- (xii) Brownian motion parameter and thermophoresis parameter diminished heat transfer rate at the wall. Also, Stefan blowing parameter had slowly weakened it.
- (xiii) The Lewis number was strongly boosted the mass transfer rate at the wall for negative blowing, but fell quickly for positive blowing, and this phenomenon happened for no concentration slip boundary condition. On the other hand, the mass transfer rate had changed very slowly for concentration slip boundary condition.
- (xiv) Bioconvection Lewis number had uplifted local microorganisms transfer rate quickly with no microorganism slip boundary condition compared to the presence of slip factor. Suction at the wall was increased local microorganisms transfer rate slowly.

#### **4.2 Possible future works**

- (i) This work can be extended to free and mixed convection.
- (ii) The unsteady condition of this work can be considered.
- (iii) It can be extended for variable fluid properties.

## CHAPTER 5: REFERENCES

---

- [1] Maxwell, J. C., *Treatise on Electricity and Magnetism*, vol. 1, Oxford: Clarendon Press, 1873.
- [2] Choi, S., "Enhancing thermal conductivity of fluids with nanoparticles, developments and applications of non-Newtonian flows," *ASME Fluids Engineering Division*, vol. 66, pp. 99-105, 1995.
- [3] Lee, C. E., "Rapid and repeated invasions of fresh water by the saltwater Copepod *Eurytemora Affinis*," *Evolution*, vol. 53, no. 5, pp. 1423–1434, 1999.
- [4] Murshed, S. M. S., Leong, K. C., and Yang, C., "Thermophysical and electrokinetic properties of nanofluids—a critical review," *Applied Thermal Engineering*, vol. 28, no. 17-18, pp. 2109-2125, 2008.
- [5] Kakaç, S., Özerinç, S., and Yazıcıoğlu, A. G., "Enhanced thermal conductivity of nanofluids: a state-of-the-art review," *Microfluids and Nanofluids*, vol. 8, no. 2, pp. 145-170, 2010.
- [6] Kaufui V. W., and Omar, D. L., "Applications of Nanofluids: Current and Future," *Advances in Mechanical Engineering*, vol. 2, 2010.
- [7] Falkner, V. M., and Skan, S. W., "Some approximate solutions of the boundary-layer equations," *Philosophical Magazine*, vol. 12, pp. 865-896, 1931.
- [8] Atalık, K., and Sonmezler, U., "Symmetry groups and similarity analysis for boundary layer control over a wedge using electric forces," *International Journal of Non-Linear Mechanics*, vol. 44, no. 8, pp. 883-890, 2009.
- [9] Atalık, K., and Sonmezler, U., "Heat transfer enhancement for boundary layer flow over a wedge by the use of electric fields," *Applied Mathematical Modeling*, vol. 35, no. 9, pp. 4516-4525, 2011.
- [10] Seddeek, M. A., Afify, A. A., and Al- Hanaya, A. M., "Similarity Solutions for a Steady MHD Falkner - Skan flow and heat transfer over a wedge considering the effects of variable viscosity and thermal conductivity," *Application and Applied Mathematics*, vol. 4, no. 2, pp. 301-313, 2009.
- [11] Hayat, T., Majid, H., Nadeem, and Meslou, S., "Falkner-Skan wedge flow of a power-law fluid with mixed convection and porous medium," *Computers and Fluids*, vol. 49, no. 1, pp. 22-28, 2011.

- [12] Yacob, N., Ishak, A., and Pop, I., "Falkner-Skan problem for a static or moving wedge in nanofluid," *International Journal of Thermal Science*, vol. 50, no. 2, pp. 133-139, 2011.
- [13] Prasad, K. V., Datti, P. S., and Vajravelu, K., "MHD mixed convection flow over a permeable non-isothermal wedge," *Journal of King Saud University-Science*, vol. 25, no. 4, pp. 313-324, 2013.
- [14] Ashwini, G., Poornima, C., and Eswara, A. T., "Unsteady MHD accelerating flow past a wedge with thermal radiation and internal heat generation/absorption," *International Journal of Mathematical Sciences and Engineering Applications*, vol. 9, no. 1, pp. 13-26, 2015.
- [15] Lee, S. Y., and Kim, H. U., "Systems strategies for developing industrial microbial strains," *Nature Biotechnology*, vol. 33, no. 10, pp. 1061-1072, 2015.
- [16] Kuznetsov, A. V., and Nield, D. A., "Natural convective boundary-layer flow of a nanofluid past a vertical plate," *International Journal of Thermal Science*, vol. 49, no. 2, pp. 243-247, 2010a.
- [17] Kuznetsov, A. V., and Nield, D. A., "Thermal instability in a porous medium layer saturated by a nanofluid: Brinkman model," *Transport in Porous Media*, vol. 81, no. 3, pp. 409-422, 2010b.
- [18] Kuznetsov, A. V., and Nield, D. A., "Effect of local thermal non-equilibrium on the onset of convection in a porous medium layer saturated by a nanofluid," *Transport in Porous Media*, vol. 33, no. 2, pp. 425-436, 2010c.
- [19] Khan, W. A., Uddin, M. J., and Ismail, A. I. M., "Free convection of non-Newtonian nanofluids in porous media with gyrotactic microorganisms," *Transport in Porous Media*, vol. 97, no. 2, pp. 241-252, 2012.
- [20] Tham, L., Nazar, R., and Pop, I., "Steady mixed convection flow on a horizontal circular cylinder embedded in a porous medium filled by a nanofluid containing gyrotactic micro-organisms," *ASME Journal of Heat Transfer*, vol. 135, no. 10, pp. 102601, 2013.
- [21] Bég, O. A., Prasad, V. R., and Vasu, B., "Numerical study of mixed bioconvection in porous media saturated with nanofluid and containing oxytactic microorganisms," *Journal of Mechanics in Medicine and Biology*, vol. 13, no. 4, pp. 1350067.1–1350067.25, 2013.
- [22] Shaw, S., Sibanda, P., Sutradhar, A., and Murthy, P. V. S. N., "Magnetohydrodynamics and Soret effects on bioconvection in a porous medium

- saturated with a nanofluid containing gyrotactic microorganisms," ASME Journal of Heat Transfer, vol. 136, no. 5, pp. 52601, 2014.
- [23] Zaimi, K., Ishak, A., and Pop, I., "Stagnation-point flow toward a stretching /shrinking sheet in a nanofluid containing both nanoparticles and gyrotactic microorganisms," ASME Journal of Heat Transfer, vol. 136, no. 4, pp. 041705, 2014.
- [24] Xu, H., and Pop, I., "Fully developed mixed convection flow in a horizontal channel filled by a nanofluid containing both nanoparticles and gyrotactic microorganisms," European Journal of Mechanics B Fluids, vol. 46, pp. 37-45, 2014.
- [25] Raees, A., Xu, H., Sun, Q., and Pop, I., "Mixed convection in gravity-driven nano-liquid film containing both nanoparticles and gyrotactic microorganisms," Applied Mathematics and Mechanics, vol. 36, no. 2, pp. 163-178, 2015.
- [26] Akbar, N. S., and Khan, Z. H., "Magnetic field analysis in a suspension of gyrotactic microorganisms and nanoparticles over a stretching surface," Journal of Magnetism and Magnetic Materials, vol. 410, pp. 72-80, 2016.
- [27] Mutuku, W. N., and Makinde, O. D., "Hydromagnetic bioconvection of nanofluid over a permeable vertical plate due to gyrotactic microorganisms," Computational Fluids, vol. 95, pp. 88-97, 2014.
- [28] Xu, H., "Lie group analysis of a nanofluid bioconvection flow past a vertical flat surface with an outer power-law stream," ASME Journal of Heat Transfer, vol. 137, no. 4, pp. 041101.1-041101.9, 2015.
- [29] Amirson, N. A., Uddin, M. J., and Ismail, A. I., "Three dimensional stagnation point flow of bionanofluid with variable transport properties," Alexandria Engineering Journals, vol. 55, no. 3, pp. 1983–1993, 2016.
- [30] Latiff, N. A., Uddin, M. J., and Ismail, A. I. M., "Stefan blowing effect on bioconvective flow of nanofluid over a solid rotating stretchable disk," Propulsion and Power Research, vol. 5, no. 4, pp. 267–278, 2016.
- [31] Babu, M. J., and Sandeep, N., "Effect of nonlinear thermal radiation on non-aligned bio-convective stagnation point flow of a magnetic-nanofluid over a stretching sheet," Alexandria Engineering Journals, vol. 55, no. 3, pp. 1931–1939, 2016.
- [32] Makinde, O. D., and Animasaun, I. L., "Thermophoresis and Brownian motion effects on MHD bioconvection of nanofluid with nonlinear thermal radiation and quartic chemical reaction past an upper horizontal surface of a paraboloid of revolution," Journal of Molecular Liquids, vol. 221, pp. 733–743, 2016.
- [33] Nellis, G., and Klein, S., Heat Transfer, 1st ed., Cambridge University Press, pp. 974-978, 2008.

- [34] Lienhard, IV J. H., and Lienhard, V J. H., A heat transfer textbook, 3rd ed., Massachusetts: Phlogiston Press, pp. 662–663, 2005.
- [35] Fang, T., "Flow and mass transfer for an unsteady stagnation-point flow over a moving wall considering blowing effects," ASME Journal of Fluids Engineering, vol. 136, no. 4, pp. 071103, 2014.
- [36] Fang, T., and Jing, W., "Flow, heat, and species transfer over a stretching plate considering coupled Stefan blowing effects from species transfer," Communication in Nonlinear Science and Numerical Simulation, vol. 19, no. 9, pp. 3086–3097, 2014.
- [37] Latiff, N. A., Uddin, M. J., and Ismail, A. I. M., "Stefan blowing effect on bioconvective flow of nanofluid over a solid rotating stretchable disk," Propulsion and Power Research, vol. 5, no. 4, pp. 267–278, 2016.
- [38] Uddin, M. J., Beg, O. A., and Beg, T. A., "Stefan blowing, Navier slip, and radiation effects on thermo-solutal convection from a spinning cone in an anisotropic porous medium," Journal of Porous Media, vol. 19, no. 7, pp. 617–633, 2016.
- [39] Amirsom, N., Uddin, M. J., and Ismail, A. I. M., "Electromagnetoconvective stagnation point flow of bionanofluid with melting heat transfer and Stefan blowing," Thermal Science, vol. 22, pp. 134-134, 2017.
- [40] Basir, M. F. M., Uddin, M. J., Béq, O. A., and Ismail, A. M., "Influence of Stefan blowing on nanofluid flow submerged in microorganisms with leading edge accretion or ablation," Journal of the Brazilian Society of Mechanical Sciences and Engineering, vol. 39, no. 11, pp. 4519-4532, 2017.
- [41] Giri, S. S., Das, K., and Kundu, P. K., "Stefan blowing effects on MHD bioconvection flow of a nanofluid in the presence of gyrotactic microorganisms with active and passive nanoparticles flux," The European Physics Journal Plus, vol. 132, no. 101, 2017.
- [42] Zohra, F. T., Uddin, M. J., Ismail, A. I. M., Beg, O. A., and Kadir, A., "Anisotropic slip magneto-bioconvection flow from a rotating cone to a nanofluid with Stefan blowing effects," Chinese Journal of Physics, vol. 56, no. 1, pp. 432-448, 2017.
- [43] Uddin, M. J., Béq, O. A., and Amin, N. S., "Hydromagnetic transport phenomena from a stretching or shrinking nonlinear nanomaterial sheet with Navier slip and convective heating: a model for bio-nano-materials processing," Journal of Magnetism and Magnetic Materials, vol. 368, pp. 252–261, 2014.
- [44] Ibrahim, W., and Shankar, B., "MHD boundary layer flow and heat transfer of a nanofluid past a permeable stretching sheet with velocity, thermal and solutal slip boundary conditions," Computers and Fluids, vol. 75, pp. 1-10, 2013.

- [45] Uddin, M. J., Khan, W. A., and Amin, N. S., "G-Jitter mixed convective slip flow of nanofluid past a permeable stretching sheet embedded in a Darcian porous media with variable viscosity," *PLoS One*, vol. 9, no. 6, pp. e99384, 2014.
- [46] Zheng, L., Zhang, C., Zhang, X., and Zhang, J., "Flow and radiation heat transfer of a nanofluid over a stretching sheet with velocity slip and temperature jump in porous medium," *Journal of the Franklin Institute*, vol. 350, no. 5, pp. 990–1007, 2013.
- [47] Uddin, M. J., Ferdows, M., and Bég, O. A., "Group analysis and numerical computation of magneto-convective non-Newtonian nanofluid slip flow from a permeable stretching sheet," *Applied Nanoscience*, vol. 4, no. 7, pp. 897–910, 2014.
- [48] Hamad, M. A. A., Uddin, M. J., and Ismail, A. I. M., "Investigation of combined heat and mass transfer by Lie group analysis with variable diffusivity taking into account hydrodynamic slip and thermal convective boundary conditions," *International Journal of Heat and Mass Transfer*, vol. 55, no. 4, pp. 1355–1362, 2013.
- [49] Mishra, U., and Singh, G., "Dual solutions of mixed convection flow with momentum and thermal slip flow over a permeable shrinking cylinder," *Computers and Fluids*, vol. 93, pp. 107–115, 2014.
- [50] Crane, L. J., and McVeigh, A. G., "Slip flow on a body of revolution," *Acta Mechanica*, vol. 224, no. 3, pp. 619–629, 2013.
- [51] Hettiarachchi, H. D. M., Golubovic, M., Worek, W. M., and Minkowycz, W. J., "Three dimensional laminar slip-flow and heat transfer in a rectangular microchannel with constant wall temperature," *International Journal of Heat and Mass Transfer*, vol. 51, no. 21-22, pp. 5088–5096, 2008.
- [52] Kuddusi, L., "Prediction of temperature distribution and Nusselt number in rectangular microchannels at wall slip condition for all versions of constant wall temperature," *International Journal of Thermal Science*, vol. 46, no. 10, pp. 998–1010, 2007.
- [53] Djukic, D. S., "On unsteady magnetic low-speed slip flow in the boundary layer," *Acta Mechanica*, vol. 18, no. 1, pp. 35–48, 1973.
- [54] Barkhordari, M., and Etemad, S. G., "Numerical study of slip flow heat transfer of non-Newtonian fluids in circular micro-channels," *International Journal of Heat and Fluid Flow*, vol. 28, pp. 1027–1033, 2007.
- [55] Kishore, N., and Ramteke, R. R., "Slip in flows of power-law liquids past smooth spherical particles," *Acta Mechanica*, vol. 226, no. 8, pp. 2555-2571, 2015.

- [56] Shateyi, S., and Mabood, F., "MHD mixed convection slip flow near a stagnation-point on a nonlinearly vertical stretching sheet in the presence of viscous dissipation," *Thermal Science*, vol. 21, no. 6B, pp. 219-219, 2015.
- [57] Khan, W. A., Uddin, M. J., and Ismail, A. I. M., "Multiple slip effects on unsteady MHD rear stagnation point flow of nanofluids in a Darcian porous medium," *Journal of Porous Media*, vol. 18, pp. 665–678, 2015.
- [58] Basir, M. F. M., Uddin, M. J., Ismail, A. M., and Bég, O. A., "Nanofluid slip flow over a stretching cylinder with Schmidt and Péclet number effects," *American Institute of Physics Advances*, vol. 6, no. 5, pp. 055316, 2016.
- [59] Rosca, N. C., Rosca, A. V., Aly, E. H., and Pop, I., "Semi-analytical solution for the flow of a nanofluid over a permeable stretching/shrinking sheet with velocity slip using Buongiorno's mathematical model," *European Journal of Mechanics B Fluids*, vol. 58, pp. 39-49, 2016.
- [60] Uddin, M. J., Alginahi, Y., Bég, O. A., and Kabir, M. N., "Numerical solutions for gyrotactic bioconvection in nanofluid-saturated porous media with Stefan blowing and multiple slip effects," *Computers and Mathematics with Applications*, vol. 72, no. 10, pp. 2562-2581, 2016.
- [61] Devi, S. P. A., and Prakash, M., "Temperature dependent viscosity and thermal conductivity effects on hydromagnetic flow over a slendering stretching sheet," *Journal of the Nigerian Mathematical Society*, vol. 34, no. 3, pp. 318-330, 2015.
- [62] Raisinghania, M. D., "Fluid dynamics with complete Hydrodynamics," S.Chand & Company Limited, 7361, Ram Nagar publication, New Delhi-110055, India, 5<sup>th</sup> ed., pp. 764-769, 2003.

## CHAPTER 6: APPENDICES

---

### 6.1 Appendix one

Vector equations are

$$\text{Continuity equation: } \nabla \cdot \vec{V} = 0, \quad (6.1.1)$$

$$\text{Momentum equation: } \rho(\vec{V} \cdot \nabla) \vec{V} = -\nabla p + \mu \nabla^2 \vec{V} + \sigma(\vec{V} \times \vec{B}) \times \vec{B}, \quad (6.1.2)$$

$$\text{Energy equation: } (\vec{V} \cdot \nabla) T = \alpha \nabla^2 T + \tau \left[ D_B \nabla C \cdot \nabla T + \left( \frac{D_T}{T_\infty} \right) \nabla T \cdot \nabla T \right], \quad (6.1.3)$$

$$\text{Concentration equation: } (\vec{V} \cdot \nabla) C = D_B \nabla^2 C + \left( \frac{D_T}{T_\infty} \right) \nabla^2 T, \quad (6.1.4)$$

$$\text{Microorganism equation: } \nabla \cdot (N \vec{V} + N \vec{\tilde{V}} - D_n \nabla N) = 0. \quad (6.1.5)$$

Here,  $\vec{V} = (u, v, 0) = u \hat{x} + v \hat{y}$  is the flow velocity.  $\nabla = \frac{\partial}{\partial x} \hat{x} + \frac{\partial}{\partial y} \hat{y}$  is the vector gradient.

The magnetic field  $\vec{B}$  is applied perpendicular to the flow (Devi and Prakash [61]),  $\therefore \vec{B} = (0, B(x), 0)$ , and  $\vec{\tilde{V}} = \frac{bW_c}{\Delta c} \nabla C$ .

From equation (6.1.1),  $\nabla \cdot \vec{V} = 0$

$$\begin{aligned} &\Rightarrow \left( \frac{\partial}{\partial x} \hat{x} + \frac{\partial}{\partial y} \hat{y} \right) \cdot (u \hat{x} + v \hat{y}) = 0 \\ &\Rightarrow \frac{\partial u}{\partial x} + \frac{\partial v}{\partial y} = 0. \end{aligned} \quad (6.1.6)$$

Let, the dependent variables  $u$  and  $v$ , and independent variables  $x$  and  $y$  are assigned the following measure of scales:  $u \sim U_\infty$ ,  $x \sim L$ , and  $y \sim \delta$ . Where,  $\delta \ll L$ . These are applied to the continuity equation to develop a scale for  $v$ .

Rewriting the continuity equation as  $\frac{\partial u}{\partial x} = -\frac{\partial v}{\partial y}$ . So,  $\frac{v}{\delta} \sim \frac{U_\infty}{L}$ . Solving for  $v$ ,  $v \sim U_\infty \frac{\delta}{L}$ .

#### 6.1.1 Momentum equation:

From equation (6.1.2),

$$\begin{aligned} &\rho(\vec{V} \cdot \nabla) \vec{V} = -\nabla p + \mu \nabla^2 \vec{V} + \sigma(\vec{V} \times \vec{B}) \times \vec{B} \\ &\Rightarrow \rho \left[ (u \hat{x} + v \hat{y}) \cdot \left( \frac{\partial}{\partial x} \hat{x} + \frac{\partial}{\partial y} \hat{y} \right) \right] (u \hat{x} + v \hat{y}) \\ &= -\left( \frac{\partial}{\partial x} \hat{x} + \frac{\partial}{\partial y} \hat{y} \right) p + \mu \left( \frac{\partial^2}{\partial x^2} + \frac{\partial^2}{\partial y^2} \right) (u \hat{x} + v \hat{y}) + \sigma [(u \hat{x} + v \hat{y}) \times B(x) \hat{y}] \times B(x) \hat{y} \\ &\Rightarrow \rho \left( u \frac{\partial}{\partial x} + v \frac{\partial}{\partial y} \right) (u \hat{x} + v \hat{y}) \end{aligned}$$



$$\begin{aligned}
 &= -\left(\frac{\partial p}{\partial x} \hat{x} + \frac{\partial p}{\partial y} \hat{y}\right) + \mu \left(\frac{\partial^2 u}{\partial x^2} \hat{x} + \frac{\partial^2 u}{\partial y^2} \hat{x} + \frac{\partial^2 v}{\partial x^2} \hat{y} + \frac{\partial^2 v}{\partial y^2} \hat{y}\right) + \sigma [\hat{z} u B(x)] \times B(x) \hat{y} \\
 \Rightarrow &\rho \left(u \frac{\partial u}{\partial x} \hat{x} + v \frac{\partial u}{\partial y} \hat{x} + u \frac{\partial v}{\partial x} \hat{y} + v \frac{\partial v}{\partial y} \hat{y}\right) \\
 &= -\left(\frac{\partial p}{\partial x} \hat{x} + \frac{\partial p}{\partial y} \hat{y}\right) + \mu \left(\frac{\partial^2 u}{\partial x^2} \hat{x} + \frac{\partial^2 u}{\partial y^2} \hat{x} + \frac{\partial^2 v}{\partial x^2} \hat{y} + \frac{\partial^2 v}{\partial y^2} \hat{y}\right) - \sigma \hat{x} u B^2(x) \cdot
 \end{aligned}$$

$$\text{The } x\text{- momentum, } \rho \left(u \frac{\partial u}{\partial x} + v \frac{\partial u}{\partial y}\right) = -\frac{\partial p}{\partial x} + \mu \left(\frac{\partial^2 u}{\partial x^2} + \frac{\partial^2 u}{\partial y^2}\right) - \sigma u B^2(x), \quad (6.1.7)$$

$$\text{The } y\text{- momentum, } \rho \left(u \frac{\partial v}{\partial x} + v \frac{\partial v}{\partial y}\right) = -\frac{\partial p}{\partial y} + \mu \left(\frac{\partial^2 v}{\partial x^2} + \frac{\partial^2 v}{\partial y^2}\right). \quad (6.1.8)$$

By the scale analysis, terms of equation (6.1.7) give

$$u \frac{\partial u}{\partial x} \sim U_\infty \frac{U_\infty}{L}, v \frac{\partial u}{\partial y} \sim U_\infty \frac{\delta U_\infty}{L \delta} = U_\infty \frac{U_\infty}{L}, \frac{\partial^2 u}{\partial x^2} \sim \frac{U_\infty}{L^2}, \text{ and } \frac{\partial^2 u}{\partial y^2} \sim \frac{U_\infty}{\delta^2}.$$

If we ignore small terms, equation (6.1.7) implies

$$u \frac{\partial u}{\partial x} + v \frac{\partial u}{\partial y} = -\frac{1}{\rho} \frac{\partial p}{\partial x} + v \frac{\partial^2 u}{\partial y^2} - \frac{\sigma u B^2(x)}{\rho} \quad (6.1.9)$$

as  $y \rightarrow \infty, u = K u_e(x),$

$$\begin{aligned}
 \therefore K u_e \frac{\partial(K u_e)}{\partial x} &= -\frac{1}{\rho} \frac{\partial p}{\partial x} + 0 - \frac{\sigma K u_e B^2(x)}{\rho} \\
 \Rightarrow -\frac{1}{\rho} \frac{\partial p}{\partial x} &= K^2 u_e \frac{d u_e}{d x} + \frac{\sigma K u_e B^2(x)}{\rho}
 \end{aligned}$$

So, equation (6.1.9) becomes

$$\begin{aligned}
 u \frac{\partial u}{\partial x} + v \frac{\partial u}{\partial y} &= K^2 u_e \frac{d u_e}{d x} + \frac{\sigma K u_e B^2(x)}{\rho} + v \frac{\partial^2 u}{\partial y^2} - \frac{\sigma u B^2(x)}{\rho} \\
 \Rightarrow u \frac{\partial u}{\partial x} + v \frac{\partial u}{\partial y} &= K^2 u_e \frac{d u_e}{d x} + v \frac{\partial^2 u}{\partial y^2} - \frac{\sigma(u - K u_e) B^2(x)}{\rho}.
 \end{aligned} \quad (6.1.10)$$

By the scale analysis, terms of equation (6.1.8) give

$$u \frac{\partial v}{\partial x} \sim U_\infty \frac{U_\infty \delta}{L} = \left(\frac{U_\infty}{L}\right)^2 \delta, v \frac{\partial v}{\partial y} \sim U_\infty \frac{\delta U_\infty \delta}{L \delta} = \left(\frac{U_\infty}{L}\right)^2 \delta, \text{ and } \frac{\partial^2 v}{\partial x^2} \sim \frac{U_\infty \delta}{L^2} = \frac{U_\infty \delta}{L^3}.$$

$p, v$  does not depend on  $y$ . So, equation (6.1.8) becomes irrelevant.

### 6.1.2 Energy equation:

From equation (6.1.3),

$$\begin{aligned}
 (\vec{V} \cdot \nabla) T &= \alpha \nabla^2 T + \tau \left[ D_B \nabla C \cdot \nabla T + \left(\frac{D_T}{T_\infty}\right) \nabla T \cdot \nabla T \right] \\
 \Rightarrow \left[ (u \hat{x} + v \hat{y}) \cdot \left(\frac{\partial}{\partial x} \hat{x} + \frac{\partial}{\partial y} \hat{y}\right) \right] T &= \alpha \left(\frac{\partial^2 T}{\partial x^2} + \frac{\partial^2 T}{\partial y^2}\right) \\
 &+ \tau \left[ D_B \left\{ \left(\frac{\partial C}{\partial x} \hat{x} + \frac{\partial C}{\partial y} \hat{y}\right) \cdot \left(\frac{\partial T}{\partial x} \hat{x} + \frac{\partial T}{\partial y} \hat{y}\right) \right\} + \left(\frac{D_T}{T_\infty}\right) \left\{ \left(\frac{\partial T}{\partial x} \hat{x} + \frac{\partial T}{\partial y} \hat{y}\right) \cdot \left(\frac{\partial T}{\partial x} \hat{x} + \frac{\partial T}{\partial y} \hat{y}\right) \right\} \right]
 \end{aligned}$$

$$\Rightarrow u \frac{\partial T}{\partial x} + v \frac{\partial T}{\partial y} = \alpha \left( \frac{\partial^2 T}{\partial x^2} + \frac{\partial^2 T}{\partial y^2} \right) + \tau \left[ D_B \left( \frac{\partial C}{\partial x} \frac{\partial T}{\partial x} + \frac{\partial C}{\partial y} \frac{\partial T}{\partial y} \right) + \left( \frac{D_T}{T_\infty} \right) \left\{ \left( \frac{\partial T}{\partial x} \right)^2 + \left( \frac{\partial T}{\partial y} \right)^2 \right\} \right]. \quad (6.1.11)$$

By the scale analysis, terms of equation (6.1.11) give

$$u \frac{\partial T}{\partial x} \sim U_\infty \frac{\Delta T}{L}, v \frac{\partial T}{\partial y} \sim U_\infty \frac{\delta \Delta T}{L \delta} = U_\infty \frac{\Delta T}{L}, \frac{\partial^2 T}{\partial x^2} \sim \frac{\Delta T}{L^2}, \frac{\partial^2 T}{\partial y^2} \sim \frac{\Delta T}{\delta^2}, \frac{\partial C}{\partial x} \frac{\partial T}{\partial x} \sim \frac{\Delta C \Delta T}{L^2}, \frac{\partial C}{\partial y} \frac{\partial T}{\partial y} \sim \frac{\Delta C \Delta T}{\delta^2},$$

$$\left( \frac{\partial T}{\partial x} \right)^2 \sim \left( \frac{\Delta T}{L} \right)^2, \text{ and } \left( \frac{\partial T}{\partial y} \right)^2 \sim \left( \frac{\Delta T}{\delta} \right)^2.$$

If we ignore small terms, equation (6.1.11) becomes

$$u \frac{\partial T}{\partial x} + v \frac{\partial T}{\partial y} = \alpha \frac{\partial^2 T}{\partial y^2} + \tau \left[ D_B \frac{\partial C}{\partial y} \frac{\partial T}{\partial y} + \left( \frac{D_T}{T_\infty} \right) \left( \frac{\partial T}{\partial y} \right)^2 \right]. \quad (6.1.12)$$

### 6.1.3 Concentration equation:

From equation (6.1.4),

$$\begin{aligned} (\vec{V} \cdot \nabla) C &= D_B \nabla^2 C + \left( \frac{D_T}{T_\infty} \right) \nabla^2 T \\ \Rightarrow \left[ (u \hat{x} + v \hat{y}) \cdot \left( \frac{\partial}{\partial x} \hat{x} + \frac{\partial}{\partial y} \hat{y} \right) \right] C &= D_B \left( \frac{\partial^2 C}{\partial x^2} + \frac{\partial^2 C}{\partial y^2} \right) + \left( \frac{D_T}{T_\infty} \right) \left( \frac{\partial^2 T}{\partial x^2} + \frac{\partial^2 T}{\partial y^2} \right) \\ \Rightarrow u \frac{\partial C}{\partial x} + v \frac{\partial C}{\partial y} &= D_B \left( \frac{\partial^2 C}{\partial x^2} + \frac{\partial^2 C}{\partial y^2} \right) + \left( \frac{D_T}{T_\infty} \right) \left( \frac{\partial^2 T}{\partial x^2} + \frac{\partial^2 T}{\partial y^2} \right). \end{aligned} \quad (6.1.13)$$

By the scale analysis, terms of equation (6.1.13) give

$$u \frac{\partial C}{\partial x} \sim U_\infty \frac{\Delta C}{L}, v \frac{\partial C}{\partial y} \sim U_\infty \frac{\delta \Delta C}{L \delta} = U_\infty \frac{\Delta C}{L}, \frac{\partial^2 C}{\partial x^2} \sim \frac{\Delta C}{L^2}, \frac{\partial^2 C}{\partial y^2} \sim \frac{\Delta C}{\delta^2}, \frac{\partial^2 T}{\partial x^2} \sim \frac{\Delta T}{L^2}, \text{ and } \frac{\partial^2 T}{\partial y^2} \sim \frac{\Delta T}{\delta^2}.$$

Equation (6.1.13) becomes

$$u \frac{\partial C}{\partial x} + v \frac{\partial C}{\partial y} = D_B \frac{\partial^2 C}{\partial y^2} + \left( \frac{D_T}{T_\infty} \right) \frac{\partial^2 T}{\partial y^2}. \quad (6.1.14)$$

### 6.1.4 Microorganism equation:

From equation (6.1.5),

$$\begin{aligned} \nabla \cdot (N \vec{V} + N \vec{V} - D_n \nabla N) &= 0 \\ \Rightarrow \left( \frac{\partial}{\partial x} \hat{x} + \frac{\partial}{\partial y} \hat{y} \right) \cdot \left[ N(u \hat{x} + v \hat{y}) + N \vec{V} - D_n \left( \frac{\partial}{\partial x} \hat{x} + \frac{\partial}{\partial y} \hat{y} \right) N \right] &= 0 \\ \Rightarrow \left( \frac{\partial}{\partial x} \hat{x} + \frac{\partial}{\partial y} \hat{y} \right) \cdot \left[ (Nu \hat{x} + Nv \hat{y}) + N \frac{bW_c}{\Delta C} \nabla C - D_n \left( \frac{\partial N}{\partial x} \hat{x} + \frac{\partial N}{\partial y} \hat{y} \right) \right] &= 0 \\ \Rightarrow \frac{\partial(Nu)}{\partial x} + \frac{\partial(Nv)}{\partial y} + \left( \frac{\partial}{\partial x} \hat{x} + \frac{\partial}{\partial y} \hat{y} \right) \cdot \left[ N \frac{bW_c}{\Delta C} \left( \frac{\partial C}{\partial x} \hat{x} + \frac{\partial C}{\partial y} \hat{y} \right) \right] &= D_n \left( \frac{\partial^2 N}{\partial x^2} + \frac{\partial^2 N}{\partial y^2} \right) \\ \Rightarrow N \left( \frac{\partial u}{\partial x} + \frac{\partial v}{\partial y} \right) + u \frac{\partial N}{\partial x} + v \frac{\partial N}{\partial y} + \frac{\partial}{\partial x} \left( N \frac{bW_c}{\Delta C} \frac{\partial C}{\partial x} \right) + \frac{\partial}{\partial y} \left( N \frac{bW_c}{\Delta C} \frac{\partial C}{\partial y} \right) &= D_n \left( \frac{\partial^2 N}{\partial x^2} + \frac{\partial^2 N}{\partial y^2} \right) \end{aligned}$$

$$\Rightarrow u \frac{\partial N}{\partial x} + v \frac{\partial N}{\partial y} + N \frac{bW_c}{\Delta C} \frac{\partial^2 C}{\partial x^2} + \frac{bW_c}{\Delta C} \frac{\partial C}{\partial x} \frac{\partial N}{\partial x} + \frac{\partial}{\partial y} (N\tilde{v}) = D_n \left( \frac{\partial^2 N}{\partial x^2} + \frac{\partial^2 N}{\partial y^2} \right). \quad (6.1.15)$$

By the scale analysis, terms of equation (6.1.15) give

$$u \frac{\partial N}{\partial x} \sim U_\infty \frac{\Delta N}{L}, v \frac{\partial C}{\partial y} \sim U_\infty \frac{\delta \Delta N}{L \delta} = U_\infty \frac{\Delta N}{L}, \frac{\partial^2 C}{\partial x^2} \sim \frac{\Delta C}{L^2}, \frac{\partial C}{\partial x} \frac{\partial N}{\partial x} \sim \frac{\Delta C \Delta N}{L^2}, \frac{\partial^2 C}{\partial y^2} \sim \frac{\Delta C}{\delta^2}, \frac{\partial^2 N}{\partial x^2} \sim \frac{\Delta N}{L^2},$$

and  $\frac{\partial^2 N}{\partial y^2} \sim \frac{\Delta N}{\delta^2}$ .

Equation (6.1.15) becomes

$$u \frac{\partial N}{\partial x} + v \frac{\partial N}{\partial y} + \frac{\partial}{\partial y} (N\tilde{v}) = D_n \frac{\partial^2 N}{\partial y^2}. \quad (6.1.16)$$

## 6.2 Appendix two

$$\text{Continuity equation: } \frac{\partial u}{\partial x} + \frac{\partial v}{\partial y} = 0, \quad (6.2.1)$$

$$\text{Momentum equation: } u \frac{\partial u}{\partial x} + v \frac{\partial u}{\partial y} = K^2 u_e \frac{du_e}{dx} + v \frac{\partial^2 u}{\partial y^2} - \frac{\sigma(u - Ku_e)B^2(x)}{\rho}, \quad (6.2.2)$$

$$\text{Energy equation: } u \frac{\partial T}{\partial x} + v \frac{\partial T}{\partial y} = \alpha \frac{\partial^2 T}{\partial y^2} + \tau \left[ D_B \frac{\partial C}{\partial y} \frac{\partial T}{\partial y} + \left( \frac{D_T}{T_\infty} \right) \left( \frac{\partial T}{\partial y} \right)^2 \right], \quad (6.2.3)$$

$$\text{Concentration equation: } u \frac{\partial C}{\partial x} + v \frac{\partial C}{\partial y} = D_B \frac{\partial^2 C}{\partial y^2} + \left( \frac{D_T}{T_\infty} \right) \frac{\partial^2 T}{\partial y^2}, \quad (6.2.4)$$

$$\text{Microorganism equation: } u \frac{\partial N}{\partial x} + v \frac{\partial N}{\partial y} + \frac{\partial}{\partial y} (N\tilde{v}) = D_n \frac{\partial^2 N}{\partial y^2}. \quad (6.2.5)$$

The boundary conditions are

$$u = N_1(x)v \frac{\partial u}{\partial y}, v = -\frac{D_B}{1-C_w} \frac{\partial C}{\partial y}, T = T_w + D_1(x) \frac{\partial T}{\partial y}, \quad (6.2.6)$$

$$C = C_w + E_1(x) \frac{\partial C}{\partial y}, N = N_w + F_1(x) \frac{\partial N}{\partial y} \text{ at } y = 0.$$

$$u = Ku_e(x) = Ka_0 x^m, T = T_\infty, C = C_\infty, N = N_\infty = 0 \text{ as } y \rightarrow \infty. \quad (6.2.7)$$

By substituting these following similarity variables into equations (6.2.1)-(6.2.7),

$$\psi = \sqrt{u_e(x)vx} f(\eta), \eta = \sqrt{\frac{u_e(x)}{vx}} y, \theta(\eta) = \frac{T-T_\infty}{\Delta T}, \phi(\eta) = \frac{C-C_\infty}{\Delta C}, \chi(\eta) = \frac{N-N_\infty}{\Delta N},$$

$$u = u_e(x) f'(\eta), v = -\left(\frac{m+1}{2}\right) \sqrt{\frac{u_e(x)v}{x}} \left[ f(\eta) + \left(\frac{m-1}{m+1}\right) \eta f'(\eta) \right], \tilde{v} = \left(\frac{bW_c}{\Delta C}\right) \frac{\partial C}{\partial y},$$

$$\Delta T = T_w - T_\infty, \Delta C = C_w - C_\infty, \Delta N = N_w - N_\infty.$$

Here  $\psi$  is the stream function defined as  $u = \frac{\partial \psi}{\partial y}$  and  $v = -\frac{\partial \psi}{\partial x}$ .

$$\begin{aligned}
 \frac{\partial u}{\partial x} &= \frac{\partial}{\partial x} \{u_e(x)f'(\eta)\} = \frac{\partial}{\partial x} \{a_0 x^m f'\} = a_0 m x^{m-1} f' + a_0 x^m f'' \frac{\partial \eta}{\partial x} \\
 &= \frac{m}{x} u_e f' + u_e f'' \frac{\partial}{\partial x} \left( \sqrt{\frac{a_0 x^m}{\nu x}} y \right) = \frac{m}{x} u_e f' + u_e f'' \left( \frac{m-1}{2} \right) x^{\frac{m-1}{2}-1} \sqrt{\frac{a_0}{\nu}} y \\
 &= \frac{m}{x} u_e f' + \frac{u_e}{x} f'' \left( \frac{m-1}{2} \right) \sqrt{\frac{a_0 x^m}{\nu x}} y = \frac{m}{x} u_e f' + \frac{u_e}{x} f'' \left( \frac{m-1}{2} \right) \sqrt{\frac{u_e}{\nu x}} y \\
 \therefore u \frac{\partial u}{\partial x} &= u_e(x) f' \left[ \frac{m}{x} u_e f' + \frac{u_e}{x} f'' \left( \frac{m-1}{2} \right) \sqrt{\frac{u_e}{\nu x}} y \right] \\
 &= \frac{u_e^2}{x} \left[ m f'^2 + \left( \frac{m-1}{2} \right) f' f'' \eta \right] \tag{6.2.8}
 \end{aligned}$$

$$\begin{aligned}
 \frac{\partial u}{\partial y} &= \frac{\partial}{\partial y} \{u_e(x)f'(\eta)\} = u_e f'' \frac{\partial \eta}{\partial y} = u_e f'' \sqrt{\frac{u_e}{\nu x}} \\
 v \frac{\partial u}{\partial y} &= - \left( \frac{m+1}{2} \right) \sqrt{\frac{u_e \nu}{x}} \left[ f + \left( \frac{m-1}{m+1} \right) \eta f' \right] u_e f'' \sqrt{\frac{u_e}{\nu x}} \\
 \therefore v \frac{\partial u}{\partial y} &= - \frac{u_e^2}{2x} [(m+1) f f'' + (m-1) \eta f' f''] \tag{6.2.9}
 \end{aligned}$$

$$K^2 u_e \frac{du_e}{dx} = K^2 u_e a_0 m x^{m-1} = \frac{m K^2}{x} u_e^2 \tag{6.2.10}$$

$$\begin{aligned}
 v \frac{\partial^2 u}{\partial y^2} &= v \frac{\partial}{\partial y} \left( u_e f'' \sqrt{\frac{u_e}{\nu x}} \right) = \nu u_e \sqrt{\frac{u_e}{\nu x}} f''' \frac{\partial \eta}{\partial y} = \nu u_e \sqrt{\frac{u_e}{\nu x}} f''' \sqrt{\frac{u_e}{\nu x}} = \frac{u_e^2}{x} f''' \\
 \therefore v \frac{\partial^2 u}{\partial y^2} &= \frac{u_e^2}{x} f''' \tag{6.2.11}
 \end{aligned}$$

$$\begin{aligned}
 u \frac{\partial T}{\partial x} &= u_e f' \frac{\partial}{\partial x} (\Delta T \theta + T_\infty) = u_e f' \Delta T \theta' \frac{\partial \eta}{\partial x} = u_e f' \Delta T \theta' \left( \frac{m-1}{2x} \right) \eta = u_e \Delta T \left( \frac{m-1}{2x} \right) \eta f' \theta' \\
 \therefore u \frac{\partial T}{\partial x} &= u_e \Delta T \left( \frac{m-1}{2x} \right) \eta f' \theta' \tag{6.2.12}
 \end{aligned}$$

$$\begin{aligned}
 v \frac{\partial T}{\partial y} &= - \left( \frac{m+1}{2} \right) \sqrt{\frac{u_e \nu}{x}} \left[ f + \left( \frac{m-1}{m+1} \right) \eta f' \right] \frac{\partial}{\partial y} (\Delta T \theta + T_\infty) \\
 &= - \frac{1}{2} \sqrt{\frac{u_e \nu}{x}} [(m+1) f + (m-1) \eta f'] \Delta T \theta' \frac{\partial \eta}{\partial y} \\
 &= - \frac{1}{2} \sqrt{\frac{u_e \nu}{x}} [(m+1) f + (m-1) \eta f'] \Delta T \theta' \sqrt{\frac{u_e}{\nu x}} \\
 &= - \Delta T \frac{u_e}{2x} [(m+1) f \theta' + (m-1) \eta f' \theta'] \\
 \therefore v \frac{\partial T}{\partial y} &= - \Delta T \frac{u_e}{2x} [(m+1) f \theta' + (m-1) \eta f' \theta'] \tag{6.2.13}
 \end{aligned}$$

$$\frac{\partial^2 T}{\partial y^2} = \frac{\partial}{\partial y} \left\{ \frac{\partial}{\partial y} (\Delta T \theta + T_\infty) \right\} = \frac{\partial}{\partial y} \left\{ \Delta T \theta' \frac{\partial \eta}{\partial y} \right\} = \frac{\partial}{\partial y} \left\{ \Delta T \theta' \sqrt{\frac{u_e}{\nu x}} \right\} = \Delta T \frac{u_e}{\nu x} \theta'' \tag{6.2.14}$$

$$\begin{aligned} \frac{\partial C}{\partial y} &= \frac{\partial}{\partial y} (\Delta C \phi + C_\infty) = \Delta C \phi' \frac{\partial \eta}{\partial y} = \Delta C \phi' \sqrt{\frac{u_e}{\nu x}} \\ \therefore \frac{\partial C}{\partial y} \frac{\partial T}{\partial y} &= \Delta C \phi' \sqrt{\frac{u_e}{\nu x}} \Delta T \theta' \sqrt{\frac{u_e}{\nu x}} = \Delta C \Delta T \phi' \theta' \frac{u_e}{\nu x} \end{aligned} \quad (6.2.15)$$

$$\left(\frac{\partial T}{\partial y}\right)^2 = \left(\Delta T \theta' \sqrt{\frac{u_e}{\nu x}}\right)^2 = (\Delta T)^2 \frac{u_e}{\nu x} \theta'^2 \quad (6.2.16)$$

$$u \frac{\partial C}{\partial x} = u_e f' \frac{\partial}{\partial x} (\Delta C \phi + C_\infty) = u_e f' \Delta C \phi' \frac{\partial \eta}{\partial x} = u_e \Delta C \left(\frac{m-1}{2x}\right) f' \phi' \eta \quad (6.2.17)$$

$$\begin{aligned} v \frac{\partial C}{\partial y} &= -\left(\frac{m+1}{2}\right) \sqrt{\frac{u_e \nu}{x}} \left[f + \left(\frac{m-1}{m+1}\right) \eta f'\right] \Delta C \phi' \sqrt{\frac{u_e}{\nu x}} = -\frac{\Delta C u_e}{2x} [(m+1)f\phi' + (m-1)\eta f'\phi'] \\ \therefore v \frac{\partial C}{\partial y} &= -\frac{\Delta C u_e}{2x} [(m+1)f\phi' + (m-1)\eta f'\phi'] \end{aligned} \quad (6.2.18)$$

$$\frac{\partial^2 C}{\partial y^2} = \frac{\partial}{\partial y} \left\{ \frac{\partial}{\partial y} (\Delta C \phi + C_\infty) \right\} = \frac{\partial}{\partial y} \left\{ \Delta C \phi' \frac{\partial \eta}{\partial y} \right\} = \frac{\partial}{\partial y} \left\{ \Delta C \phi' \sqrt{\frac{u_e}{\nu x}} \right\} = \Delta C \frac{u_e}{\nu x} \phi'' \quad (6.2.19)$$

$$u \frac{\partial N}{\partial x} = u_e f' \frac{\partial}{\partial x} (\Delta N \chi + N_\infty) = u_e f' \Delta N \chi' \frac{\partial \eta}{\partial x} = u_e \Delta N \left(\frac{m-1}{2x}\right) f' \chi' \eta \quad (6.2.20)$$

$$\begin{aligned} \frac{\partial N}{\partial y} &= \frac{\partial}{\partial y} (\Delta N \phi + N_\infty) = \Delta N \chi' \frac{\partial \eta}{\partial y} = \Delta N \chi' \sqrt{\frac{u_e}{\nu x}} \\ v \frac{\partial N}{\partial y} &= -\left(\frac{m+1}{2}\right) \sqrt{\frac{u_e \nu}{x}} \left[f + \left(\frac{m-1}{m+1}\right) \eta f'\right] \Delta N \chi' \sqrt{\frac{u_e}{\nu x}} = -\frac{\Delta N u_e}{2x} [(m+1)f\chi' + (m-1)\eta f'\chi'] \\ \therefore v \frac{\partial N}{\partial y} &= -\frac{\Delta N u_e}{2x} [(m+1)f\chi' + (m-1)\eta f'\chi'] \end{aligned} \quad (6.2.21)$$

$$\begin{aligned} \frac{\partial}{\partial y} (N \tilde{v}) &= \frac{\partial}{\partial y} \left( (\Delta N \chi + N_\infty) \frac{bW_c}{\Delta C} \frac{\partial C}{\partial y} \right) = \frac{bW_c}{\Delta C} \left[ \frac{\partial C}{\partial y} \Delta N \chi' \frac{\partial \eta}{\partial y} + \Delta N \chi \frac{\partial^2 C}{\partial y^2} \right] (\because N_\infty = 0) \\ \therefore \frac{\partial}{\partial y} (N \tilde{v}) &= \frac{bW_c}{\Delta C} \left[ \Delta C \phi' \sqrt{\frac{u_e}{\nu x}} \Delta N \chi' \sqrt{\frac{u_e}{\nu x}} + \Delta N \chi \Delta C \frac{u_e}{\nu x} \phi'' \right] \end{aligned} \quad (6.2.22)$$

$$\frac{\partial^2 N}{\partial y^2} = \frac{\partial}{\partial y} \left\{ \frac{\partial}{\partial y} (\Delta N \chi + N_\infty) \right\} = \frac{\partial}{\partial y} \left\{ \Delta N \chi' \frac{\partial \eta}{\partial y} \right\} = \frac{\partial}{\partial y} \left\{ \Delta N \chi' \sqrt{\frac{u_e}{\nu x}} \right\} = \Delta N \frac{u_e}{\nu x} \chi'' \quad (6.2.23)$$

Using the above equations, the governing system of partial differential equations become,

### 6.2.1 Momentum equation:

$$\begin{aligned} u \frac{\partial u}{\partial x} + v \frac{\partial u}{\partial y} &= K^2 u_e \frac{du_e}{dx} + v \frac{\partial^2 u}{\partial y^2} - \frac{\sigma(u - Ku_e)B^2(x)}{\rho} \\ \Rightarrow \frac{u_e^2}{x} \left[ m f'^2 + \left(\frac{m-1}{2}\right) f' f'' \eta \right] &- \frac{u_e^2}{2x} [(m+1)ff'' + (m-1)\eta f' f''] \\ &= \frac{mK^2}{x} u_e^2 + \frac{u_e^2}{x} f''' - \frac{\sigma(u - Ku_e)B^2(x)}{\rho} \end{aligned}$$

$$\begin{aligned}
 &\Rightarrow mf'^2 + \left(\frac{m-1}{2}\right) f' f'' \eta - \left(\frac{m+1}{2}\right) f f'' - \left(\frac{m-1}{2}\right) \eta f' f'' \\
 &\quad = mK^2 + f''' - \frac{\sigma(u-Ku_e)B^2(x)}{\rho} \frac{x}{u_e^2} \\
 &\Rightarrow f''' + mK^2 - mf'^2 + \left(\frac{m+1}{2}\right) f f'' - \frac{\sigma(u_e f' - Ku_e)B^2(x)}{\rho} \frac{x}{u_e^2} = 0 \\
 &\Rightarrow f''' + mK^2 - mf'^2 + \left(\frac{m+1}{2}\right) f f'' - (f' - K) \frac{\sigma x B^2(x)}{\rho a_0 x^m} = 0 \\
 &\Rightarrow f''' + mK^2 - mf'^2 + \left(\frac{m+1}{2}\right) f f'' - (f' - K) \frac{\sigma B^2(x) x^{1-m}}{\rho a_0} = 0 \\
 &\Rightarrow f''' + mK^2 - mf'^2 + \left(\frac{m+1}{2}\right) f f'' - (f' - K) \frac{\sigma B_0^2(x)}{\rho a_0} = 0 \\
 &\Rightarrow f''' + mK^2 - mf'^2 + \left(\frac{m+1}{2}\right) f f'' - M(f' - K) = 0. \tag{6.2.24}
 \end{aligned}$$

$$\text{Here, } M = \frac{\sigma B_0^2(x)}{\rho a_0}.$$

### 6.2.2 Energy equation:

$$\begin{aligned}
 &u \frac{\partial T}{\partial x} + v \frac{\partial T}{\partial y} = \alpha \frac{\partial^2 T}{\partial y^2} + \tau \left[ D_B \frac{\partial C}{\partial y} \frac{\partial T}{\partial y} + \left(\frac{D_T}{T_\infty}\right) \left(\frac{\partial T}{\partial y}\right)^2 \right] \\
 &\Rightarrow u_e \Delta T \left(\frac{m-1}{2x}\right) \eta f' \theta' - \Delta T \frac{u_e}{2x} [(m+1)f\theta' + (m-1)\eta f' \theta'] \\
 &\quad = \alpha \Delta T \frac{u_e}{vx} \theta'' + \tau D_B \Delta C \Delta T \phi' \theta' \frac{u_e}{vx} + \tau \left(\frac{D_T}{T_\infty}\right) (\Delta T)^2 \frac{u_e}{vx} \theta'^2 \\
 &\Rightarrow \frac{\alpha}{v} \theta'' + \frac{\tau D_B \Delta C}{v} \phi' \theta' + \frac{\tau \Delta T D_T}{v T_\infty} \theta'^2 + \left(\frac{m+1}{2}\right) f \theta' = 0 \\
 &\Rightarrow \frac{1}{Pr} \theta'' + \left(\frac{m+1}{2}\right) f \theta' + \frac{\tau D_B \Delta C}{\alpha} \frac{\alpha}{v} \phi' \theta' + \frac{\tau \Delta T D_T}{\alpha T_\infty} \frac{\alpha}{v} \theta'^2 = 0 \\
 &\Rightarrow \frac{1}{Pr} \theta'' + \left(\frac{m+1}{2}\right) f \theta' + \frac{Nb}{Pr} \phi' \theta' + \frac{Nt}{Pr} \theta'^2 = 0 \\
 &\Rightarrow \theta'' + Pr \left(\frac{m+1}{2}\right) f \theta' + Nb \phi' \theta' + Nt \theta'^2 = 0. \tag{6.2.25}
 \end{aligned}$$

$$\text{Here, } Pr = \frac{v}{\alpha}, Nb = \frac{\tau D_B \Delta C}{\alpha}, \text{ and } Nt = \frac{\tau D_T \Delta T}{T_\infty \alpha}.$$

### 6.2.3 Concentration equation:

$$\begin{aligned}
 &u \frac{\partial C}{\partial x} + v \frac{\partial C}{\partial y} = D_B \frac{\partial^2 C}{\partial y^2} + \left(\frac{D_T}{T_\infty}\right) \frac{\partial^2 T}{\partial y^2} \\
 &\Rightarrow u_e \Delta C \left(\frac{m-1}{2x}\right) f' \phi' \eta - \frac{\Delta C u_e}{2x} [(m+1)f\phi' + (m-1)\eta f' \phi'] \\
 &\quad = D_B \Delta C \frac{u_e}{vx} \phi'' + \left(\frac{D_T}{T_\infty}\right) \Delta T \frac{u_e}{vx} \theta'' \\
 &\Rightarrow \frac{D_B \Delta C}{v} \phi'' + \frac{\Delta T D_T}{v T_\infty} \theta'' + \Delta C \left(\frac{m+1}{2}\right) f \phi' = 0 \\
 &\Rightarrow \phi'' + \frac{\Delta T D_T}{\Delta C D_B T_\infty} \theta'' + \left(\frac{m+1}{2}\right) \frac{v}{D_B} f \phi' = 0
 \end{aligned}$$

$$\begin{aligned} \Rightarrow \phi'' + \left(\frac{m+1}{2}\right) \frac{v}{\alpha D_B} f \phi' + \frac{\tau \Delta T D_T}{\alpha T_\infty} \frac{\alpha}{\tau \Delta C D_B} \theta'' &= 0 \\ \Rightarrow \phi'' + \left(\frac{m+1}{2}\right) Le Pr f \phi' + \frac{Nt}{Nb} \theta'' &= 0. \end{aligned} \quad (6.2.26)$$

Here,  $Le = \frac{\alpha}{D_B}$ ,  $Pr = \frac{v}{\alpha}$ ,  $Nb = \frac{\tau D_B \Delta C}{\alpha}$ , and  $Nt = \frac{\tau D_T \Delta T}{T_\infty \alpha}$ .

#### 6.2.4 Microorganism equation:

$$\begin{aligned} u \frac{\partial N}{\partial x} + v \frac{\partial N}{\partial y} + \frac{\partial}{\partial y} (N \tilde{v}) &= D_n \frac{\partial^2 N}{\partial y^2} \\ \Rightarrow u_e \Delta N \left(\frac{m-1}{2x}\right) f' \chi' \eta - \frac{\Delta N u_e}{2x} [(m+1)f\chi' + (m-1)\eta f' \chi'] \\ &+ \frac{bW_c}{\Delta C} \left[ \Delta C \phi' \sqrt{\frac{u_e}{vx}} \Delta N \chi' \sqrt{\frac{u_e}{vx}} + \Delta N \chi \Delta C \frac{u_e}{vx} \phi'' \right] = D_n \Delta N \frac{u_e}{vx} \chi'' \\ \Rightarrow \chi'' + \left(\frac{m+1}{2}\right) \frac{v}{D_n} f \chi' - \frac{bW_c}{D_n} [\phi' \chi' + \phi'' \chi] &= 0 \\ \Rightarrow \chi'' + \left(\frac{m+1}{2}\right) Lb f \chi' - Pe [\phi' \chi' + \phi'' \chi] &= 0. \end{aligned} \quad (6.2.27)$$

Here,  $Lb = \frac{v}{D_n}$ , and  $Pe = \frac{bW_c}{D_n}$ .

#### 6.2.5 Boundary conditions

The boundary conditions are transformed as,

$$\begin{aligned} u &= N_1(x) v \frac{\partial u}{\partial y} \\ \Rightarrow u_e(x) f'(\eta) &= N_1(x) v u_e(x) f''(\eta) \sqrt{\frac{u_e(x)}{vx}} \\ \Rightarrow f'(\eta) &= N_1(x) v f''(\eta) \sqrt{\frac{a_0 x^m}{vx}} \\ \Rightarrow f'(\eta) &= N_1(x) x^{\frac{m-1}{2}} f''(\eta) \sqrt{v a_0} \\ \Rightarrow f'(\eta) &= (N_1)_0 f''(\eta) \sqrt{v a_0} \\ \Rightarrow f'(\eta) &= a f''(\eta) \\ \therefore f'(0) &= a f''(0). \end{aligned} \quad (6.2.28)$$

Here,  $a = (N_1)_0 \sqrt{v a_0}$ , and  $(N_1)_0 = N_1(x) x^{\frac{m-1}{2}}$ .

$$\begin{aligned} v &= -\frac{D_B}{1-c_w} \frac{\partial C}{\partial y} \\ \Rightarrow -\left(\frac{m+1}{2}\right) \sqrt{\frac{u_e(x)v}{x}} [f(\eta) + \left(\frac{m-1}{m+1}\right) \eta f'(\eta)] &= -\frac{D_B}{1-c_w} \Delta C \phi'(\eta) \sqrt{\frac{u_e}{vx}} \end{aligned}$$

$$\begin{aligned}
 &\Rightarrow \left(\frac{m+1}{2}\right) \left[ f(\eta) + \left(\frac{m-1}{m+1}\right) \eta f'(\eta) \right] = \frac{D_B}{v} \frac{\Delta C}{1-C_w} \phi'(\eta) \\
 &\Rightarrow \left(\frac{m+1}{2}\right) \left[ f(0) + \left(\frac{m-1}{m+1}\right) \cdot 0 \cdot f'(0) \right] = \frac{D_B}{v} \frac{\Delta C}{1-C_w} \phi'(0), (\eta = 0) \\
 &\Rightarrow \left(\frac{m+1}{2}\right) f(0) = \frac{1}{\frac{D_B}{v}} S \phi'(0) \\
 &\Rightarrow f(0) = \frac{2S}{(m+1)} \frac{1}{\frac{v}{\alpha} \frac{1}{D_B}} \phi'(0) \\
 &\Rightarrow f(0) = \frac{2S}{(m+1)} \frac{1}{PrLe} \phi'(0) \cdot \tag{6.2.29}
 \end{aligned}$$

$$\text{Here, } S = \frac{\Delta C}{1-C_w}.$$

$$\begin{aligned}
 T &= T_w + D_1(x) \frac{\partial T}{\partial y} \\
 &\Rightarrow \Delta T \theta(\eta) + T_\infty = T_w + D_1(x) \Delta T \theta'(\eta) \sqrt{\frac{u_e}{\nu x}} \\
 &\Rightarrow \Delta T \theta(\eta) = T_w - T_\infty + D_1(x) \Delta T \theta'(\eta) \sqrt{\frac{a_0 x^m}{\nu x}} \\
 &\Rightarrow \Delta T \theta(\eta) = \Delta T + D_1(x) x^{\frac{m-1}{2}} \Delta T \theta'(\eta) \sqrt{\frac{a_0}{\nu}} \\
 &\Rightarrow \theta(\eta) = 1 + (D_1)_0 \sqrt{\frac{a_0}{\nu}} \theta'(\eta) \\
 &\Rightarrow \theta(\eta) = 1 + b \theta'(\eta) \\
 \therefore \theta(0) &= 1 + b \theta'(0) \cdot \tag{6.2.30}
 \end{aligned}$$

$$\text{Here, } b = (D_1)_0 \sqrt{\frac{a_0}{\nu}}, \text{ and } (D_1)_0 = D_1(x) x^{\frac{m-1}{2}}.$$

$$\begin{aligned}
 C &= C_w + E_1(x) \frac{\partial C}{\partial y} \\
 &\Rightarrow \Delta C \phi(\eta) + C_\infty = C_w + E_1(x) \Delta C \phi'(\eta) \sqrt{\frac{u_e}{\nu x}} \\
 &\Rightarrow \Delta C \phi(\eta) = C_w - C_\infty + E_1(x) \Delta C \phi'(\eta) \sqrt{\frac{a_0 x^m}{\nu x}} \\
 &\Rightarrow \Delta C \phi(\eta) = \Delta C + E_1(x) x^{\frac{m-1}{2}} \Delta C \phi'(\eta) \sqrt{\frac{a_0}{\nu}} \\
 &\Rightarrow \phi(\eta) = 1 + (E_1)_0 \sqrt{\frac{a_0}{\nu}} \phi'(\eta) \\
 &\Rightarrow \phi(\eta) = 1 + d \phi'(\eta) \\
 \therefore \phi(0) &= 1 + d \phi'(0) \cdot \tag{6.2.31}
 \end{aligned}$$



Here,  $d = (E_1)_0 \sqrt{\frac{a_0}{v}}$  and  $(E_1)_0 = E_1(x) x^{\frac{m-1}{2}}$ .

$$\begin{aligned}
 N &= N_w + F_1(x) \frac{\partial N}{\partial y} \\
 \Rightarrow \Delta N \chi(\eta) + N_\infty &= N_w + F_1(x) \Delta N \chi'(\eta) \sqrt{\frac{u_e}{vx}} \\
 \Rightarrow \Delta N \chi(\eta) &= N_w - N_\infty + F_1(x) \Delta N \chi'(\eta) \sqrt{\frac{a_0 x^m}{vx}} \\
 \Rightarrow \Delta N \chi(\eta) &= \Delta N + F_1(x) x^{\frac{m-1}{2}} \Delta N \chi'(\eta) \sqrt{\frac{a_0}{v}} \\
 \Rightarrow \chi(\eta) &= 1 + (F_1)_0 \sqrt{\frac{a_0}{v}} \chi'(\eta) \\
 \Rightarrow \chi(\eta) &= 1 + e \chi'(\eta) \\
 \therefore \chi(0) &= 1 + e \chi'(0). \tag{6.2.32}
 \end{aligned}$$

Here,  $e = (F_1)_0 \sqrt{\frac{a_0}{v}}$ , and  $(F_1)_0 = F_1(x) x^{\frac{m-1}{2}}$ .

$$\begin{aligned}
 u &= u_e(x) f'(\eta) \\
 \Rightarrow K u_e(x) &= u_e(x) f'(\eta) \\
 \Rightarrow f'(\infty) &= K, \text{ (as } y \rightarrow \infty, \eta \rightarrow \infty). \tag{6.2.33}
 \end{aligned}$$

$$\begin{aligned}
 \theta(\eta) &= \frac{T - T_\infty}{\Delta T} \\
 \Rightarrow \theta(\infty) &= 0, \text{ (as } y \rightarrow \infty, \eta \rightarrow \infty, \text{ and } T = T_\infty). \tag{6.2.34}
 \end{aligned}$$

$$\begin{aligned}
 \phi(\eta) &= \frac{C - C_\infty}{\Delta C} \\
 \Rightarrow \phi(\infty) &= 0, \text{ (as } y \rightarrow \infty, \eta \rightarrow \infty, \text{ and } C = C_\infty). \tag{6.2.35}
 \end{aligned}$$

$$\begin{aligned}
 \chi(\eta) &= \frac{N - N_\infty}{\Delta N} \\
 \Rightarrow \chi(\infty) &= 0, \text{ (as } y \rightarrow \infty, \eta \rightarrow \infty, \text{ and } N = N_\infty = 0). \tag{6.2.36}
 \end{aligned}$$

### 6.3 Appendix three

#### 6.3.1 Skin friction coefficient

$$\begin{aligned} C_{fx} &= \frac{\nu}{u_e^2(x)} \left( \frac{\partial u}{\partial y} \right)_{y=0} = \frac{\nu}{u_e^2(x)} \left( u_e(x) f''(\eta) \sqrt{\frac{u_e}{\nu x}} \right)_{y=0} \\ &= \left( \sqrt{\frac{\nu}{xu_e(x)}} f''(\eta) \right)_{y=0} = Re_x^{-\frac{1}{2}} f''(0) \end{aligned}$$

$$\therefore C_{fx} Re_x^{\frac{1}{2}} = f''(0). \quad (6.3.1)$$

#### 6.3.2 Local Nusselt number

$$\begin{aligned} Nu_x &= \frac{xq_w}{k\Delta T} = \frac{x \left( -k \left( \frac{\partial T}{\partial y} \right)_{y=0} \right)}{k\Delta T} = -\frac{x}{\Delta T} \left( \Delta T \theta'(\eta) \sqrt{\frac{u_e}{\nu x}} \right)_{y=0} \\ &= -\left( \theta'(\eta) \sqrt{\frac{xu_e}{\nu}} \right)_{y=0} = -Re_x^{\frac{1}{2}} \theta'(0) \end{aligned}$$

$$\therefore Re_x^{-\frac{1}{2}} Nu_x = -\theta'(0). \quad (6.3.2)$$

#### 6.3.3 Local Sherwood number

$$\begin{aligned} Sh_x &= \frac{xq_m}{D_B \Delta C} = \frac{x \left( -D_B \left( \frac{\partial C}{\partial y} \right)_{y=0} \right)}{D_B \Delta C} = -\frac{x}{\Delta C} \left( \Delta C \phi'(\eta) \sqrt{\frac{u_e}{\nu x}} \right)_{y=0} \\ &= -\left( \phi'(\eta) \sqrt{\frac{xu_e}{\nu}} \right)_{y=0} = -Re_x^{\frac{1}{2}} \phi'(0) \end{aligned}$$

$$\therefore Re_x^{-\frac{1}{2}} Sh_x = -\phi'(0). \quad (6.3.3)$$

#### 6.3.4 Local density number of the motile microorganisms

$$Nn_x = -\frac{x}{\Delta N} \left( \Delta N \chi'(\eta) \sqrt{\frac{u_e}{\nu x}} \right)_{y=0} = -\left( \chi'(\eta) \sqrt{\frac{xu_e}{\nu}} \right)_{y=0} = -Re_x^{\frac{1}{2}} \chi'(0)$$

$$\therefore Re_x^{-\frac{1}{2}} Nn_x = -\chi'(0). \quad (6.3.4)$$

$$\text{where, } Re_x = \frac{xu_e(x)}{\nu}.$$